TECHNISCHE UNIVERSITÄT MÜNCHEN

Lehrstuhl für Biochemische Pflanzenpathologie

NO-mediated modification of nuclear proteins: S-Nitrosylation of *Arabidopsis* HD2 proteins

Azam Shekariesfahlan

Vollständiger Abdruck der von der Fakultät Wissenschaftszentrum Weihenstephan für Ernährung, Landnutzung und Umwelt der Technischen Universität München zur Erlangung des akademischen Grades eines

Doktors der Naturwissenschaften

genehmigten Dissertation.

Vorsitzender:	Univ.- Prof. Dr. Siegfried Scherer
Prüfer der Dissertation:	1. Univ.- Prof. Dr. Jörg Durner 2. apl. Prof. Dr. Erich Glawischnig

Die Dissertation wurde am 05.11.2015 bei der Technischen Universität München eingereicht und durch die Fakultät Wissenschaftszentrum Weihenstephan für Ernährung, Landnutzung und Umwelt am 12.01.2016 angenommen.

Abstract

Nitric oxide (NO) is a diatomic molecule and contains an unpaired electron. In mammals NO is a particularly known highly reactive intermediate molecule involved in various physiological and immunological processes. Discovery of NO function as a signaling molecule in cardiovascular system won the Nobel Prize in 1998. S-Nitrosylation is an NO-dependent post-translational modification wherein NO reacts with the thiol group of redox-sensitive cysteine residues of proteins. In plants, growing number of studies reveals S-nitrosylation as an important regulatory check-point in relying cellular signaling processes during growth, development and in stress-related responses. To generate a map of NO-regulated nuclear candidates, nuclear proteins of pathogen-treated *Arabidopsis* cell cultures were isolated; S-nitrosylated nuclear proteins were then enriched and labeled via biotin switch method and identified by mass spectrometry. In total, 137 proteins were identified, whereas nuclear localization and possession of at least one cysteine residue was defined for 123 and 117 proteins, respectively. Those proteins were involved in protein and RNA metabolism, stress response, and cell organization and division. Two HD2 type histone deacetylases (HDACs) were identified and S-nitrosylation of all HD2 isoforms (HD2A-HD2D) was further verified *in-vitro*.

Analysis of function of HD2C's S-nitrosylation was pursued, since it involves in *Arabidopsis* ABA and salt stress responses. HD2C contains only 2 cysteine residues belong to its zinc finger domain which has been hypothesized to be involved in protein-protein interactions. As putative function of S-nitrosylation, zinc ion was released from recombinant HD2C. Although, HDAC activity could not be detected for HD2C, Co-Immuonoprecipitation (Co-IP) analysis suggested an alternative function. Absence of histones, HDACs and DNA binding proteins among Co-IP candidates and - in turn - significantly high enrichment of three core proteins of C/D box snoRNP complex involved in RNA methylation, besides HD2C's nucleolar localization propose an rRNA processing-related function for HD2C. Likewise, identification of three core proteins of C/D box as candidates of S-nitrosylation highlights the putative regulatory role of NO in rRNA processing which has to be further determined. Since, HD2C involves in modulation of ABA-induced pathways and ABA - in turn - induces NO production in *Arabidopsis; hd2c-1* plants transformed by *HD2C* mutated at the bases coding cysteine(s) were treated with ABA. *hd2c-1/HD2C-C269/272H* line associated with the lowest inhibition of rosette growth by ABA in comparison to WT. These data indicate that cysteine residues are important in function of HD2C and their S-nitrosylation might switch off the putative positive part of modulatory role of HD2C in ABA-induced pathways.

Index of figures

Index of supplementary figures

Index of tables

Index of supplementary tables

Abbreviations:

2,4-D	2,4-Dichlorophenoxyacetic acid
aa	Amino acid
ABA	Abscisic Acid
ACN	Acetonitrile
ANOVA	Analysis of variance
APS	Ammonium Persulfate
AS	Alternative splicing
BCIP	5-Bromo- 4-Chloro-3-Indolyl Phosphate
Biotin-HPDP	N-[6-(biotinamido)hexyl]-3'-(2'-pyridyldithio)propionamide
bp/Kb	Base pair(s)/kilo base pair
BSA	Bovine serum albumin
BST	Biotin switch technique
C	Carboxyl
Co-IP	Co-Immunoprecipitation
cDNA	Complementary DNA
CFU	Colony-forming unit
cGMP	Cyclic guanosine monophosphate
CPTIO	2-(4-Carboxyphenyl)-4,4,5,5-tetramethylimidazoline-1-oxyl-3-oxide
CTAB	Cetyltrimethylammoniumbromide
DAF-FM	4-amino-5-methylamino-2’,7’-difluororescein diacetat
DAPI	4', 6-diamidino-2-phenylindole, dihydrochloride
ddH_2O	Double distilled water
DMSO	Dimethylsulfoxid
DNA	Deoxyribonucleic acid
dNTPs	Deoxynucleotide-5’-triphosphates
DSP	Dithiobis[succinimidyl propionate
DTT	Dithiothreitol
E. coli	*Escherichia coli*
EDTA	Ethylendiamintetraacetate
GAPDH	Glyceraldehyde-3-phosphate dehydrogenase
GSH	Glutathione
GSNO	S-nitrosoglutathione
GSNOR	S-nitrosoglutathione reductase
h	Hour(s)
hd2c-1	T-DNA insertion line *hd2c-1*/Salk_129799.19.60
HDAC	Histone deacetylase
HEPES	4-(2-hydroxyethyl)-1-piperazineethanesulfonic acid
HR	Hypersensitive response
kDa	Kilo Dalton
LC-MS	Liquid chromatography mass spectrometry
LB	Luria-Bertani
MES	2-(N-morpholino) ethanesulfonic acid
min	Minute(s)
MMTS	Methyl methanethiosulfonate
mRNA	messenger RNA

MS	Murashigge & Skoog
N	Amino
NAD	Nicotinamide adenine dinucleotide
NADPH	Nicotinamide adenine dinucleotide phosphate
NBT	Nitro-blue tetrazolium
NEB/NIB	Nuclear extraction/isolation buffer
NIA	Nitrate reductase
NLB	Nuclear lysis buffer
NO	Nitric oxide
NOS	Nitric oxide synthase
NP-40	Nonyl phenoxypolyethoxylethanol
NPR1	Nonexpressor of pathogenesis-related gene 1
NR	Nitrate reductase
OD	Optical density
PAR	4-(2-pyridylazo) resorcinol
PCD	Programmed cell death
PCR	Polymerase chain reaction
PMSF	Phenylmethanesulfonylfluoride
PR	Pathogenesis-related
PSI-BLAST	Position-Specific Iterative Basic Local Alignment Search Tool
Pst avr	*Pseudomonas syringae* pv tomato DC3000 avrRpm1
Pst vir	*Pseudomonas syringae* pv tomato DC3000
PVDF	Polyvinylidene difluoride
RNA	Ribonucleic acid
RNS	Reactive nitrogen species
rpm	Revolutions per minute
rRNA	Ribosomal RNA
RT	Room temperature
S	Second(s)
SA	Salicylic acid
SDS	Sodium Dodecyl Sulfate
SDS-PAGE	Sodium dodecyl sulfate polyacrylamide gel electrophoresis
SEM	Standard error of the mean
sGC	Soluble guanylate cyclase
SNAP	S-nitroso-N-acetylpenicillamine
SNO	S-nitrosothiol
snoRNA	Small nucleolar RNAs
snoRNP	Small nucleolar ribonucleoprotein
TAE	Tris-Acetate-EDTA
Taq	*Thermus aquaticus*
TEMED	N,N,N',N'- Tetramethylethylenediamine
Tris	2-amino-2-hydroxymethyl-1,3-propanediol
v/v	Volume per volume
WT	Wild type
w/v	Weight per volume
x g	(times) earth gravity

Introduction

1. Nitric oxide (NO)

NO is a highly reactive radical gas, as a result of the presence of an unpaired electron in its outer orbital; thereby, it can exist in 3 redox-related species; nitric oxide radical (NO°), nitrosonium cation (NO^{+}), and nitroxyl anion (NO^{-}) (Lindermayr & Durner, 2007, Abat et al., 2008a). NO reacts with O_2 and O_2^{-} and generates NO_x and peroxynitrite, respectively, the last one is a strong oxidant that reacts with many biologic molecules, causing cell damage (Lindermayr & Durner, 2007). Each of those reactive nitrogen species (RNS) preserves its own specific reactivity in biological systems (Abat et al., 2008a). NO is known as an important regulatory molecule in a various range of physiological processes in plants including immunity. Extensive studies were commenced in order to define the molecular mechanisms underlying NO functions in plants (Lamotte et al., 2014). Regarding to plant stress, NO is involved in responsive mechanisms against abiotic and biotic stressors by participating in processes such as hormonal signaling, stomatal closure, cross-talk with reactive oxygen species, and transcriptional regulation of defense-related genes.

1. 1. NO synthesis in plants

There are extensive studies which demonstrate that NO generation occurs in plants via both enzymatic and non-enzymatic pathways. However, how NO is synthesized in plants is still a quarrelling field. Plants lack any nitric oxide synthase (NOS)-like enzyme. A gene in *Arabidopsis thaliana* (At3g47450) homologous with a snail (*Helix pomatia*) gene encoding a protein involving in NO synthesis was identified as AtNOS1 (Guo et al., 2003). AtNOS1 could show NOS activity using a commercial kit which converted L-arginine to L-citrulline. Later on, some other studies questioned its NOS activity (Guo, 2006, Zemojtel et al., 2006, Crawford, 2006). On the other hand, several studies showed that NO synthesis and responses that require NO are undeniably failed in the *Atnos1* mutant (Neill et al., 2008). Therefore, AtNOS1 was re-named to *Arabidopsis thaliana* nitric oxide-associated 1 (AtNOA1) (Neill et al., 2008). Nitrate reductase (NR) generates NO from nitrite via an nicotinamide adenine dinucleotide phosphate (NADPH)-dependent manner (Mur et al., 2006, Kaiser et al., 2002, Sakihama et al., 2002). NIA1 and NIA2 are two *Arabidopsis* NR isoforms. *Arabidopsis nia1 nia2* mutants are impaired in both ABA-induced NO generation and stomatal closure (Desikan et al., 2002) which demonstrates that NO synthesis mediated by NR is a main step in ABA signaling in

guard cells (Besson-Bard et al., 2008). However, the production of NO due to adding nitrite to *nia* mutants suggests that NR is not the only nitrite-derived source of NO in plants (Moreau et al., 2010). Moreover, there is an evidence of triggering NO production by polyamines such as spermine and spermidine in phloem of *Vicia faba* (Tun et al., 2006). Plant tissues also can synthesize NO in apoplasts - non-enzymatically - from nitrite as a response to accumulation of gibberellin and ABA (Bethke et al., 2004). Both of those hormones make an acidic environment which is required for the occurrence of the reaction (Bethke et al., 2004). NO production has been shown in several different compartments such as peroxisomes (Corpas et al., 2009b), mitochondria (Gupta et al., 2009) and chloroplast (Jasid et al., 2006). This commends a probable specific role of NO in each organelle, possibly local signaling pathways (Mur et al., 2013). Finally, different studies have demonstrated the formation of NO and its derivatives in the root of several plants including pea, pepper and *Arabidopsis* (Corpas & Barroso, 2015, Corpas et al., 2006, Corpas et al., 2009a, Airaki et al., 2015, Stohr & Stremlau, 2006). Regarding to biochemical aspect, at present, a strong data is accumulated from diverse experiments which indicate that an arginine-utilizing pathway can produce NO in planta. Although, this does not necessarily leads to the co-formation of citrulline which is a particular characteristic of a typical NOS enzyme (Mur et al., 2013). Moreover, roles of NO are associated with its concentration in different compartments of plants. This highlights the importance of accuracy of measuring methods of NO levels in planta (Mur et al., 2013). Although impressive efforts have been made, it should be considered that NO detection methods in plants are generally inefficient and that the accuracy and tissue specificity of methods used for measuring NO formation can be questioned (Mur et al., 2013).

1. 2. NO signaling in plants

In animal field, cyclic guanosine monophosphate (cGMP)-dependent signaling is known as the classical NO signaling and it has been characterized very well. cGMP is synthesized by activation of NO-sensitive soluble guanylate cyclase (sGC) and can be degraded by cyclic nucleotide phosphodiesterases (Francis et al., 2010). sGC is a hemoprotein and binding of NO to the heme center of sGC activates its catalytic domain which leads to producing cGMP from guanosine triphosphate. cGMP-dependent NO signaling occurs through affecting 3 different main targets: cGMP-dependent protein kinases, cGMP-gated cation channels and phosphodiesterases (Francis et al., 2010). In contrast to the animal system, the occurrence

and importance of cGMP-dependent NO signaling is not very clear in plants. Due to several independent studies in *Arabidopsis* (Durner et al., 1998), tobacco (Donaldson et al., 2004) and barley (Penson et al., 1996), the presence of cGMP in plants is generally accepted. But, since cGMP exists in much less concentrations (femtomolar range) in plants in compare with animals, its measurement and investigation of its role is challenging (Isner & Maathuis, 2011). Another important NO signaling pathway is associated with the binding of NO to metal center of cytochrome c oxidase and the inhibition of its activity in mitochondria and consequently the mitochondrial respiration (Kovacs & Lindermayr, 2013, Tan et al., 2010). Cytochrome c oxidase is the last enzyme in the electron transport chain of mitochondrial respiration. Those 2 signaling pathways occur via metal nitrosation which is the direct binding of NO to transition metal ions of proteins (Kovacs & Lindermayr, 2013) (Fig. 1a).

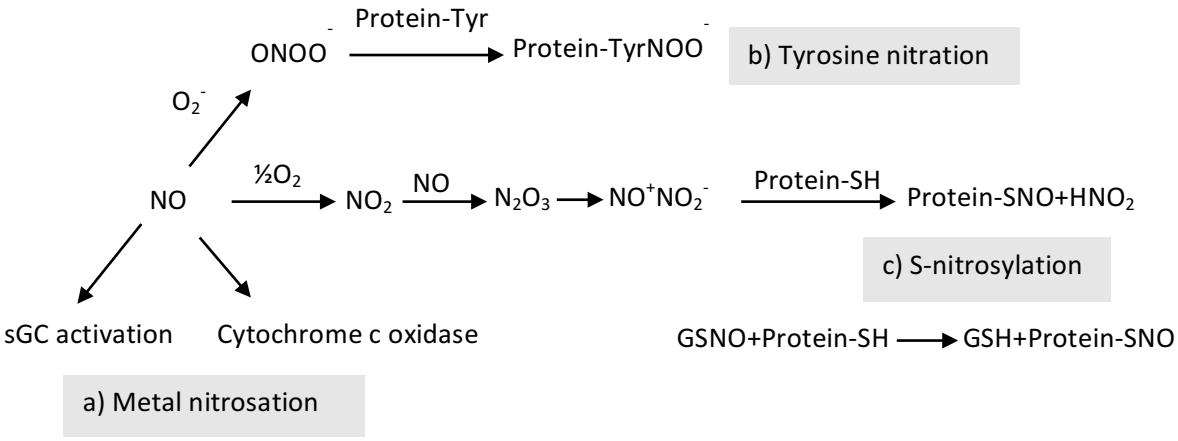

Fig. 1. Nitric oxide signaling in plants. a) Metal nitrosation is the direct binding of NO to transition metal ions of proteins, b) Tyrosine nitration is the covalent modification of tyrosine residues by RNS, such as peroxynitrite ($ONOO^-$) and c) S-Nitrosylation is the covalent attachment of an NO moiety to the sulfhydryl group of a cysteine residue of a target protein.

Other NO-mediated signaling mechanisms are through the post-translational modification of proteins via reaction of NO-derived molecules with cysteine and tyrosine residues (Fig. 1b and c). RNS can intervene different post-translational modifications of proteins including tyrosine nitration and S-nitrosylation (Martinez & Andriantsitohaina, 2009) which all can alter protein structure, and consequently protein functions. Tyrosine nitration is the covalent modification of tyrosine residues by RNS, such as peroxynitrite ($ONOO^-$) (Fig. 1b). However, the most known and biologically relevant NO mediated signaling in plants is S-nitrosylation (Fig. 1c). This reversible modification can result in altered protein conformation, function/activity and translocation. Such changes accomplish the regulatory function of S-

nitrosylation during different processes. A growing number of studies indicate the important regulatory role of S-nitrosylation in plants.

1. 2. 1. Biochemistry of S-nitrosylation

S-Nitrosylation assigns to the covalent attachment of an NO moiety to the sulfhydryl group of a cysteine residue of a target protein (Moreau et al., 2010). Therefore, first the properties of cysteine which make it unique among other amino acids are commented. Cysteine is an ambiguous amino acid; on one side it is one of the least abundant amino acids in proteins of living organisms, on the other side it often appears in important functional sites such as regulatory, catalytic and co-factor binding (Marino & Gladyshev, 2010a, Requejo et al., 2010). Low abundance of cysteine residues on proteins surfaces might be due to evolutionary selective removal of cysteines as a result of their high reactivity (Marino & Gladyshev, 2010a). Thiol group of cysteines have unique reactivity, because of creating disulphide bonds with other thiols, reversible oxidation to sulfenic acid and overoxidation to sulfinic acid and coordinating metal ions (Marino & Gladyshev, 2012). The Cysteine sulfhydryl group has a crucial role in the antioxidant function of glutathione serving as an electron donor. Moreover, cysteines that are exposed on the surface of proteins and are not involved in the enzymatic function of protein seem to have an important role in the antioxidant defence (Requejo et al., 2010). Comprising all those functions, cysteines are the primary targets of nitrosative stress which leads to S-nitrosylation of proteins (Requejo et al., 2010).

NO is not able to react with nucleophiles under anaerobic conditions (Sun et al., 2006). But S-nitrosylation can be mediated by NO-oxides such as N_2O_3 and S-nitrosothiols (SNOs) and S-nitrosoglutathione (GSNO) as an S-nitrosocysteine (Dalle-Donne et al., 2009). The basis of the determination of a NO-sensitive target residue is still not well understood. The presence of an acid-base or a hydrophobic motif flanking the cysteine residue has been considered essential (Stamler et al., 2001). According to a study, using 70 known S-nitrosylated peptides, it is important for the NO-sensitivity of cysteine residue to be close to exposed charged groups of an acid-base motif in 3D structure of protein; however it is a bit farther in amino acid sequence (Marino & Gladyshev, 2010b). Other studies have also proposed that it is not only the primary structure but also the three-dimensional environment determines S-nitrosylation sensitive residues in proteins (Taldone et al., 2005). It is further proposed that

S-nitrosylation of cysteine residues is associated with the low pKa value of the target residue. The predictability potential of NO-sensitivity of cysteine residues has been drawn attention to develope several different prediction tools. Some of the widely used databases and prediction tools of SNOs are including: dbSNO (http://140.138.144.145/~dbSNO/index.php) (Chen et al., 2015), iSNO-AAPair (http://app.aporc.org/iSNO-AAPair/index.html) (Xu et al., 2013), GPS-SNO (http://sno.biocuckoo.org/) (Xue et al., 2010b) and PSNO (http://59.73.198.144:8088/PSNO/) (Zhang et al., 2014).

S-Nitrosylation of GSH - the most plentiful low-molecular weight thiol (up to 10 mM) in living organisms leads to generation of S-nitrosoglutathione (GSNO), which mediates S-nitrosylation of proteins via trans-nitrosylation. S-Nitrosylated hemoglobin, thioredoxin, caspase 3, and glyceraldehyde-3-phosphate dehydrogenase (GAPDH) can also trans-nitrosylate their NO group to a binding partner protein (Lamotte et al., 2014). In addition, reaction of GSH with SNOs can lead to S-glutathionylation of proteins (Dalle-Donne et al., 2009).

S-Nitrosothiols are highly labile, a property which provides S-nitrosylation to be a sensitive mechanism for regulating cellular processes (Lindermayr et al., 2005). Reversibility of S-nitrosylation (de-nitrosylation) does not arise spontaneously (Benhar et al., 2009). Exposure to light, heat, reductants and nucleophilic compounds results in cleavage of the sulphur-nitrogen bond and decomposition of SNOs to yield radical or ionic species (Benhar et al., 2008). Besides, transition metal ions might also catalyse decomposition of SNOs (Benhar et al., 2009). Furthermore, enzymatic decomposition of SNOs has been shown with GSNO reductase and thioredoxin systems (Liu et al., 2001, Benhar et al., 2008, Tada et al., 2008b).

1. 2. 2. S-Nitrosylation in response to biotic and abiotic stresses in plants

Alteration in cellular redox status is a remarkable feature of immune responses following pathogen challenge. The rapid synthesis of ROS and NOS changes the equilibrium between them and their scavengers. By increasing the concentration of ROS and NOS in a cellular environment, protein cysteine residues can be oxidized into sulphenic, sulphinic, sulphonic acids, or to an S-nitrosothiol. Composition of sulphinic and sulphonic are usually irreversible (Dalle-Donne et al., 2009). These irreversible modifications following an oxidative burst are part of oxidative damage and can lead to the cell death. S-nitrosylation which is reversible (Lindermayr & Durner, 2007) is mainly involved in signaling pathways.

A well-studied plant S-nitrosylation signaling pathway is associated with nonexpressor of pathogenesis-related gene 1 (NPR1). S-Nitrosylation of NPR1 triggers its oligomerization and stabilization in cytoplasm (Fig. 2a). NPR1 is a key positive regulator of salicylic acid (SA)-dependent signaling that triggers plant immunity responses. SA increases cellular redox status which leads to reduction of disulphide bonds in NPR1 oligomer and releasing monomers. The monomer translocates to nucleus and activates several TGA-class transcription factors that consequently activate pathogenesis-related (PR) genes (Tada et al., 2008a, Lindermayr et al., 2010) (Fig. 2b). Activity of TGA1 is enhanced by S-nitrosylation and increases its interaction with NPR1 (Lindermayr et al., 2010) (Fig. 2c).

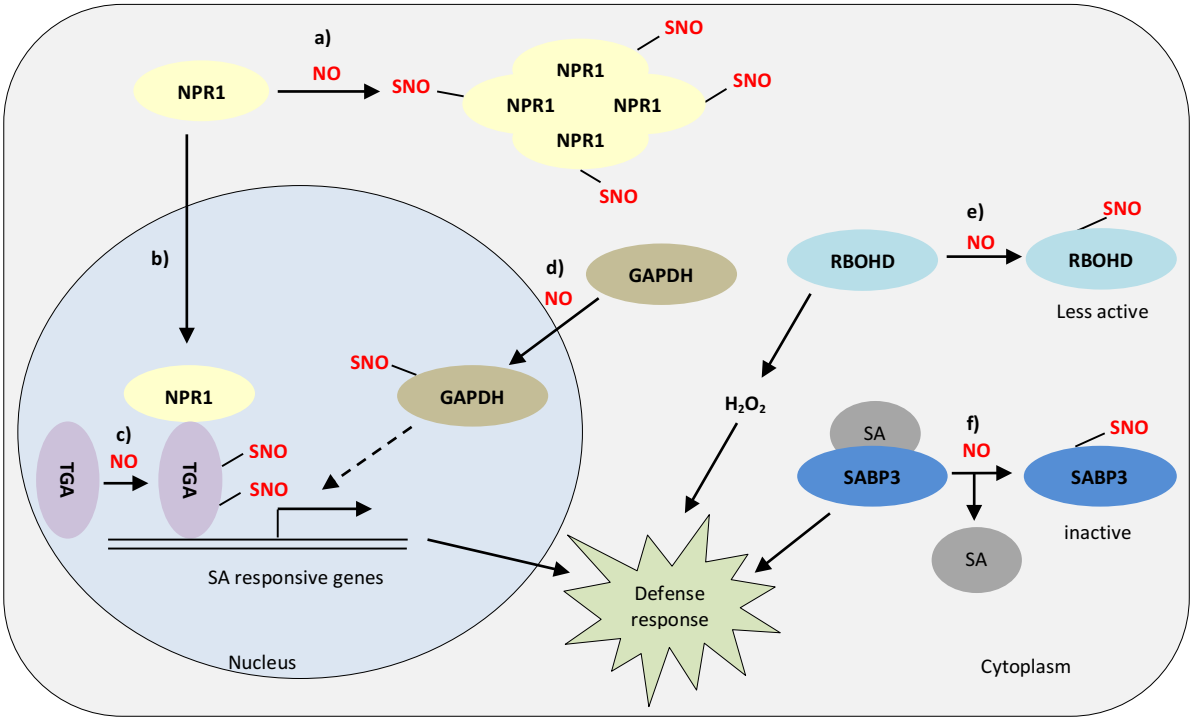

Fig. 2. Schematic model of protein S-nitrosylation in plant responses to biotic and abiotic stresses. a) S-Nitrosylation of NPR1 promotes its oligomerization and stabilization in cytoplasm. b) De-nitrosylation of NPR1 oligomers releases it monomers which can translocate to nucleus and bind to TGA1 activating the expression of SA responsive genes. c) TGA1 activation is increased by S-nitrosylation. d) S-Nitrosylation of GAPDH induces its nuclear localization wherein it putatively involves in gene regulation with trans-nitrosylating of nuclear proteins. e) Activity of RBOHD decreases due to S-nitrosylation which leads to production of less reactive oxygen species and limited defense response. f) S-Nitrosylation of SABP3 represses its SA binding activity promoting a negative feed loop back in plant immunity responses.

GAPDH is an essential glycolytic enzyme which lacks a nuclear localization signal (Mengel et al., 2013b). In animals, GAPDH is S-nitrosylated due to stress which leads it to form a complex with seven in absentia homolog 1 (Siah1), an E3 ubiquitin ligase and consequently enables the translocation of the complex to the nucleus (Hara et al., 2005). S-Nitrosylated

GAPDH trans-nitrosylates nuclear proteins including deacetylating enzyme sirtuin 1, histone deacetylase 2, and DNA-activated protein kinase; this consequently affects gene transcription (Kornberg et al., 2010). S-Nitrosylation and S-glutathionylation of GAPDH (isoforms GapC1 and 2) has been shown in *Arabidopsis* (Holtgrefe et al., 2008). Cys155 and Cys159 have been demonstrated as targets of both redox modifications and at the same time nuclear localization and DNA binding activity of the protein was shown (Holtgrefe et al., 2008). The authors suggested that, since in animal system DNA binding activity of GAPDH occurs upon stress conditions, a similar process can happen in plant system as well (Holtgrefe et al., 2008). In tobacco, NtGAPCa and NtGAPCb isoforms of GAPDH interact with salt-stress-activated protein kinase NtOSAK, and S-nitrosylation of those GAPDH isoforms triggers translocation of the complex into the nucleus (Wawer et al., 2010a) suggesting its probable role in regulation of gene expression (Fig. 2d).

S-Nitrosylation of NADPH oxidase, AtRBOHD, at Cys890, decreases its ability to produce reactive oxygen intermediates which consequently leads to a limited hypersensitive response (Yun et al., 2011). Mutation of Cys890 showed increased activity of RBOHD during the defense response, with higher accumulation of reactive oxygen intermediates and cell death development (Yun et al., 2011). Interestingly, this cysteine is evolutionarily conserved and its S-nitrosylation has been shown in both human and fly NADPH oxidases (Yun et al., 2011) (Fig. 2e).

S-Nitrosylation of *Arabidopsis* salicylic acid-binding protein 3 (AtSABP3) decreases its SA-binding and carbonic anhydrase activity. Carbonic anhydrase activity of SABP3 is required for the expression of plant defense responses. The inhibition of SABP3's activity makes a negative loop feedback modulating plant immunity responses (Wang et al., 2009) (Fig. 2f).

1. 2. 3. Detection and identification of candidates for protein S-nitrosylation

Since S-nitrosothiols are highly labile due to low bond energy of SNOs (29 kcal/mol) (Chen et al., 2013), identification of endogenous S-nitrosylated proteins is challenging. Until present, several methods have been developed for identification of S-nitrosylated proteins which work either directly or indirectly, and either qualitatively or quantitatively. Mass spectrometry and X-ray crystallography have been used for the direct detection of S-nitrosothiols (Kovacs & Lindermayr, 2013). Replacement of hydrogen on S-H group with an NO group makes a 29 Da increase of mass in compare with an unmodified peptide; This

increase is detectable by mass spectrometry (Chen et al., 2013). This procedure can lead to direct identification of S-nitrosylated cysteine on a unique peptide (Chen et al., 2013). However, labile nature of the S-NO bond and the difficulty of the optimization of sample preparation and the instrument parameters have been restricted this method from being used in the large-scale S-nitrosoproteomic approaches (Chen et al., 2013). Besides direct methods, the indirect methods of identification of S-nitrosothiols have been established. Indirect methods are at the base of either measuring NO levels after breaking of the S-NO bonds or altering nitrosothiols to a detectable tag (Kovacs & Lindermayr, 2013).

Biotin switch technique (BST) - the most commonly used method for indirect detection of S-nitrosylated proteins - was invented by Jaffrey et al (Jaffrey et al., 2001). In the plant field, Lindermayr et al adopted BST for identification of S-nitrosylated proteins in *Arabidopsis* (Lindermayr et al., 2005). Since its invention, biotin switch and its variations have been applied comprehensively, because of its big advantage to detection of particular protein-SNOs in a complex mixture, as well as to identify novel S-nitrosylated proteins (Forrester et al., 2009). Before starting BST a protein cysteine residue can be present as a free thiol, a disulphide or a nitrosothiol. BST contains 3 steps: I) the free thiols are blocked by MMTS and the residue of MMTS is removed, II) the nitrosothiols are selectively reduced by ascorbate III) and labelled by biotin-HPDP (Fig. 3). Afterward the biotin-labeled proteins are detected by antibiotin antibody, purified by avidin affinity and identified by mass spectrometry (Jaffrey et al., 2001, Lindermayr et al., 2005). The specificity of BST to S-nitrosothiols is theoretically on the base of the fact that ascorbate can convert SNOs to SHs but not SSGs and other S-oxides (Forrester et al., 2009) (Fig. 3). Thermodynamic measurements support this specificity (Jaffrey et al., 2001), however there are some controversial reports about specificity of ascorbate. Some authors indicate that ascorbate is an inefficient reducer and needs longer time of incubations and others suggest that it speeds up the biotinylation reaction and increase the false-positive signals (Kovacs & Lindermayr, 2013). Although, the same amounts of material for different treatments and controls are used in BST, the quite high number of chemical steps and acetone precipitations makes it rather a qualitative method. Another important challenge of BST is producing false-positives due to insufficient blocking by methyl methanethiosulfonate (MMTS) (Chen et al., 2013). Besides the controversial reports about technical problems of the BST, another challenge is to characterize the physiological role of the identified candidates which has already crossed the

number of 3000 among all the studied organisms (Kovacs & Lindermayr, 2013). For the quantitative analysis of S-nitrosylated proteins, an approach which combines two-dimensional gel electrophoresis with BST has been developed (Huang et al., 2009).

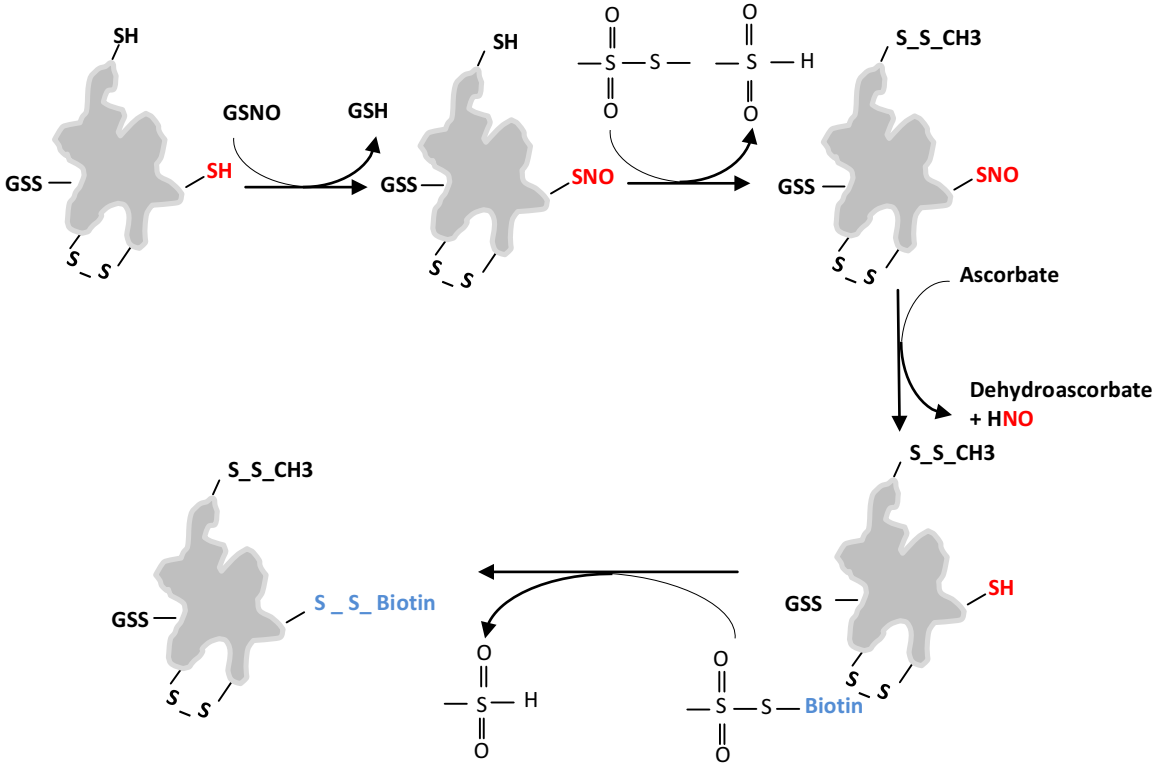

Fig. 3. Biotin switch method. A protein with possible –SH, –SSG, –S–S– and –SNO groups exists or –SNO formation has occurred due to treatment with NO donors such as GSNO. The free thiols are blocked with MMTS and further S-nitrosothiols are selectively reduced with ascorbate. The newly formed free thilos then are biotinylated using biotin-HPDP.

Until today, S-nitrosylation candidates have been identified in *Arabidopsis* extracts treated with GSNO (Lindermayr et al., 2005), NO-fumigated *Arabidopsis* plants (Lindermayr et al., 2005), mitochondria of *Arabidopsis* leaves (Palmieri et al., 2010), *Arabidopsis* cell cultures treated with salt (Fares et al., 2011a), *Arabidopsis* plants undergoing defense (Maldonado-Alconada et al., 2011a) and hypersensitive response (Romero-Puertas et al., 2008), *Kalanchoe pinnata* leaves (Abat et al., 2008b), *Solanum tuberosum* leaves and tubers (Kato et al., 2013), *Oryza sativa* leaves (Lin et al., 2012), peroxisomes of *Pisum sativum* (Ortega-Galisteo et al., 2012) and salt-treated mitochondria of pea (Camejo et al., 2013).

From the above mentioned studies the main categories of proteins that identified are including: stress-related, redox-related, signaling-related, antioxidant defense-related, cytoskeleton and cell wall proteins, metabolism- related proteins, transport proteins,

photosynthetic proteins, respiratory and/or photorespiratory-related and genetic information processing proteins (reviewed by (Kovacs & Lindermayr, 2013). Last but not least, recently a site-specific identification of *Arabidopsis* endogenously S-nitrosylated proteins has been performed (Hu et al., 2015). Hu et al identified 1,195 endogenously S-nitrosylated peptides from 926 proteins which is the largest dataset of S-nitrosylatad proteins among all organisms, up to present. Significant number of the endogenously identified proteins is involved in chlorophyll metabolism, photosynthesis, carbohydrate metabolism, and stress responses (Hu et al., 2015). However, until now no actions have been taken to analyze S-nitrosylation of *Arabidopsis* nuclear proteins specifically.

1. 2. 4. Regulation of gene expression by NO

Plants lack the adaptive immune system similar that of animals in which migrant defender cells carry out the antigen-specific immune response (Jones & Dangl, 2006). Therefore, the ability of each plant cell to reprogram its transcription to defend against pathogens is crucial. This procedure arises from the infection sites by producing and mediating systemic signals (mainly phytohormones) (Berr et al., 2012). NO signaling has been demonstrated to act upstream and/or downstream of hormonal signaling (Freschi, 2013) suggesting its relevance in this vital transcriptional reprogramming. Moreover, several studies on plants, based on altered NO-levels, have also recently contributed genetic evidence for the participation of NO in gene induction. For a general survey of NO- dependent gene expression, two large-scale transcriptional analyses of *Arabidopsis* performed using custom-made or commercial DNA-microarrays (Huang et al., 2002, Parani, 2004). Additionally, a comprehensive transcript profiling by cDNA-amplification fragment length polymorphism (AFLP) identified a number of NO-regulated *Arabidopsis* genes that are associated with signal transduction, stress response, disease resistance, cellular transport, photosynthesis, and basic metabolism (Polverari et al., 2003). Furthermore, a search for common transcription factor-binding sites in promoter regions of NO-regulated genes, has been done based on microarray analyses using Genomatix Gene 2 Promotor and MatInspector (Palmieri et al., 2008). According to this study, particular transcription factor binding sites, such as octopine synthase gene (ocs) elements and WRKY-sites were enriched (Palmieri et al., 2008). This raised the question whether NO influence transcription directly by S-nitrosylation of transcription factors or indirectly by modifying their regulators (Mengel et al., 2013b). Evidences for NO

accumulation in the nucleus of stomatal and epidermal cells in response to various stress conditions like heat, green light, osmotic stress, and elicitors have been reported (Foissner et al., 2000, Gould K et al., 2003, Vitecek et al., 2008). Moreover, S-nitrosylation has been studied in plants, in some nuclear-localized proteins such as Non-expressor of Pathogenesis-related genes 1 (NPR1), transcription factor TGA1, glyceraldehyde-3-phosphate dehydrogenase, aldolase, and MYB transcription factors (Holtgrefe et al., 2008, Lindermayr et al., 2010, van der Linde et al., 2011, Tavares et al., 2014).

The S-nitrosylation of GAPDH and NPR1 was mentioned in the section of '1. 2. 2'. Myb transcription factors are highly abundant in *Arabidopsis*, establishing around 9% of all of its estimated transcription factors (Mengel et al., 2013b). Among plant Myb transcription factors, R2R3-MYB factors consist of a highly conserved cysteine residue which is found in fungi and animals as well (Serpa et al., 2007). It has been shown that the DNA binding activity of *Arabidopsis* M2D is inhibited due to S-nitrosylation at the conserved cysteine at position 53 (Serpa et al., 2007). The equivalent conserved cysteine of chicken c-Myb to Cys53 is Cys130 which also has been demonstrated to be S-nitrosylated with different NO donors. This S-nitrosylation leads to severe inhibition in chicken c-Myb's DNA binding activity (Brendeford et al., 1998). Chromatin modifications such as RNA-directed DNA methylation, histone methylation, demethylation, acetylation, deacetylation and ATP-dependent chromatin remodelling are the key transcriptional reprogramming mechanisms orchestrating plant abiotic and biotic responses (Luo et al., 2012a, Berr et al., 2012). Histone deacetylases repress the gene expression by deacetylating lysine residues of histone tails. In human, S-nitrosylation of HDAC2 has been shown in neurons (Nott et al., 2008). Cys262 and Cys274 of HDAC2 were identified as targets of S-nitrosylation. S-nitrosylation did not affect the HDAC activity of human HDAC2 (Nott et al., 2008). Whereas, it caused the releasing HDAC2 from chromatin and consequently increasing of the histone acetylation at particular promoter regions which leads to the transcription of genes such as c-fos, egr1, VGF, and nNos involving in neuronal development (Nott et al., 2008, Riccio et al., 2006). According another study in muscle cells, it has been demonstrated that S-nitrosylation of HDAC2 decreases its HDAC activity (Colussi et al., 2008), this might be due to S-nitrosylation of different Cys residues in neurons and muscle cells (Nott & Riccio, 2009, Mengel et al., 2013b). *Arabidopsis* HDA6 and HDA19 contain 2 conserved cysteines with Cys262 and Cys274 of HDAC2 (Mengel et al., 2013b) which studying their sensitivity to S-nitrosylation would be interesting.

Aim of this work

The primary aim of this work was to identify NO-sensitive nuclear candidate proteins in infected and uninfected *Arabidopsis* cell cultures to get deeper insight into the regulatory function of NO in the nucleus. For generating a map of S-nitrosylated nuclear proteins, a biotin switch assay shall be employed and followed by affinity chromatography purification and mass spectrometry analysis.

The secondary aim was to verify S-nitrosylation of selected interesting candidates using standard characterization methods. For this aim, one needed to produce recombinant proteins, verify the S-nitrosylation and further analyze the function of S-nitrosylation *in-vitro* and *in-vivo*.

1. Identification of nuclear target proteins for S-nitrosylation in pathogen-treated *Arabidopsis* cell cultures

The involvement of NO in defense signaling was one of the first functions known for NO in plants (Delledonne et al., 1998, Durner et al., 1998). Moreover, a direct function of NO in regulation of nuclear proteins has been already demonstrated (Lindermayr et al., 2008, van der Linde et al., 2011, Holtgrefe et al., 2008, Tavares et al., 2014). But a comprehensive survey of S-nitrosylated nuclear proteins was not available. Here a map of nuclear target proteins for S-nitrosylation is generated from pathogen-treated *Arabidopsis* cell cultures.

1. 1. NO production in pathogen-treated *Arabidopsis* cell cultures

It is known that NO production increases after stimulation with pathogens (Delledonne et al., 1998). To study protein S-nitrosylation in plant defense response, first the profile of NO production was monitored after infection of *Arabidopsis* cell cultures with *P. syringae*. NO was detected using the NO-sensitive fluorescent dye DAF-FM. *Arabidopsis* cell cultures were pre-treated with 5 µM DAF-FM and infected then with the avirulent strain of *P. syringae* pv. tomato DC3000 (*Pst* avrRpm1) for 28 h.

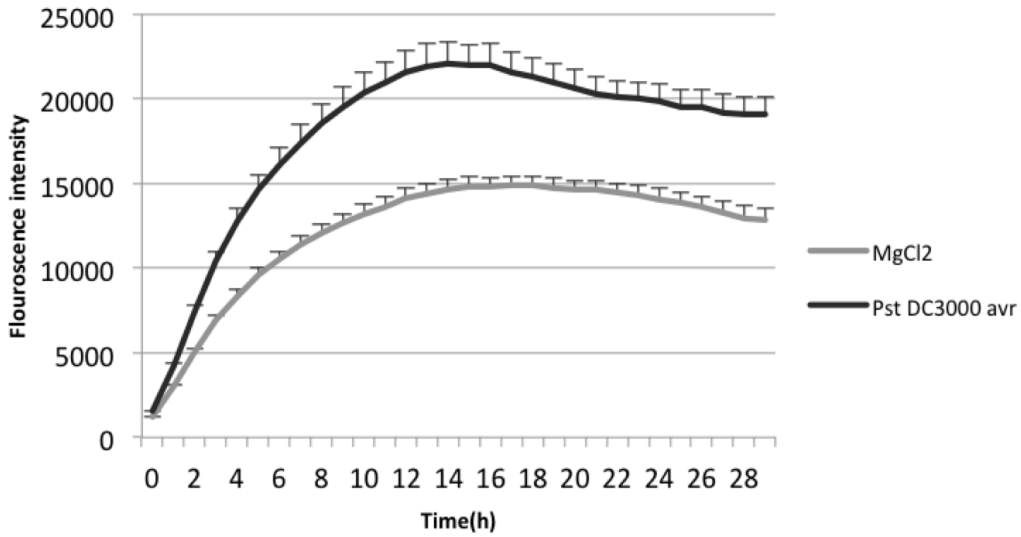

Fig. 4. Detection of NO in pathogen treated-*Arabidopsis* cell cultures. The accumulation of NO in *Arabidopsis* cell cultures was detected using the NO-sensitive fluorescent dye DAF-FM. The cell cultures were pre-treated with 5 µM DAF-FM for 1 h, followed by treatment with 5 mM $MgCl_2$ or *Pst* avrRpm1 for 28h. Fluorescence intensity was measured every hour using a Tecan fluorescence plate reader. Data are the mean ± SEM of two biological replicates (The NO production in pathogen-treated *Arabidopsis* cell cultures was performed by Dr. Mounira Chaki).

NO production strongly increased directly after the infection and continued up to 14 h. In $MgCl_2$-treated cell culture NO production could be also observed, but the levels were lower

than in the pathogen treated cells (Fig. 4). Therefore, an early (2 h) and a late (13 h) time point after infection were selected for identification of candidates for S-nitrosylation.

1. 2. Detection and purification of S-nitrosylated proteins in pathogen-treated *Arabidopsis* nuclear enriched extracts

Since S-nitrosothiols are quite unstable, their isolation from nuclei is a big challenge, because the modification might be lost during the long procedure of protein extraction. Therefore, in parallel to the isolation of *in-vivo* S-nitrosylated nuclear proteins, an *in-vitro* S-nitrosylation approach was performed - meaning the treatment of extracted nuclear proteins with the S-nitrosylating agent GSNO. First, *Arabidopsis* cell cultures were treated with $MgCl_2$ or *Pst* avrRpm1. Besides $MgCl_2$-treatment, a treatment with virulent *P. syringae* pv. tomato DC3000 (*Pst* vir) was used as control, since this pathogen does not induce NO production (Holzmeister et al., 2011). Nuclei were isolated after 2 h ($MgCl_2$, *Pst* avrRpm1) and 13 h ($MgCl_2$, *Pst* avrRpm1, and *Pst* vir) and visualized by DAPI (Supplementary Fig. S1). Afterward nuclear proteins were extracted. Immunoblot analysis using anti-H3ac and anti-H4ac antibodies demonstrated the enrichment of nuclear proteins (Supplementary Fig. S2).

The nuclear extracts were separated and treated either with water or 250 µM GSNO for 20 min in dark. The water-treated samples represent the *in-vivo* S-nitrosylated protein, while the GSNO-treatment results in S-nitrosylation of nearly all putative S-nitrosylation targets present in the nuclear extract. Afterwards, all samples were subjected to the biotin switch assay for biotin-labelling of S-nitrosylated cysteine residues. Control treatments demonstrated the specificity of the biotin switch assay (Supplementary Fig. S3). Biotinylated proteins were visualized by immuno-blotting using monoclonal anti-biotin antibody (Fig. 5a).

In all samples a significant difference in the S-nitrosylation pattern could be observed between GSNO-treated samples and *in-vivo* samples. Regarding the treatment with the avirulent strain at the early time point (2 h) more candidates for S-nitrosylation seems to be present in the cells than in the later time point (13 h). S-Nitrosylated proteins could also be detected in the *Pst* vir samples after GSNO-treatment. However, here three times more protein had been loaded in comparison to the *Pst* avrRpm1 samples (Fig. 5a-left gel).

Biotinylated proteins were purified by affinity chromatography using neutravidin agarose beads, separated by SDS-PAGE and visualized by silver staining (Fig. 5b). According to the results of the silver-stained gel, more S-nitrosylated proteins were purified in the GSNO-

treated samples in comparison to the control samples. These results were consistent with the results of western blot.

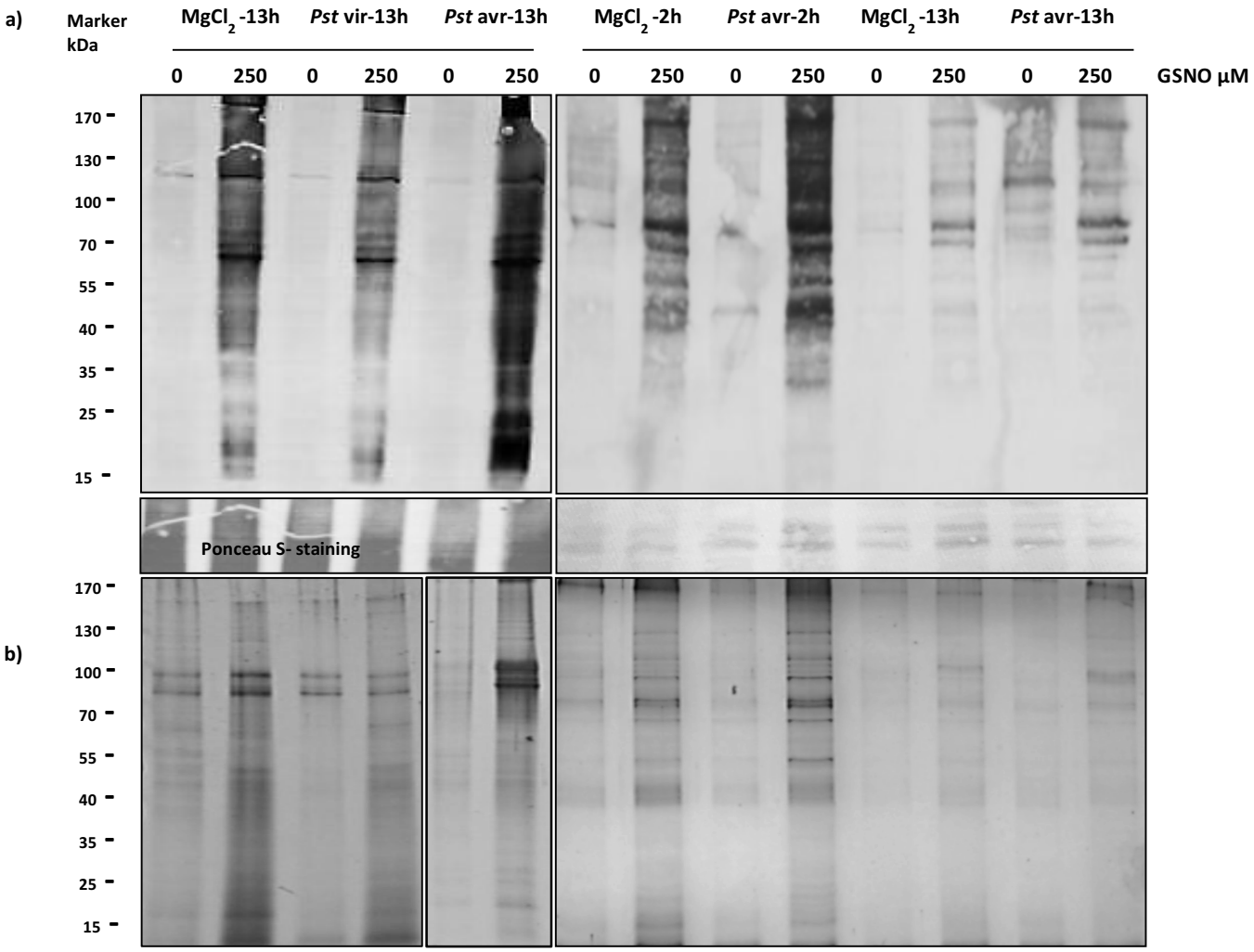

Fig. 5. Detection and purification of S-nitrosylated proteins in pathogen-treated *Arabidopsis* nuclear enriched extracts. *Arabidopsis* cell cultures were treated with 10 mM $MgCl_2$ and *Pst* DC3000 avrRpm1 for 2 h and 13 h and with *Pst* DC3000 vir for 13 h. Extracted proteins from nuclei enriched fractions were treated with either ddH_2O or 250 µM GSNO and subjected to the biotin switch assay. a) Biotinylated proteins were separated with SDS-PAGE and visualized by immunoblotting using anti-biotin antibody. The Ponceau S-stained membrane is shown in the bottom of the figures. b) After immuonoblot detection, the rest of biotinylated samples were purified by neutravidin agarose beads, separated by SDS-PAGE and visualized by silver staining. The relative masses of protein standards are shown on the left. This experiment was repeated 3 times and similar results were achieved. All steps of experiment including bacterial infection, protoplast isolation, nuclear isolation, nuclear protein extraction, biotin switch of nuclear extracts, immunoblot and silver-staining analysis were optimized for 13 h time point (left membrane and gel). The left gels in bottom; besides 2 other - similar - independently produced gels were analyzed by mass spectrometry. Due to some incompatibility problems of mass spectrometry analysis with silver-stained gels, the analysis of those two gels was failed. Afterward, the production of right gel and membrane was performed by Dr. Mounira Chaki (for *Pst* avr-treated cell cultures with 2 time points of infection) using the same procedure except nuclear isolation (methods: 2. 2. 5. 4). Mass spectrometry analysis was then performed on eluted samples instead of silver-stained gels. Here the data from right and left gels (bottom) are analyzed (Table. 1, Table. 2, Fig.6, Fig. 7 and Supplementary Table. S1).

1. 2. 1. Identification of candidate proteins for S-nitrosylation by mass spectrometry

The purified proteins were identified by nano LC-MS/MS analysis performed by the proteome facility of HMGU. All MS/MS spectra were analysed using Mascot software version (Matrix Science). Mascot was installed to search The *Arabidopsis* Information Resource (TAIR) database (www.arabidopsis.org). Scaffold (version Scaffold_2_02_03; Proteome Software) was used to verify MS/MS-based peptide and protein identifications. To get highly significant results, stringent conditions were used for protein identification. Peptide identifications were approved if they could be established at the probability greater than 95.0% as described by the peptide prophet algorithm (Keller et al., 2002). Protein identifications were approved if they could be established at the probability greater than 99.0% and consist of at least two identified unique peptides. In total, 137 proteins were identified (Supplementary Table. S1 and Table. 1).

Table 1. Total number of identified candidates for S-nitrosylation from different treatments. (Collected from the data of 2 different analyzed gels (Fig. 5b)). *Arabidopsis* cell cultures were treated with 10 mM $MgCl_2$ and *Pst* DC3000 avrRpm1 for 2 h and 13 h and with virulent *Pst* DC 3000 for 13 h. Nuclear enriched fractions were treated with either ddH_2O or 250 µM GSNO and subjected to the biotin switch assay. Biotinylated proteins were purified by affinity chromatography using neutravidin agarose. The biotinylated proteins were identified by LC-MS/MS analysis. Peptide identifications were accepted if they could be established at greater than 95.0% probability as specified by the Peptide Prophet algorithm. Protein identifications were accepted if they could be established at greater than 99.0% probability and contained at least two identified peptides.

	$MgCl_2$_2h_H_2O	$MgCl_2$_2h_GSNO	*Pst* avr_2h_H_2O	*Pst* avr_2h_GSNO	$MgCl_2$_13h_H_2O	$MgCl_2$_13h_GSNO	*Pst* avr_13h_H_2O	*Pst* avr_13h_GSNO	*Pst* vir_13h_H_2O	*Pst* vir_13h_GSNO	Common in 2h and 13h of *Pst* avr -GSNO	Common in 13h of *Pst* avr and *Pst vir* -GSNO	All treatments
Total proteins	24	33	22	99	12	18	36	42	0	22	24	6	137
Nuclear proteins	23	30	18	88	11	15	33	39	0	22	22	6	123
Nuclear proteins with cysteines	22	29	17	88	11	14	31	37	0	19	19	6	117

According to the *Arabidopsis* eFP Browser database (http://bar.utoronto.ca/efp/cgi-bin/efpWeb.cgi) 123 (89,78%) of those 137 proteins were described as nuclear proteins and 117 (85.40%) have at least one cysteine residue. In all GSNO-treated samples more S-nitrosylated proteins were identified in comparison to the corresponding *in-vivo* S-nitrosylated samples (water treated samples) (Table. 1). *In-vivo* 22 and 17 S-nitrosylated proteins were identified 2 h after treatment with $MgCl_2$ and *Pst* avrRpm1, respectively. GSNO-treatment boosted the number of S-nitrosylated proteins to 29 ($MgCl_2$) and 88 (*Pst* avrRpm1) proteins. After 13 h, 11 and 37 *in-vivo* S-nitrosylated proteins were identified in $MgCl_2$ and *Pst* avrRpm1-treated samples, respectively (Table. 1). At this time point GSNO-treatment resulted only in a slight increase of S-nitrosylated proteins.

1. 2. 2. Identification of NO-sensitive cysteine residues of nuclear targets of S-nitrosylation by GPS-SNO 1.0 software

For a better perspective of the function of protein S-nitrosylation in plants, identification of the NO-sensitive cysteine residues is necessary. Until now different methods are available to identify/predict NO-sensitive cysteine residues, including computer-based methods and methods related to the biotin switch assay. Both have advantages and disadvantages (Chaki et al., 2014). Here the GPS-SNO 1.0 software (Xue et al., 2010b) (http://sno.biocuckoo.org/) was employed to predict NO-sensitive cysteine residues within the identified S-nitrosylated nuclear proteins. 117 amino acid sequences contain at least one cysteine residue were extracted from the TAIR database. The amino acid sequences with a total of 781 cysteine residues were analyzed with the GPS-SNO 1.0 software using the high threshold. In total, 103 S-nitrosylation sites (13.18% of all Cys residues) were predicted in 64 proteins, which comprise 54.70% of the identified nuclear candidate proteins for S-nitrosylation (Supplementary Table. S2).

S-Nitrosylation consensus sequences are still object of intense discussion and until now several different S-nitrosylation motifs are described in the literature. Analysis of the NO transfer in hemoglobin proteins revealed an acid–base motif comprised of acidic (D,E) and basic (R,H,K) residues flanking the NO-sensitive cysteine residue ([KRHDE]-C-[DE]) (Stamler et al., 1997). Moreover, a GSNO binding consensus sequence has been described containing charged and hydrophobic amino acid residues ([HKR]-C-[hydrophobic]X[DE]) (Hess et al., 2005). Here the Motif-X algorithm (http://motif-x.med.harvard.edu) (Xue et al., 2010b) was employed to deduce a putative consensus sequence in the 155 predicted S-nitrosylation

sites. One apolar motif (.....C...I....) was found (Fig. 6). Motif score was 8.34. Apolar motifs were also found in *Arabidopsis thaliana* cell cultures and plantlets (Fares et al., 2011b, Puyaubert et al., 2014).

Fig. 6. Predicted S-Nitrosylation motif for *Arabidopsis* nuclear S-nitrosylation candidates. 117 amino acid sequences belong to nuclear S-nitrosylation candidate proteins which contained at least one cysteine residue were extracted from the TAIR database. The amino acid sequences with a total of 781 cysteine residues were analyzed with the GPS-SNO 1.0 software using the high threshold. In total, 103 S-nitrosylation sites were predicted in 64 proteins (Supplementary Table. S2). The Motif-X algorithm (http://motif-x.med.harvard.edu) was used to deduce a putative consensus sequence in those 103 predicted S-nitrosylation sites. Motif score was 8.34.

1. 2. 3. Functional classification of *Arabidopsis* S-nitrosylated nuclear proteins

To analyze the functional classification of the S-nitrosylated nuclear proteins, MapMan Ontology of *Arabidopsis thaliana* proteins (http://mapman.gabipd.org/web/guest/mapman) was employed (Fig. 7). The results showed that 38% of S-nitrosylated candidates involved in protein metabolism, 11% in stress response, 10% in RNA metabolism, 9% in cell organization and division, 7% in transport, 5% in nucleotide metabolism and DNA synthesis, 3% in TCA/organic acid transformation, 3% in development, and 8% in other categories, such as photosynthesis, glycolysis, mitochondrial electron transport/ATP synthesis, amino acid metabolism, lipid metabolism, hormone metabolism, redox, miscellaneous, and metal handling (Fig. 7a). A very similar functional classification could be found for the identified *in-vivo* S-nitrosylated nuclear proteins (Fig. 7b). Most of the *in-vivo* S-nitrosylated nuclear proteins are involved in protein metabolism (39%), cell organization (13%), stress (12%), transport (6%), RNA metabolism (6%) and organic acid transformation (6%) (Fig. 7b).

1. 2. 4. Selected *Arabidopsis* S-nitrosylated nuclear proteins

From 117 identified nuclear proteins with cysteine residues, 48 proteins were localized with highest/higher abundance in nucleus in comparison to other organelles using eFP browser database.

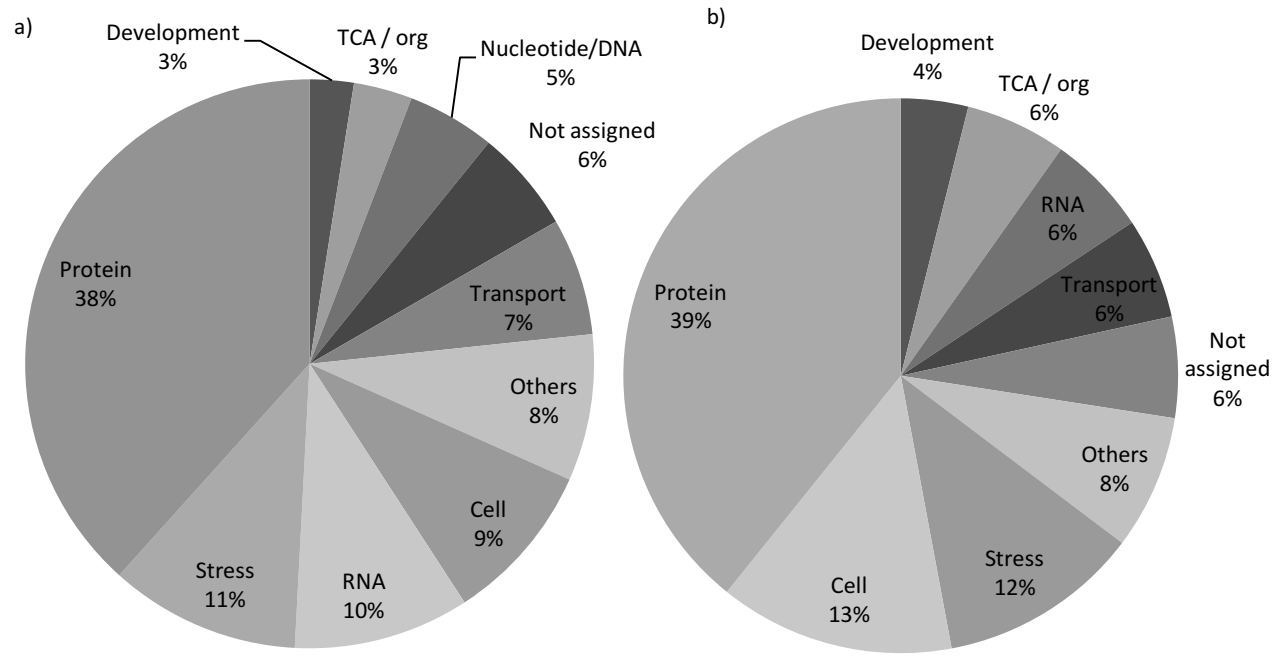

Fig. 7. Functional classification of *Arabidopsis* nuclear S-nitrosylation candidates. *Arabidopsis* cell cultures were treated with avirulent and virulent *Pst* DC3000 for 2 h and 13 h and only 13 h, respectively. Control samples were treated with 10 mM $MgCl_2$. The nuclear extracts were separated and treated either with water or 250 µM GSNO for 20 min in dark. The water-treated samples represent the *in-vivo* S-nitrosylated protein. Biotinylated proteins were purified and identified by LC-MS/MS analysis. Functional classification of a) *Arabidopsis* S-nitrosylated nuclear candidates and b) *in-vivo* S-nitrosylated candidates was performed using MapMan Ontology tool version 3.5.1R2.

Localization of 20 of those 48 proteins in nucleolus is noticeable (Supplementary Table. S1). 30 of those 48 candidate proteins were selected mainly based on to be found in GSNO and/or *Pst* avrRpm1 treated samples (Table. 2). A few proteins were selected according to be identified also in *in-vivo* samples besides the GSNO treated samples. Some interesting candidates were identified including two plant specific histone deacetylases, stress inducible proteins Hop1 and Hop2, core proteins of C/D box ribonucleoprotein complex such as fibrillarin1 and NOP56, a CCCH type zinc finger protein, a DEA(D/H)-box RNA helicase, nuclear transport proteins, translation elongation factors, ribosomal proteins and DNA binding proteins (Table. 2). Some of the selected identified proteins or their closely related relative proteins have been identified in the context of redox regulation in literature (Table. 2).

Table. 2. Selected identified nuclear candidate proteins for S-nitrosylation. *Arabidopsis* cell cultures were treated with 10 mM $MgCl_2$ and *Pst* DC3000 avrRpm1 for 2 h and 13 h and with virulent *Pst* DC 3000 for 13 h. Nuclear enriched fractions were treated with either ddH_2O or 250 µM GSNO and subjected to the biotin switch assay. Biotinylated proteins were purified by affinity chromatography using neutravidin agarose. The biotinylated proteins were identified by LC-MS/MS analysis. Peptide identifications were accepted if they could be established at greater than 95.0% probability as specified by the Peptide Prophet algorithm. Protein identifications were accepted if they could be established at greater than 99.0% probability and contained at least two identified peptides. C; Predicted as a NO-sensitive cysteine residue to S-nitrosylation by GPS-SNO 1.0 software using high threshold condition.

	AGI code	Description	NO-sensitive cysteine residue(s) predicted by GPS-SNO1.0 software	$MgCl_2$-2h-H_2O	$MgCl_2$-2h-GSNO	*Pst* avr_2h_H_2O	*Pst* avr_2h_GSNO	$MgCl_2$-13h-H_2O	$MgCl_2$-13h-GSNO	*Pst* avr_13h_H_2O	*Pst* avr_13h_GSNO	*Pst* vir_13h_H_2O	*Pst* vir_13h_GSNO	Hints to redox regulation
1	AT1G06220.1	Ribosomal protein S5/Elongation factor G/III/V	ADPVVSFCETVVESS				+							
2	AT1G12270.1	Hop1, Stress-inducible protein, putative	EMGKYNECIEDCNKA LLDGVKRCVQQINKA		+		+							
3	AT1G20960.1	Emb1507, U5 small nuclear ribonucleoprotein helicase	KAENILLCAPTGAGK TGSGKTICAEFAILR				+							
4	AT1G24360.1	NAD(P)-binding Rossmann-fold superfamily protein	NLTGVFLCTQAAVKI NINVNVVCPGFIASD	+			+							(Lozano-Juste et al., 2011)
5	AT1G48920.1	ATNUC-L1, Nucleolin like 1					+	+		+				
6	AT1G56110.1	NOP56, Homolog of nucleolar protein NOP56	SLTNLAKCPSSTLQI SIASRIDCFADGATT			+	+			+	+		+	
7	AT1G62740.1	Hop 2, Stress-inducible protein	EMGKYDECIKDCDKA AYSNRAACYTKLGAM LLDGVKRCVQQINKA				+				+			(Hu et al., 2015)
8	AT1G67230.1	Little nuclei1	KVSWFRKCTSKMLKL QQEEGIHCTQATATA				+			+	+			

Table. 2. Continued.

	AGI code	Description	NO-sensitive cysteine residue(s) predicted by GPS-SNO1.0 software	$MgCl_2$-2h-H_2O	$MgCl_2$-2h-GSNO	*Pst* avr_2h_H_2O	*Pst* avr_2h_GSNO	$MgCl_2$-13h-H_2O	$MgCl_2$-13h-GSNO	*Pst* avr_13h_H_2O	*Pst* avr_13h_GSNO	*Pst* vir_13h_H_2O	*Pst* vir_13h_GSNO	Hints to redox regulation
9	AT2G02160.1	CCCH-type zinc finger family protein					+							(Kroncke & Carlberg, 2000b)
10	AT2G19480.1	Nucleosome assembly protein 1;2	AGERPPECKQQ****				+							
11	AT2G33340.1	MOS4-associated complex 3B	*****MNCAISGEVP				+							
12	AT2G39990.1	EIF2, Eukaryotic translation initiation factor 2					+							
13	AT2G40660.1	Nucleic acid-binding, OB-fold-like protein	QMILSALCKHFSLDP				+							(Hu et al., 2015)
14	AT3G01800.1	Ribosome recycling factor					+							
15	AT3G05060.1	NOP56-like pre RNA processing ribonucleoprotein	RKFLKANCQGETLAV			+	+				+		+	
16	AT3G25520.1	ATL5, Ribosomal protein L5			+		+							
17	AT3G58510.1	DEA(D/H)-box RNA helicase family protein					+							(Hu et al., 2015)
18	AT3G60240.2	Eukaryotic translation initiation factor 4G	PQEKDLKCDNRTASD TEKIMHACIQKLLGY EKMKMLSCKQELSSR DENEIGMCMKDMNSP		+		+			+				
19	AT4G16143.1	IMPA-2, Importin alpha isoform 2					+							(Hu et al., 2015)

Table. 2. Continued.

	AGI code	Description	NO-sensitive cysteine residue(s) predicted by GPS-SNO1.0 software	$MgCl_2$-2h-H_2O	$MgCl_2$-2h-GSNO	*Pst* avr_2h_H_2O	*Pst* avr_2h_GSNO	$MgCl_2$-13h-H_2O	$MgCl_2$-13h-GSNO	*Pst* avr_13h_H_2O	*Pst* avr_13h_GSNO	*Pst* vir_13h_H_2O	*Pst* vir_13h_GSNO	Hints to redox regulation
20	AT4G20890.1	Tubulin beta-9 chain	LHIQGGQCGNQIGAK		+		+			+				(Hu et al., 2015)
21	AT4G36020.1	Cold shock domain protein 1	VGHFARDCTQKVAAG				+		+					(Hu et al., 2015)
22	AT5G03740.1	Histone deacetylase 2C											+	(Nott et al., 2008, Cibelli et al., 2002)
23	AT5G20290.1	Ribosomal protein S8e family protein					+							
24	AT5G22650.1	Histone deacetylase 2B					+				+			(Nott et al., 2008, Cibelli et al., 2002)
25	AT5G27640.1	TIF3B1, Translation initiation factor 3B1					+			+			+	
26	AT5G46070.1	Guanylate-binding family protein	FMEADLRCTSTIQRM EKQLRAACHASNANM				+							(Hu et al., 2015)
27	AT5G48650.1	Nuclear transport factor 2					+							
28	AT5G52470.1	FIBRILLARIN 1, SnoRNA binding	VISIKANCIDSTVAA								+		+	
29	AT5G57870.1	MIF4G domain-containing protein	LLGEALQCVEELGLP QAADIEACRNL****				+							(Hu et al., 2015)
30	AT5G67630.1	P-loop containing nucleoside triphosphate hydrolases superfamily protein	AQTKFVQCPEGELQK				+							(Hu et al., 2015)

2. Characterization of S-nitrosylation of *Arabidopsis* HD2 proteins

Two HD2 type HDACs were identified as targets of S-nitrosylation (HD2B and HD2C) (Table. 2 and Supplementary Table. S1). HD2 type HDACs were chosen for further analysis, because HDACs play important role in many different processes in plants including growth, development, reproduction and stress responses. Furthermore, HD2 isoforms were known as plant specific HDACs - however they can be found in other organisms except vertebrates - pointing that they may have plant specific function(s).

Histone acetyltransferases (HATs) catalyse the transfer of an acetyl group to the lysine residues of histone tails. Doing this, they neutralize the positive charge of histone tails and consequently enable the negatively charged chromatin to open up and let transcription factors and RNA polymerases to have access to DNA (Hollender & Liu, 2008). Histone deacetylases oppose the activity of HATs by restoring the positive charge of the lysine residues which explains their transcriptional repression activity (Bannister & Kouzarides, 2011). *Arabidopsis* HD2A, HD2B and HD2C have been demonstrated to mediate transcriptional repression, if they target to the promoter of a reporter gene (Wu et al., 2003, Wu et al., 2000); however, their HDAC activity was not shown experimentally. Moreover, according to a phylogenetic analysis plant HD2 proteins show a considerable diversification; this could accompany by a functional diversity (Pandey et al., 2002). HD2A and HD2C contain a single Cys2His2 type zinc finger domain in the carboxyl terminus, which could enable DNA/RNA-binding activity or mediate protein-protein interactions. HD2B and HD2D do not have a zinc finger domain suggesting that they might function in a different way. It was also known that HD2 type proteins involve in biotic and abiotic responses (Luo et al., 2012b, Sridha & Wu, 2006, Bourque et al., 2011). Therefore, it was interesting to know whether S-nitrosylation affect the function of HD2 isoforms. Since mechanism of function of HD2 isoforms was unclear as well, it had to be investigated in parallel.

2. 1. Sequence alignment and phylogenetic tree of *Arabidopsis* HD2 proteins

Arabidopsis thaliana contain 18 HDACs that based on sequence homology to yeast HDACs are categorized in three types. The type I HDACs are homologous to the yeast RPD3 (reduced potassium deficiency 3) and consist of 12 members that all contain a characteristic histone deacetylase domain and require Zn^{2+} cofactor for deacetylase activity (Liu et al., 2014).

Type I HDACs are categorized into class I (HDA6, HDA7, HDA9 and HDA19), class II (HDA5, HDA15 and HDA18), class III (HDA2 and its two other isoforms) and unclassified (HDA8, HDA10, HDA14 and HDA17). The type II HDACs - which are also called HD-tuins and/or HD2 type HDACs - include HDT1-4 (HD2A-HD2D). They have distinct structure with type I HDACs but sequence similarity to FKBP family peptidyl-prolyl cis-trans isomerases. Type III HDACs show homology to yeast silent information regulator 2 (Sir2) protein including SRT1 and SRT2. Unlike type I and II HDACs, sirtuins are nicotinamide adenine dinucleotide (NAD)-dependent and their activity is not inhibited by common HDAC inhibitors (Hollender & Liu, 2008).

To analyse the relationship within the HD2 type HDACs, a percentage identity matrix of all HD2 isoforms was created using clustalW2 (http://www.ebi.ac.uk/). According clustalW2, HD2 isoforms have variable and rather a low sequence similarity with together (Table. 3).

Table. 3. Percentage identity matrix of amino acid sequence of *Arabidopsis* HD2 proteins. Percentage identity matrix of *Arabidopsis* HD2 isoforms was created by ClustalW2 (http://www.ebi.ac.uk/).

	HD2A	**HD2B**	**HD2C**	**HD2D**
HD2A	100.00	60.25	44.44	36.08
HD2B	60.25	100.00	38.60	34.67
HD2C	44.44	38.60	100.00	34.85
HD2D	36.08	34.67	34.85	100.00

Moreover, the phylogenetic tree of HD2 type HDACs was drawn using phylogeny.fr online tool (http://www.phylogeny.fr/) (Fig. 8). According percentage identity matrix, the highest identity belongs to HD2A and HD2B (62.25 %) and the lowest identity belongs to HD2B and HD2D (34.67%) (Table 3), this is shown in the phylogenetic tree as well (Fig. 8).

Fig. 8. Phylogenetic tree of *Arabidopsis* HD2 proteins. Phylogenetic tree of HD2 isoforms was created using phylogeny.fr online tool (http://www.phylogeny.fr/).

Furthermore, the HD2 type isoforms were aligned using clustalW2 sequence alignment webserver (Fig. 9). According to the alignment result, around 100 aminocids of N-terminus

region of HD2 isoforms are highly conserved. The N-terminal domain composes an invariable pentapeptide (MEFWG) motif. Two conserved residues, a histidine at position 25 and an aspartate at position 75 (glutamate in HD2C) have been considered to be critical for HDAC activity (Dangl et al., 2001). The middle (from around AA120 to AA200) and C-terminus regions (from around AA240 to the C-terminus end) are very less conserved. Those two unconserved regions are separated from each other by a short more conserved region (from around AA200 to AA240). HD2B and HD2C share an acidic region (rich in Aspartate (D) and glutamate (E)) at around AA160 to AA200 (Fig. 9).

```
                10        20        30        40        50        60
HD2D      MEFWGIEIKPGKPFKVIQKDGFMVHASQVTLGDVEKVKKDETFAVYVKIGDDENGFMIGN
HD2C      MEFWGVEVKNGKPLHLDPGLDRLVHISQVALGESK-NNVTEPIQLYVTVGSD--KLLIGT
HD2A      MEFWGIEVKSGKPVTVTPEEGILIHVSQASLGECK-NKKGEFVPLHVKVGNQ--NLVLGT
HD2B      MEFWGVAVTPKNATKVTPEEDSLVHISQASL-DCT-VKSGESVVLSVTVGGA--KLVIGT
          *****: :.  :   :      ::* **.:* :    :  * . : *.:*     :::*.

                70        80        90        100       110       120
HD2D      LS-QKFPQFSIDLYLGHEFEISHNST-SSVYLIGYRTFDAFD----ELDEEIDSDSE---
HD2C      LSHEKFPQLSTEIVLERNFALSHTWKNGSVFFSGYKVDASDPEPEDLIDDQLEAAG----
HD2A      LSTENIPQLFCDLVFDKEFELSHTWGKGSVYFVGYKTPNIEPQGYSEEEEEEEE-VPA-
HD2B      LSQDKFPQISFDLVFDKEFELSHSGTKANVHFIGYKSPNIEQDDFTSSDDEDVPEAVPAP
          ** :::**:  :: : ::* :**.   ..*.: **:            :::

                130       140       150       160       170       180
HD2D      -------------------LDEYMEQQIAALPQNEINPEEDDESDSD-------------
HD2C      ---------------FKAAPKSAAKQVNFQLPNEDVKAKQDDDADGSEEDSSDDDDSENS
HD2A      --------GN----AAKAVAKPKAKPA-------EVKPAVDDEED-E-------------
HD2B      APTAVTANGNAGAAVVKADTKPKAKPA-------EVKPAEEKPES-DEEDESDDEDESEE
                           .   :         :::   :.  . .

                190       200       210       220       230       240
HD2D      -----EMGLDEDDDSSD-------EEDVEAEAPLKVAPPSKKMPNGAFEIAK-GGKK---
HD2C      GDEEEEKVTAESDSEEDDSSDDEEDDSSEEETPKKPEEPKKRSAEPNSSKNPASNKKAKF
HD2A      --SD-SDGMDEDDSDGE-------DSEEEEPTPKKPA-SSKKRANETTPKAPVSAKKAKV
HD2B      DDDS-EKGMDVDEDDSDDDEEEDSEDEEEEETPKKPEPINKKRPNESVSKTPVSGKKAKP
               .     .:.. :       :.. *  :* *    .*:  :        . **

                250       260       270       280       290       300
HD2D      ------------NKSSGG------------------------------KKRCPFPCGPSC
HD2C      -----VTPQKTDSKKPHVHVATPHPSKQAGKNSGGGSTGETSKQQQTPKSAGAFGCK-SC
HD2A      A----VTPQKTDEKKKGGKAANQSP-----------------------KSASQVSCG-SC
HD2B      AAAPASTPQKTEEKKKGGHTATPHPAKKGGKSPVN--------ANQSPKSGGQSSGGNNN
                     .*.                                  *.        .

                310       320
HD2D      KK-------------------------
HD2C      TRTFTSEMGLQSHTKAKHSAAA-----
HD2A      KKTFNSGNALESHNKAKHAAAK-----
HD2B      KKPFNSGKQFGGSNNKGSNKGKGKGRA
            .:
```

Fig. 9. Sequence alignment of *Arabidopsis* HD2 proteins. Sequence alignment of HD2 isoforms was performed using ClustalW2 sequence alignment webserver (http://www.ebi.ac.uk/). The cysteine residues are marked by gray color.

One cysteine residue in N-terminal region of HD2A and HD2B and another 2 cysteine residues of HD2A, HD2C and HD2D in the C-terminal region are conserved (Fig. 9).

2. 2. Cloning wild type HD2 genes (HD2A-HD2D) of *Arabidopsis*

To confirm that the identified HD2 proteins are S-nitrosylated, recombinant proteins of different HD2 isoforms had to be produced. cDNAs of *HD2A*, *HD2B*, and *HD2D* with a coding sequence for TEV cleavage site (GCAGGCTTCGAGAATCTTTATTTTCAGGGC) and of *HD2C* without a TEV cleavage site were amplified using primers designed for Gateway cloning system and cDNA which was synthesized using total RNA extracted from *Arabidopsis* cell cultures. The size of amplified PCR product for each construct was verified by agarose gel electrophoresis. The PCR products were then cloned by Gateway cloning system using pDONR221 and pDEST17 vectors. The presence and order of sequences of all isoforms in donor and destination vectors were verified by enzyme digestion and further sequencing.

2. 3. Production and purification of *Arabidopsis* recombinant HD2 proteins (HD2A-HD2D) in *E. coli*

The pDEST17 vectors (N-terminal 6X histidine-tagged) carrying cDNAs of *HD2A*, *HD2B*, *HD2C* and *HD2D* were transformed into *E. coli* competent cells BL21 (DE3) cc4 for protein production. The *E. coli* competent cells were grown in ZYM-5052 auto inductive medium (Studier 2005) for 4 h at 37°C (until OD_{600} of 1 to 2) and further at 18°C overnight. The bacterial cells were then lysed and the lysate was transferred to a column containing Ni-NTA agarose beads which have high affinity to histidine tag. The beads were washed appropriately for removing non-specific bound proteins and the recombinant proteins were then eluted using elution buffer containing imidazole which binds strongly to Ni-NTA agarose beads.

For performing accurate analyses, the purity of recombinant proteins is critical. To detect the purified proteins and also to check their purity, the eluted recombinant proteins were analysed using coomassie stained SDS-PAGE. The approximate sizes of HD2 isoforms from TAIR database are as follow: HD2A: 26kDa, HD2B: 32kDa, HD2C: 31kDa, and HD2D: 22.5kDa. A big band was detected for first elution fraction of all HD2 isoforms with a size approximately 6kDa bigger than which was expected (after taking the size of His-tag (~1kDa) and TEV cleavage site (~1kDa) to account) and with no non-specific band(s) (Fig. 10a). Since, all isoforms showed a gel shifting in comparison to their calculated molecular weight; therefore the purified recombinant proteins were further analysed by western blot using

anti-histidine antibody. Bands with similar sizes of the ones observed via coomassie stained SDS-PAGE were detected for all corresponding HD2 isoforms (Fig. 10b).

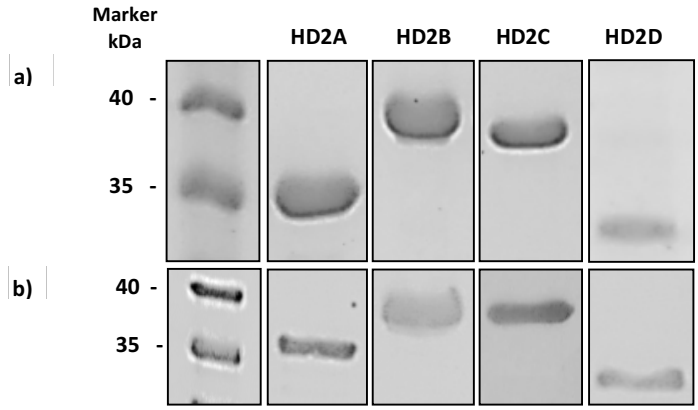

Fig. 10. Analysis of purified recombinant proteins of *Arabidopsis* HD2 proteins. 5 µg of purified 6X his-tagged recombinant proteins were loaded in the SDS-PAGE and the gel was then visualized using a) coomassie blue staining solution or followed by b) immunoblotting using monoclonal anti-polyhistidine primary antibody and anti-mouse IgG-alkaline phosphatase secondary antibody. The relative masses of protein standards are shown on the left.

2. 4. S-Nitrosylation of recombinant HD2 proteins of *Arabidopsis in-vitro*

To demonstrate, if different HD2 isoforms can be indeed S-nitrosylated, the purified recombinant proteins had to be analyzed. Therefore, all four isoforms (HD2A-D) were treated either with ddH_2O, 250 µM GSNO or 1 mM GSH and subjected to the biotin switch assay. S-Nitrosylation was analyzed by immunoblotting using anti-biotin antibodies and could be demonstrated for all four isoforms (Fig. 11).

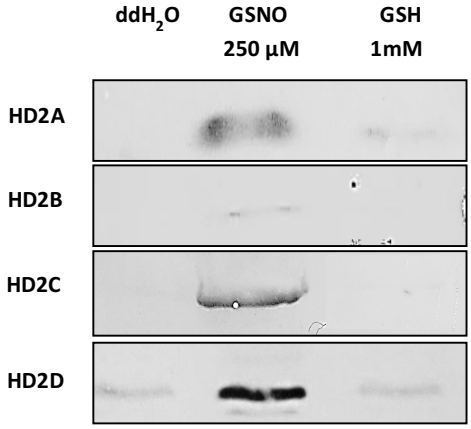

Fig. 11. Immunoblot analysis of S-nitrosylation of recombinant proteins of HD2 isoforms treated with GSNO *in-vitro*. 5 µg of recombinant HD2 proteins were used as the starting material and underwent the biotin switch assay by treating either with ddH_2O, 250 µM GSNO or 1 mM GSH. Biotinylated proteins were visualized by immunoblotting using monoclonal antibiotin alkaline phosphatase antibody.

However, S-nitrosylation of HD2B with GSNO resulted in a very weak signal, the NO-donor SNAP showed a more efficient S-nitrosylation of HD2B (Supplementary Fig. S4). Probably the different S-nitrosylation efficacy of the different NO-donors is due to stereo-chemical and structural differences of the NO-donors, remembering that HD2B contains only one cysteine residue. In the samples treated with 1 mM GSH only a weak protein band was detected, confirming that the results are correlated to S-nitrosylation (Fig. 11). These results could be reproduced with 3 independent biological replicates for all 4 isoforms.

3. Putative physiological function of S-nitrosylated HD2C

Arabidopsis HD2C is involved in plant abiotic responses and tobacco HD2C involves in biotic responses (Sridha & Wu, 2006, Luo et al., 2012b, Bourque et al., 2011); in spite of other HD2 type HDACs of *Arabidopsis* which their role in plant's defense responses has not been demonstrated yet. Therefore, HD2C was chosen for further studies to get deeper insight into its role in plant stress responses specially behalf modification by S-nitrosylation.

3. 1. NO releases zinc ion from recombinant HD2C *in-vitro*

NO can release zinc ion from zinc finger proteins and consequently affect the activity/function of those proteins (Kroncke, 2001, Rodriguez-Munoz et al., 2011, Sanchez-Blazquez et al., 2012, Kroncke et al., 1994). Both HD2A and HD2C contain a Cys2His2 zinc finger domain in which a zinc ion is coordinated with 2 histidine and 2 cysteine residues. Since HD2C only contains 2 cysteine residues belong to its zinc finger domain; seeking for the effect of S-nitrosylation on HD2C, the releasing of zinc ion from the recombinant protein was studied after treating with NO donors.

In a purified sample of a recombinant protein, a portion of the protein molecules might not uptake the metals due to different reasons such as metal deficiency in competent cells' medium. This can lead to an inaccurate and unreproducible experimental result. For solving this problem a protocol from literature was performed in which first the zinc ion is loaded to recombinant protein, then the recombinant protein is washed several times to remove extra zinc ions (Sanchez-Blazquez et al., 2012). Two different zinc indicators (zincon and (4-(2-pyridylazo) resorcinol (PAR)) were tested. Applying zincon was not successful in this work, because it showed low sensitivity to low amounts of released zinc ion from recombinant HD2C, therefore it was replaced by PAR. A similar protocol has been used widely for

measuring zinc ion released from recombinant proteins by PAR (Citiulo et al., 2012, Ravi et al., 2004). PAR binds Zn^{2+} in a 2: 1 complex and consequently its color dramatically changes to orange with strong absorbance at 490 nm. For estimation of amount of released zinc ion, standard curves for HS buffer and HS buffer containing each reagent of experiment were created and were used for corresponding samples. First, zinc ion was loaded to HS buffer and all protein samples at RT for 1 h, then the protein samples were washed 5-7 times using 10kd spin columns until the absorption of their follow through was similar to HS buffer (Supplementary Fig. S5). The protein samples were treated with different concentrations of SNAP, GSNO, GSH and H_2O_2 and incubated for 10 min in darkness at RT (with or without further adding 1 mM DTT for 5 min). PAR was added to the samples and the absorption was detected at 490 nm by tecan reader. The amount of released zinc ion (nanomole) was calculated using corresponding standard curves for before and after treatments. The released zinc ion was calculated in treated samples relative to the untreated corresponding samples (%). The experiment was repeated with 3 biological replicates. Data analysis was performed by anova single factor.

There was a significant difference between SNAP treated and non-treated samples of HD2C. However, there was not a significant difference between SNAP treated and non-treated samples of HS buffer, HD2A (another zinc finger containing protein) and HD2D as a negative control (Fig. 12a). HD2A was partially precipitated due to loading zinc ion; and when it was tested without loading zinc ion it could show releasing of zinc ion after treating with SNAP but the results were not reproducible (data is not shown here). Using cPTIO as an NO scavenger was not possible due to its strong color and consequently its interference with the absorption at 490 nm.

To test whether the zinc releasing effect of S-nitrosylation is reversible, the effect of 2 NO donors (GSNO and SNAP) and also H_2O_2 and GSH was studied on recombinant protein of HD2C with or without adding DTT as a reducing agent. The aim was to test if bounds of -SNO, -SOH or -SSG can be reduced to -SH by DTT. This way, theoretically, newly reproduced free thiols will uptake zinc ion and restore the effect of the applied reagents.

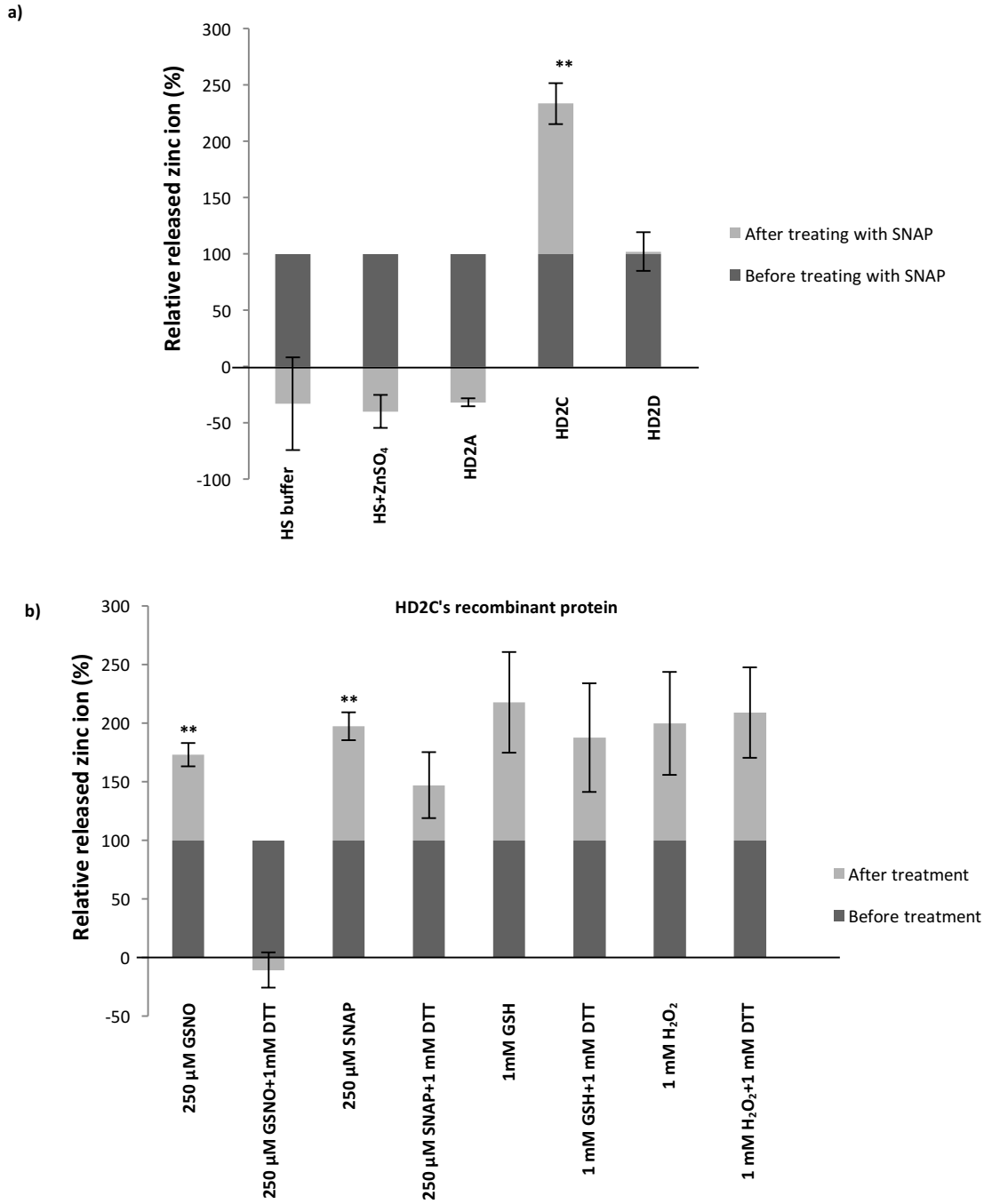

Fig. 12. NO releases zinc ion from recombinant protein of HD2C. 0.1 mM $ZnSO_4$ was loaded to HS buffer and all protein samples at RT for 1 h, then the samples were washed 5-7 times until their follow through was similar to HS buffer. a) The protein samples were treated with 250 µM SNAP and incubated at RT for 10 min in darkness. b) Two sets of protein samples were treated with GSNO, SNAP, GSH or H_2O_2 and incubated at RT for 10 min in darkness. One set of those samples were further treated with DTT at RT for 5 min in darkness. The zinc indicator PAR was added to the samples and the absorption was detected at 490 nm by tecan reader. A standard curve was made using different concentrations of $ZnCl_2$ for HS buffer and HS buffer containing each reagent. The absorption data of the samples were converted to nanomolar values using corresponding standard curve. The released zinc ion was calculated in treated samples relative to the untreated corresponding samples (%). Data are the mean ± SEM of three independent experiments. The data analysis was performed by anova single factor. ** indicates that p-value of treatment is less than 0.01 in comparision to the corresponding untreated samples.

Similar to first experiment (Fig. 12a) the effect of GSNO and SNAP on releasing zinc ion from HD2C was significant (Fig. 12b). Treating with GSH and H_2O_2 also could release zinc ion, but because of their high standard error, their effect was not statistically significant. DTT could restore the effect of GSNO totally and that of SNAP partially. However, DTT could not restore the effect of H_2O_2 and GSH (Fig. 12b). This result indicates the reversibility of S-nitrosylation.

3. 2. Generation of recombinant HD2C proteins with replaced cysteine residue(s) by serine(s)

S-nitrosylation of recombinant HD2C could be demonstrated using biotin switch assay. However, since HD2C contains 2 cysteine residues, to analyze if both are target of S-nitrosylation; HD2C's cysteine mutants were generated. Cysteine residues of HD2C were replaced by serine residues using the QuickChange™ site-directed mutagenesis with some modifications (Zheng et al., 2004). pDONR221-*HD2C* was used as template for site- directed mutagenesis reaction. After amplification, the parental and hemiparental template DNA were digested with DpnI. The amplified plasmids were transformed into *E. coli* DH5α and the mutations were verified by sequencing. The *HD2C* in pDONR221 mutated at base(s) coding cysteine(s) to serine(s) were shifted into pDEST17. The entry and expression vectors carrying the constructs of interest including *HD2C*-C269S, *HD2C*-C272S and *HD2C*-C269/272S were verified by sequencing.

The pDEST17 vectors carrying *HD2C* mutated at base(s) coding cysteine(s) were transformed into *E. coli* competent cells BL21 (DE3) cc4 and grown in ZYM-5052 auto inductive medium (Studier 2005) for 4 h at 37°C (until OD_{600} of 1 to 2) and further at 18°C overnight. The bacterial cells were then lysed and the lysate was added to a column containing Ni-NTA agarose beads. The beads were washed appropriately and the recombinant proteins were eluted. The eluted samples were analysed via coomassie stained SDS-PAGE and immunoblot using anti-histidine antibody. The bands with expected sizes were detected for all mutants in both analyses (Fig. 13). However, 2 non-specific bands with approximate sizes of 25 and 70 kDa were appeared in the samples which were not removable with extra washing steps.

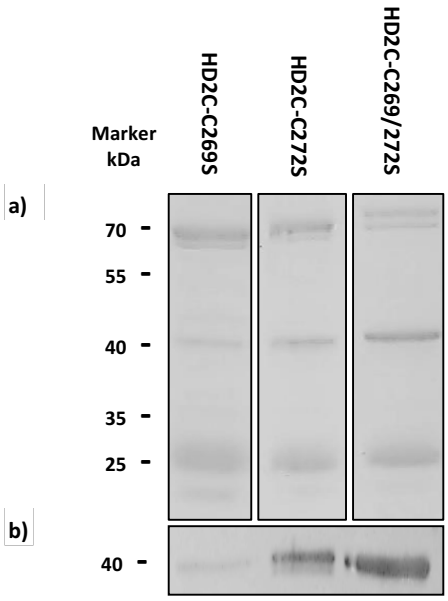

Fig. 13. Analysis of purified recombinant HD2C proteins with replaced cysteine residue(s) by serine(s). 5 µg of purified 6X his-tagged recombinant proteins were loaded in the SDS-PAGE and the gel was then visualized using a) coomassie blue staining solution or followed by b) immunoblot analysis using monoclonal anti-polyhistidine primary antibody and anti-mouse IgG-alkaline phosphatase secondary antibody. The relative masses of protein standards are shown on the left.

3. 2. 1. Cysteine residue 272 of HD2C is a target of S-nitrosylation

To identify the target cysteine residue(s) of HD2C, S-nitrosylation of different HD2C recombinant proteins with replaced cysteine(s) by serine(s) was analyzed. Recombinant proteins were treated with the S-nitrosylating agent SNAP and subjected to the biotin switch assay. By treating with 10 and 100 µM of SNAP, HD2C-C269S showed much stronger bands in compare with HD2C-C272S. Therefore, Cys272 is indeed the target of S-nitrosylation (Fig. 14). HD2C-C269/272S which had no cysteine did not show any band (Fig. 14). This experiment was repeated twice and both experiments could demonstrate similar results.

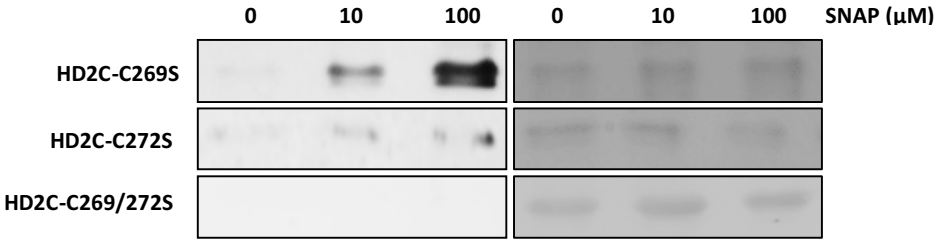

Fig. 14. Immunoblot analysis of S-nitrosylation of recombinant HD2C proteins with replaced cysteine(s) by serine(s) with SNAP *in-vitro*. 5 µg of recombinant protein was used as the starting material for biotin switch assay by treating either with ddH_2O or 10 and 100 µM. The whole sample was loaded in the gel. Biotinylated proteins were visualized by immunoblotting using monoclonal anti-biotin alkaline phosphatase antibody. This experiment was repeated twice and both experiments could demonstrate similar results. The ponceau S-stained membranes are shown in the right.

3. 3. Histone deacetylase activity of recombinant HD2C could not be detected

After confirming the S-nitrosylation of HD2C *in-vitro*, the next step was to characterize the effect of S-nitrosylation on its activity/function. *Arabidopsis* HD2 type proteins are classified as plant specific HDACs; however their HDAC activity has not been shown experimentally, yet. To investigate whether S-nitrosylation affects the known enzymatic activity of HD2C, first one had to show whether it has an HDAC activity. For this aim, EpigenaseTM HDAC Activity/Inhibition Direct Assay Kit (Epigentek, USA) was used which measures the HDAC activity. This experiment was performed by Alexander Mengel. The HDAC activity for recombinant HD2C could not be demonstrated *in-vitro*.

3. 4. Putative function of HD2C as an adopter protein rather than an enzyme (data-based analysis)

HD2 type proteins have been described as plant specific HDACs, however the evidences related to their HDAC activity are indirect. For instance, it was shown that maize HD2 accepted all core histones *in-vitro*, and it was sensitive to deacetylase inhibitors, but a direct enzymatic activity could not be detected (Brosch, Lusser et al. 1996). In *Arabidopsis,* although it has been demonstrated that HD2 family can repress the expression of a reporter gene and may function as a transcription repressor (Wu, Tian et al. 2003), the molecular mechanism of the function of HD2 type proteins is still unclear (Luo, Wang et al. 2012). On the other hand, HD2 isoforms do not contain HDAC domain like type I HDACs (Hollender and Liu 2008), instead they represent the predicted HDAC catalytic residues (a histidine and an aspartic acid residue) which are conserved in their N-terminus region (Wu, Tian et al. 2000). Moreover, HD2A and HD2C contain a C-terminus zinc finger domain which is not exists in *Arabidopsis* type I HDACs (Hollender and Liu 2008). Altogether, it was worthwhile to use different available online tools to predict the activity/function of the main candidate of this work - HD2C. Here, the results from those tools are summarized and suggest that HD2C can be an adopter/interactor protein which may bind to protein, RNA and DNA molecules rather than possesing enzymatic activity.

3. 4. 1. High homology of HD2C with RNA binding and FK506-binding proteins rather than type I HDACs according amino acid sequence alignment and PSI-Blast

Alignment of amino acid sequence of HD2C with that of 12 type I HDAC isoforms of *Arabidopsis* using ClustalW2 webserver (http://www.ebi.ac.uk/) showed that HD2C has the

identity between 11.22% (with HDA6) to 19.73% (with HDA18) with different type I HDACs which is not high. Whereas, the identity of HD2C with HD2A, HD2B and HD2D ar 48.77, 34.70 and 37.00, respectively (Table. 3). However, type I HDACs, themselves show high identity with each other. For instance, *Arabidopsis* HDA6 and HDA19 show identity of 64.02%.

Moreover, predict protein webserver (https://www.predictprotein.org/) was used for PSI-Blast of HD2C. PSI-Blast showed 440 homologous proteins for HD2C from various species. The homologous (440) proteins of HD2C belong to different protein families from various species including uncharacterized proteins (38%), peptidyl-prolyl cis-trans isomerases (27%), FK506-binding nuclear proteins (13%), HD2 type histone deacetylases (8%), RNA binding proteins (5%), LPXTG-domain-containing protein cell wall (1%), genomic scaffold (1%), nucleophosmin (1%) and others (6%). PSI-blast alignment of HD2C did not show any type I HDAC.

3. 4. 2. Prediction of protein-protein interaction, RNA and DNA binding activity for HD2C

Different online tools were used for prediction of activity/function of HD2C. Since, in many cases different tools showed similar results, the results of one online tool for each function is represented here (Fig. 15). HD2C was predicted to contain protein-protein interfaces and RNA binding sites; besides a putative highly disordered structure which fits with those kind of interactions. DNA binding activity also was predicted for HD2C, but with a lower probability (Fig. 15). Protein-protein interaction was predicted using SPPIDER (Porollo & Meller, 2007) (http://sppider.cchmc.org/). RNA binding sites were predicted by pPRINT (Kumar et al., 2008) (http://www.imtech.res.in/raghava/pprint/submit.html). For DNA binding prediction DP-bind was employed (Kuznetsov et al., 2006) (http://lcg.rit.albany.edu/dp-bind/). Prediction of disordered regions was done by PONDR (Romero et al., 2001) (http://www.pondr.com/cgi-bin/PONDR/pondr.cgi). Molecular Recognition Features (MoRFs) was predicted by MoRFpred (Disfani et al., 2012) (http://biomine.ece.ualberta.ca/MoRFpred/).

The residues predicted as protein- protein interaction sites are located in N-terminus and C-terminus regions of protein. Two cysteine residues of HD2C's zinc finger are also predicted as protein interfaces sites. The 'SKK' domain is a linker that can be found in the zinc finger proteins which interact with proteins (Brayer and Segal 2008). Moreover, RNA binding sites

and RNA recognition motifs (Maris, Dominguez et al. 2005) were predicted. DP-bind webserver could identify DNA binding sites for HD2C, however different predictors of DNA-binding sites which are specific for zinc finger proteins such as Zinc Finger Protein-DNA Scoring Form (http://zf.princeton.edu/form.php) and Zif-predict (http://web.iitd.ac.in/~sundar/zifpredict/zifpred_home.html) required a protein with more than one zinc finger for prediction of DNA binding sites.

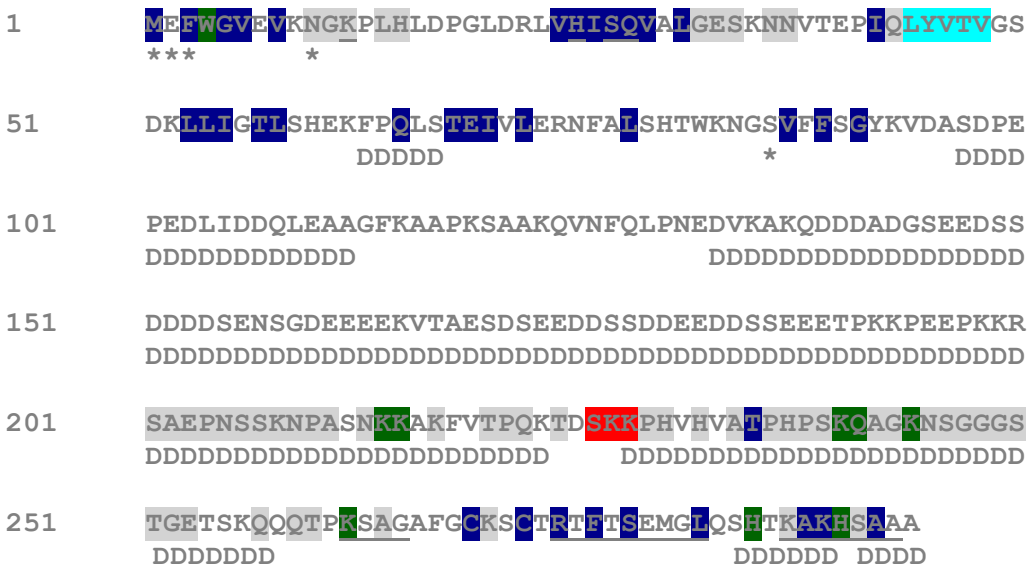

Fig. 15. Prediction of protein-protein interaction, RNA and DNA binding activity for HD2C. Protein-protein interfaces (dark blue), RNA binding sites (gray), DNA binding sites (underlined residues), disordered regions (D) and molecular recognition features (*) were predicted using SPPIDER, pPRINT, DP-bind, PONDR and MoRFpred, respectively. The amino acid residues marked by green are the overlapped regions of protein-protein interaction and RNA binding sites. SKK (red) is a linker which can be found in protein-protein interacting zinc finger proteins (Brayer and Segal 2008). LYVTV (light blue) is an RNA recognition motif (Maris, Dominguez et al. 2005). First line is the residues and the second line is the disordered region predicted by PONDR.

The middle region of HD2C was not predicted as a binding site. Instead, it was predicted as a long disordered region (91 amino acids). Different disordered protein predictors including DisEMBL (Linding, Jensen et al. 2003) (http://dis.embl.de/), FOLDindex (http://bip.weizmann.ac.il/fldbin/findex), Globplot2 (Linding, Russell et al. 2003) (http://globplot.embl.de/cgiDict.py) predict HD2C as a highly disordered structure protein which here only the results from PONDR is shown (Fig. 15). Moreover, according to the prediction from SLIDER webserver (http://biomine-ws.ece.ualberta.ca/SLIDER/index.php) HD2C has a long disorder segment (SLIDER score of 0.9203); the higher the score the more likely a protein has a long (>= 30 AAs) disordered segment. Disordered regions (DRs) are entire proteins or regions of proteins which lack a fixed tertiary structure and are partially or

fully unfolded. Such disordered regions are involved in a variety of functions, including DNA recognition, modulation of specificity/affinity of protein binding and control of protein half-life. Additionally, first 3 amino acid residues of HD2C are predicted as molecular recognition features (MoRFs) (Fig. 15); which are highly conserved in HD2 proteins (Fig. 9). MoRFs are short binding regions bind to protein partners via disorder-to-order transitions.

3. 4. 3. Identifying various non-enzymatic domains for HD2C using MOTIF search

To find out the motifs of HD2C, MOTIF search (http://www.genome.jp/tools/motif/) was employed. MOTIF search found 11 Pfam motifs for middle and C-terminus regions of HD2C including: YL1 nuclear protein, Nop14-like family, zinc finger, C2H2 type, SDA1, zinc-finger double-stranded RNA-binding, transcription initiation factor IIF, alpha subunit (TFIIF-alpha), Vta1 like, Mpp10 protein and CDC45-like protein motifs (Fig. 16). However, according MOTIF search all 12 HDAC isoforms of *Arabidopsis* contain only an HDAC motif except HDA18 which contains a CCDC92 motif as well. Middle region of HD2C is also predicted as a highly disordered region by PONDR (Fig. 15 and Fig. 16).

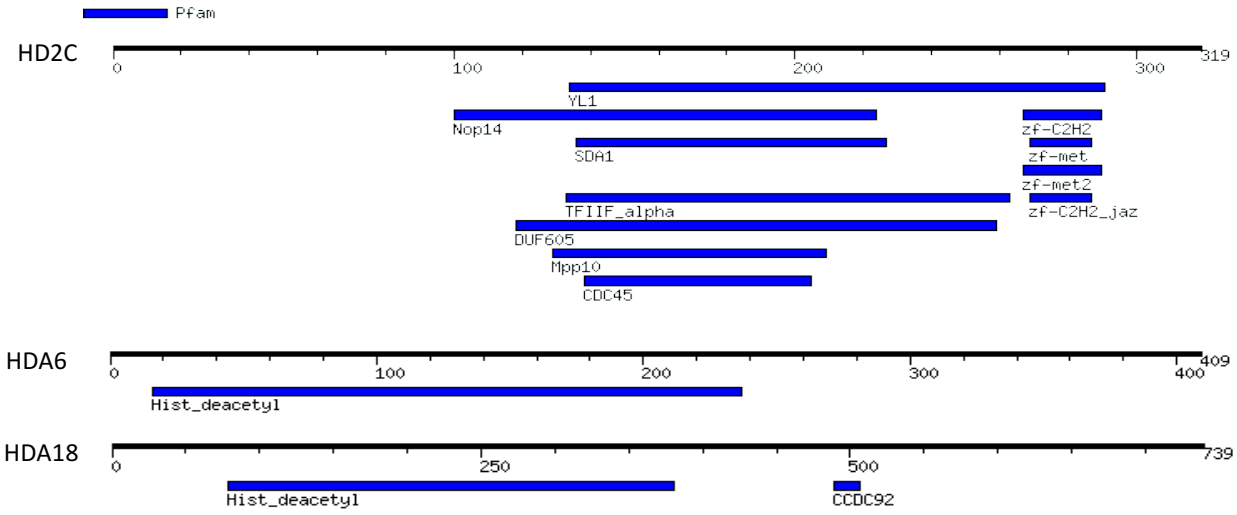

Fig. 16. Motif analysis of HD2C protein. Motif analysis was performed by MOTIF search (http://www.genome.jp/tools/motif/). MOTIF search found 11 Pfam motifs for HD2C including: YL1 nuclear protein (PF05764), Nop14-like family (PF04147), zf-C2H2 Zinc finger C2H2 type (PF00096), SDA1 (PF05285), zf-met Zinc-finger of C2H2 type (PF12874), zf-met2 Zinc-binding (PF12907), zf-C2H2_jaz zinc-finger double-stranded RNA-binding (PF12171), TFIIF_alpha, transcription initiation factor IIF, alpha subunit (PF05793), Vta1 like (PF04652), Mpp10 protein (PF04006) and CDC45-like protein (PF02724). MOTIF search found only 1 Pfam (Hist_deacetyl:, Histone deacetylase domain (PF00850)) for HDA2, HDA5, HDA6, HDA7, HDA8, HDA9, HDA14, HDA15, HDA17 and HDA19. HDA6 is shown as an example of type I HDACs. For HDA18, another PFam motif was found as well (CCDC92, Coiled-coil domain of unknown function (PF14916)). No Pfam was found for HDA10.

3. 4. 4. Co-expression of HD2C with co-chaperones, FK506 binding and heat shock proteins according databased protein expression tools

To estimate gene functions, ATTED II (Obayashi, Hayashi et al. 2009) (http://atted.jp) and GENEVESTIGATOR (https://genevestigator.com/gv/user/userProfile.jsp) were employed; those data-based tools provide co-regulated gene relationships. Using ATTED II, a RAN binding protein, 5 heat shock proteins, a glutathione S-transferase family protein, 3 chaperone proteins, 2 FK506 binding proteins, a SGS domain-containing protein, gametophytic factor 2, a Tetratricopeptide repeat (TPR)-like superfamily protein and an ankyrin repeat family protein were found as co-expressed gene network of HD2C. Important co-expressed proteins of HD2C using GENEVESTIGATOR were HD2A, HD2D and some other proteins such as a pentatricopeptide repeat protein and a transducin/WD40 repeat like superfamily protein. According ATTED II and GENEVESTIGATOR, no type I HDAC has been identified in co-expression network of HD2C, up to now.

3. 5. Detection of putative interaction partners for HD2C using Co-Immunoprecipitation (Co-IP)

According to the bioinformatics characterization, the protein-protein interaction was the most promising predicted function for HD2C (Fig. 15). C2H2 zinc finger domains are originally identified as DNA binding domains, however some C2H2 zinc fingers also facilitate protein-protein interactions and RNA binding. More than 100 C2H2 zinc finger protein-protein interactions have been identified (Brayer, Kulshreshtha et al. 2008). Moreover, C-terminal zinc fingers (like in HD2C) are involved in protein-protein interactions, rather than DNA binding (McCarty, Kleiger et al. 2003). Additionally HD2C contains a 'SKK' linker (Fig. 15) which could be found in some zinc finger proteins which interact with proteins; while it lacks 'TGEKP' linker which is common in around 50% of DNA binding zinc finger proteins (Brayer and Segal 2008). Therefore, first the protein-protein interaction of HD2C was studied.

3. 5. 1. Genotyping *hd2c* mutant (T-DNA insertion line *hd2c-1*)

HD2C T-DNA insertion line *hd2c-1* (Salk_129799.19.60) was used as negative control of Co-IP experiment; for this purpose a homozygous line was needed. To verify the homozygous mutants, a PCR-based genotyping was performed using specific primers (LBa1 of pBIN-pROK2 for SALK lines (T-DNA left border primer), HD2C-LP (left border primer) and HD2C-RP (right border primer)) from the website of SIGnal Salk Institute Genomic Analysis Laboratory

(http://signal.salk.edu/cgi-bin/tdnaexpress) and Extract-N-AmpTM plant PCR kit (sigma, Germany) following the manufacturer's instructions. Since T-DNA is inserted in the middle of genomic DNA of HD2C, according to information from Salk website by using the three primers (LBa1+LP+RP) for Salk_129799.19.60 line, WT (no insertion) should yield a product of about 900-1100 bps (from LP to RP), homozygous lines (insertions in both chromosomes) should produce a DNA fragment of 410+N bps (from RP to insertion site 300+N bases), and heterozygous lines (one of the pair chromosomes with insertion) should yield both PCR products (http://signal.salk.edu/cgi-bin/tdnaexpress). The lines which could amplify a PCR product with approximate size of 800 bp using LB+RP primers and no fragment using LP+RP primers were considered to be homozygous. In WT samples, only LP+RP primers could amplify a PCR product with an approximate size of 1050 bp (Supplementary Fig. S6). After genotyping, the homozygous line was grown for seed production and its seeds were used for Co-IP experiment and also for the entire project.

3. 5. 2. Quantity and quality analysis of antibody to HD2C

The antibody specific for *Arabidopsis* HD2C was purchased from Agrisera, Sweden (AS11 1753) which was its only commercially available antibody. First, it was necessary to know about the sensitivity of the antibody. For this aim, different dilutions (1:200, 1:500, 1:1000, 1:2000 and 1: 5000) of antibody were used to detect different amounts of recombinant HD2C via dot blot analysis. The antibody recognized up to 5 ng of recombinant HD2C protein (Fig. 17). This result showed that the antibody is sensitive enough for a Co-IP experiment.

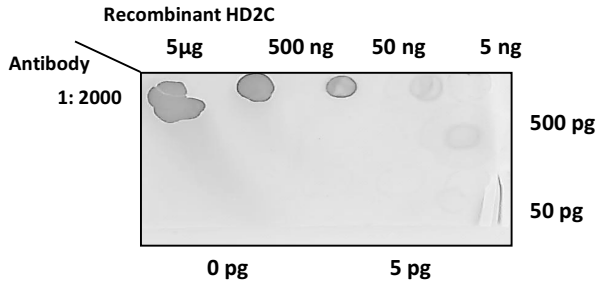

Fig. 17. Dot blot quantification analysis of specific antibody to HD2C. Different amounts of recombinant protein of HD2C were underwent a dot blot analysis using different concentrations of primary antibody to HD2C and anti-rabbit IgG–alkaline phosphatase secondary antibody.

For Co-IP experiment large amounts of plant material was needed and since the stage before floral transition is one of the production peaks of HD2C according GENEVESTIGATOR (databased protein expression tool) (Supplementary Table. S7); therefore 4 weeks old plants

grown in long day light condition were used for nuclear protein extraction in whole experiment. The nuclear protein was extracted from 2 g of starting material of WT and *hd2c-1* line (300 µl), concentrated using the 10kd spin columns to 25 µl and loaded then on the gel and further analyzed by immuonoblott using antibody to HD2C. To precise test of the specificity of the antibody, the recombinant proteins of HD2C and HD2A were also loaded on the gel as positive and negative controls, respectively. Antibody to HD2C was able to detect HD2C in nuclear enriched fraction of 4 weeks old WT plants but not in *hd2c-1* line (Fig. 18). The antibody was very specific, since it did not detect any non-specific band in WT and not in *hd2c-1* nuclear enriched fractions. Moreover, the antibody detected the recombinant protein of HD2C, but not HD2A –very close relative HD2 type protein (Fig. 18).

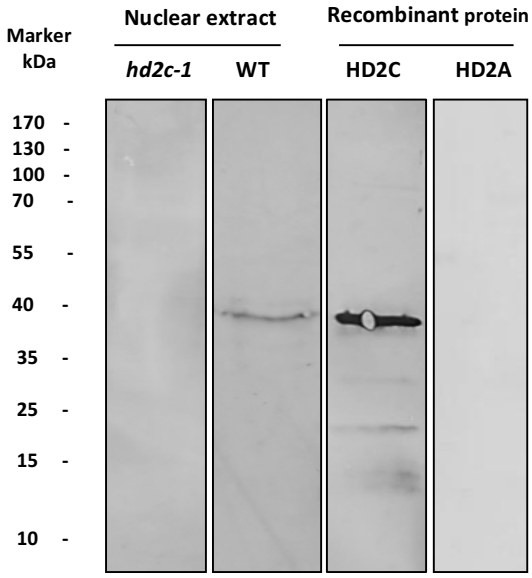

Fig. 18. Specificity analysis of antibody to HD2C. The nuclei of 2 g of 4 weeks old WT and *hd2c-1* plants were isolated and lysed. The nuclear protein samples (300 µl) were concentrated to 25 µl and afterward were separated by SDS-PAGE and further immunoblotted using primary antibody to HD2C and anti-rabbit IgG–alkaline phosphatase secondary antibody. Recombinant proteins of HD2C and HD2A were used as positive and negative controls, respectively. The relative masses of protein standards are shown on the left.

3. 5. 3. Optimization of nuclear protein extraction and IP

Since, there was no information about how stable are the probable protein-protein interaction bounds, an amine reactive cross linker Dithiobis [succinimidyl propionate (DSP) was used before IP to be able to capture the interaction partners. For this aim, 2 g of plant material of WT and *hd2c-1* line were used for nuclei isolation with and without cross-linking and the nuclear proteins were then extracted. The nuclear lysates were incubated with protein A dynabeads and antibody to HD2C and the eluted samples were further analyzed

via western blot. Using cross linker (DSP) was not successful, because pull down of HD2C was not possible in DSP treated samples (Fig. 19). However, HD2C could be pull down after IP in WT samples which were not treated with DSP and not in *hd2c-1* samples (Fig. 19). So, the Co-IP was performed without any cross-linking.

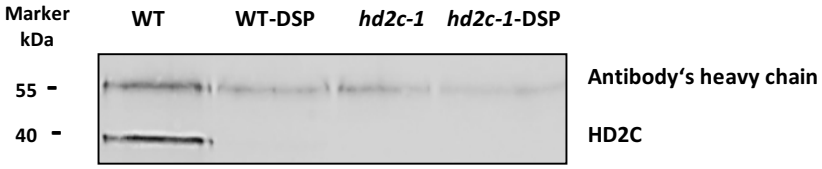

Fig. 19. Immunoblot analysis of pull-down of HD2C from WT and *hd2c-1* line after Co-IP. Co-IP was performed using 2 g of 4 weeks old WT and *hd2c-1* line. The nuclei were isolated with and without adding DSP cross linker. The nuclei enriched fractions were lysed. The nuclear lysates were incubated with Dynabeads and antibody to HD2C. The eluted sample was immunoblotted using primary antibody to HD2C and anti-rabbit IgG–alkaline phosphatase secondary antibody. The relative masses of protein standards are shown on the left.

For a Co-IP experiment, nuclear isolation and nuclear protein extraction are crucial steps; since, protein-protein bounds can be quite unstable and break with harsh detergents and sonications. On the other hand, the background proteins which are pulled down non-specifically are the big challenge of Co-IPs. To optimize the Co-IP, basically, a published protocol (Fiil et al., 2008) was combined with a protocol of a commercial Dynabeads® Co-Immunoprecipitation Kit (life technologies 14321D) with some modifications which has been mentioned in detail in methods section. In summary, for nuclei isolation buffers (I, II, and III) low concentration of detergents were used to avoid from losing putative interaction partners. And for nuclear lysis buffers, 3 different ones including NLBA, NLBB and NLBC (the IP buffer from the kit) were tested. 2 sonication tips (5mm and 2mm) were tested and the 2mm tip which made more smooth sonication without foaming and protein degradation was chosen for breaking nuclear membranes. Afterward, the quality of nuclear protein extracts was checked by coomassie stained SDS-PAGE gel, it had to show single clear bands instead of a smear of proteins (Supplementary Fig. S8). For nuclear protein extraction, different nuclear lysis buffers showed no detectable difference; however, since the same nuclear lysis buffers were then used as IP buffers and washing buffers, the compatibility of IP with different nuclear lysis buffers was further tested.

For optimizing IP, 3 different beads were tested including I) protein A agarose beads and II) protein A Dyanabeads which by using both, antibody binds to the protein A and III)

dynabeads from the Dynabeads® Co-Immunoprecipitation Kit in which antibody directly binds to the beads. The later beads make it possible to elute the bait protein and its partner(s) without eluting the heavy and light chains of antibody, however using them need more amount of antibody. Nuclear lysates were incubated with different beads according their protocol which is mentioned in methods section; the beads were then washed and the bait protein and probable partner proteins were eluted and analyzed by silver stained SDS-PAGE. The experiment was started with 2 g of plant material; this amount of plant material was enough to detect the pulling down of HD2C via western blot (Fig. 19); while it was not enough to observe visible bands of HD2C and its putative partner proteins via silver-stained SDS-PAGE. Therefore, the amount of starting material was increased to 10 g for the rest of experiment. Since, protein A agarose beads made a high background in both WT and *hd2c-1* samples, the experiment was not further continued with them (Fig. 20a). Using NLBA also did not lead to a successful pull down of putative interactors of HD2C, then it was not used anymore (Fig. 20a and Fig. 20c1). Protein A Dynabeads showed lower background in compare with protein A agarose beads and since using them needed low amount of antibody in compare with dynabeads from the kit, then they were used for optimizing nuclear lysis buffer/IP buffer/washing buffer. A nuclear lysis buffer from literature which was compatible with Co-IP experiments (NLBB) was compared with IP buffer from the kit (NLBC) and its modified version (NLBD). The results showed almost no difference between NLBB and NLBC; while NLBD could pull down more interacting proteins with lower level of protein degradation (Fig. 20b3). However, the disadvantage of protein A agarose beads was the eluting high amounts of heavy and light chains of antibody which covered the probable partner proteins on the gel; to solve this problem Dynabeads from the kit were used with a small modification in nuclear lysis buffer (NLBE) which lead to the best result with the lowest background bands, no protein degradation and highest number of putative partner proteins in WT samples (Fig. 20c2). The silver-stained gel showed a band with the same size of HD2C detected by western blot and several other bands for WT but almost no visible band for *hd2c-1* line except light and heavy chains of antibody, indicating a successful Co-IP (Fig. 20c2).

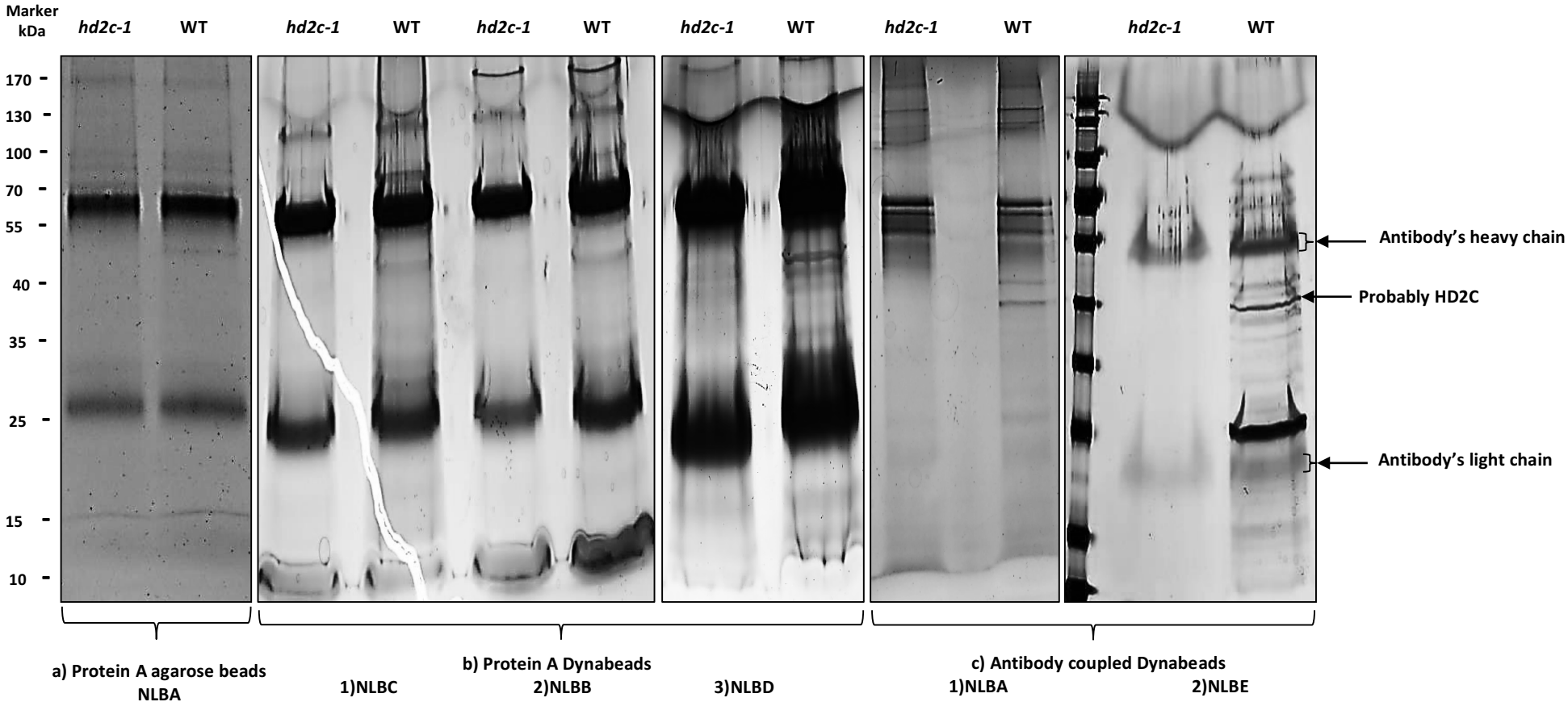

Fig. 20. Silver-stained SDS-PAGE analysis of Co-IP eluates of WT and *hd2c-1* line. Co-IP was performed by 10 g of 4 weeks old WT and *hd2c-1* line. The nuclei enriched fractions were resuspended in nuclear lysis buffer (NLBA or NLBB or NLBC or NLBD or NLBE), sonicated and centrifuged. The lysates were incubated with (a) protein A agarose beads or (b) protein A Dyanabeads or (c) Dynabeads from the Dynabeads® Co-Immunoprecipitation Kit. The beads were washed and the bait and putative partner protein(s) were eluted with elution buffer and analyzed by silver-stained SDS-PAGE. The relative masses of protein standards are shown on the left.

The experiment was repeated 3 times independently and similar pattern of bands was achieved. Since the elution buffer from the kit was not compatible with the mass spectrometry analysis, the experiment was performed with 3 other biological replicates and the samples were eluted using 2X SDS PAGE reducing loading buffer.

3. 5. 4. Identification of putative partner proteins of HD2C by mass spectrometry

The eluates were analyzed by nano LC-MS/MS analysis and quantification analysis was performed by the proteome facility of HMGU (Dr. Christine Von Toerne). Afterward the analysis of proteins to find the most promising putative partner proteins of HD2C was performed. 324 of identified proteins demonstrated the confidence score more than 30 which was used as the confidence threshold of the analysis. 156 of those 324 proteins were identified in 3 replicates. And 90 of those 156 proteins including HD2C itself, were identified with higher abundance in WT samples in compare with *hd2c-1* line in 3 replicates. From those 90 proteins, all the proteins which showed any spectral count (spectral count is the total number of spectra identified for a protein, has achieved acceptance as a practical, label-free, semiquantitative measure of protein abundance) (Lundgren et al., 2010) in *hd2c-1* samples were eliminated, then 55 putative partner proteins were remained (Supplementary Table. S3).

3. 5. 5. Analysis of putative partner proteins of HD2C by *Arabidopsis* interactions viewer

To get more knowledge about the protein-protein interaction of identified candidate partner proteins (Supplementary Table. S3), those 55 proteins were analyzed by *Arabidopsis* Interactions Viewer (http://bar.utoronto.ca/interactions/cgi-bin/arabidopsis_interactions_viewer.cgi) which is a database of known and predicted protein interactions. Using the options of only published data sets, mapman analysis and query interaction from STRING, BioGrid, IntAct and Bar, the interaction network of the proteins was created by *Arabidopsis* Interactions Viewer (Fig. 21). In the represented network, NUP50 (At1g52380)-it was not identified in Co-IP list- is the protein which interacts with both HD2C and ribosomal protein L1p/L10e (AT3G63490) and this way it connects HD2C with a complex of proteins mainly localized in nucleus, plastid and plasma membrane with different functions including more in RNA and protein metabolism (Fig. 21).

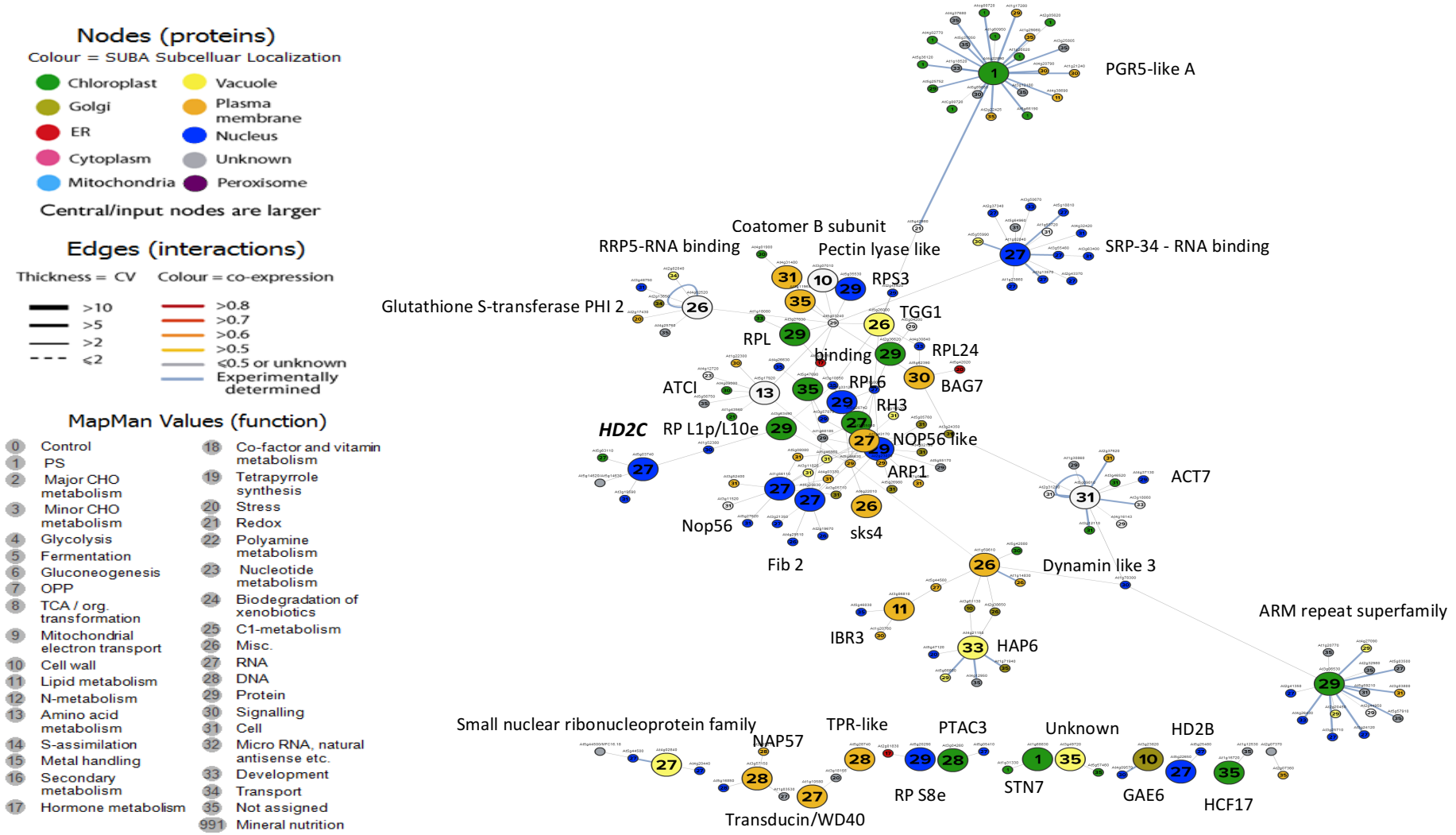

Fig. 21. Interaction network analysis of 54 putative partner proteins of HD2C using *Arabidopsis* interactions viewer. HD2C and its 54 putative partner proteins (Supplementary Table. S3) were analyzed by *Arabidopsis* Interactions Viewer using the options of only published data sets, mapman analysis and query interactions from STRING, BioGrid, IntAct and Bar and the interaction network was then created. Only the big nodes are the input proteins and their name is mentioned. The colors and numbers are correlated with subcellular localization and mapman values, respectively (left side). HD2C is shown in ***bold.***

3. 5. 6. Significantly high enriched putative partners of HD2C are involved in RNA methylation

To find the most promising candidate partners, a variation analysis among aboundance of replicates of WT and replicates of *hd2c-1* besides a t-test between WT and *hd2c-1* were performed for HD2C and its 54 putative partner proteins. The proteins were then arranged by variation among WT replicates from smallest to largest (Supplementary Table. S3). Afterward, the proteins with t-test value ≥ 0.05 were marked red, this way the proteins with WT variation ≥ 0.4 were marked red as well (Lowest fidelity). Then the proteins with variation ≥ 1 among *hd2c-1* replicates and/or identified unique peptides (A unique peptide is a peptide that exists only in one protein of a proteome of interest, even though if this peptide may appear more than once in the same protein (Zhao & Lin, 2010)) less than 2 in any replicate were marked orange (medium fidelity). The 7 un-colored remained proteins have the highest fidelity of being partner proteins of HD2C (Supplementary Table. S3, Table. 4).

Regarding abundance and spectral count, SKU5 similar 4 (sks4), HD2B and DEAD box RNA helicase (RH3) were the best candidates, since their mean normalized abundance in WT samples were only around 5 – 12 times less than that of HD2C. According maximum fold change (describing how much normalized abundance quantity changes) in WT in compare to *hd2c-1* samples which was statistically significant, the best candidates were fibrillarin 2, NOP56-like pre RNA processing ribonucleoprotein, and tetratricopeptide repeat (TPR)-like superfamily protein (AT5G28740.1) (Supplementary Table. S3).

Four best proteins which could have all criteria of high abundance, spectral count, maximum fold change (WT in compare to hd2c-1 samples) and statistically significant fold change were SKU5 similar 4, fibrillarin 2, NOP56-like pre RNA processing ribonucleoprotein and NOP56. SKU5 similar 4, fibrillarin 2, NOP56-like pre RNA processing ribonucleoprotein and NOP56 could be enriched in WT samples approximately 7, 15, 27 and 22 (mean maximum fold change of 3 replicates) folds in compare with *hd2c-1* samples, respectively. However, mean normalized abundance of SKU5 similar 4, fibrillarin 2, NOP56-like pre RNA processing ribonucleoprotein and NOP56 in WT samples were approximately 5.8, 25.3, 43 and 35 times less than that of HD2C, respectively. Three later proteins are core proteins of C/D box snoRNP complex that are localized in nucleolus similar to HD2C and involve in RNA methylation (Table. 4).

Table. 4. **Significantly high enriched putative partner proteins of HD2C identified by Co-IP.** Nuclear protein fractions were extracted from 10 g of 4 weeks old *Arabidopsis* WT and *hd2c-1* line. The nuclear lysates were incubated with the Dynabeads from the Dynabeads® Co-Immunoprecipitation Kit which had already been bound to the antibody to HD2C. The eluted samples were analyzed by mass spectrometry. 324 of identified proteins demonstrated the confidence score more than 30 (the confidence threshold of the analysis). 90 of proteins were identified with higher abundance in WT in compare with *hd2c-1* samples in 3 biological replicates. 55 of those 90 proteins, showed no spectral count in *hd2c-1* samples. A variation analysis among abundance of replicates of WT and *hd2c-1* samples besides a t-test was performed for the remained 55 proteins. The proteins were then arranged by variation in WT samples from smallest to largest. The proteins with p-value less than 0.05, WT variations less than 0.4, *hd2c-1* variation less than 1 and identified unique peptides more than 2 in any replicate are represented here. MW: molecular weight, N: Nucleus, N^N: Nucleolus, C: Cytosol, Cy: cytoskeleton, ER: Endoplasmic reticulum, E: Extracellular, G: Golgi, PM: Plasma membrane, P: Plastid, Pe: peroxisome, V: Vacuole and M: mitochondrion. Bold letters shows the highest localization of protein in the corresponding organelle.

	AGI code	Description	MW kDa	Localization (eFB browser)	Biological processes involved in (Tair database)
	AT5G03740.1	HD2C, Histone deacetylase 2C	31.83	C, ER, E, G, **N^N**	RNA methylation, chromatin modification, cullin deneddylation, negative regulation of transcription, DNA-templated, photomorphogenesis, response to abscisic acid, response to salt stress, response to water deprivation and transcription
1	AT4G22010.1	sks4, SKU5 similar 4	60.45	ER, E, G, M, PM, V	Anther development, anthocyanin accumulation in tissues in response to UV light, cell tip growth, cell wall organization, multidimensional cell growth, oxidation-reduction process, polysaccharide biosynthetic process, regulation of hormone levels, regulation of meristem growth, root hair elongation and sterol biosynthetic process
2	AT4G25630.1	FIB2, Fibrillarin 2	33.65	C, **N^N**, PM, P	RNA methylation, purine and pyrimidine ribonucleotide biosynthetic process and rRNA processing
3	AT3G05060.1	NOP56-like pre RNA processing ribonucleoprotein	59.00	C, ER, E, G, **N^N**, PM	RNA methylation, purine and pyrimidine ribonucleotide biosynthetic process and ribosome biogenesis
4	AT1G56110.1	NOP56, homolog of nucleolar protein	58.67	C, M, **N^N**, PM,P	RNA methylation, pyrimidine ribonucleotide biosynthetic process
	AT5G63420.1	emb2746, RNA-metabolising metallo-beta-lactamase family protein	100.55	C, M, N, PM, **P**	Auxin transport, chloroplast organization, embryo development ending in seed dormancy, longitudinal axis specification, metabolic process
6	AT5G26742.1	DEAD box RNA helicase (RH3)	81.15	C, M, **N**, PM,P	RNA secondary structure unwinding, embryo development ending in seed dormancy
7	AT5G28740.1	Tetratricopeptide repeat (TPR)-like	107.05	C, M, **N**, P	Generation of catalytic spliceosome for first transesterification step

To verify the interaction of putative partner proteins with HD2C via *in-vitro* pull-down, N-terminal 6X histidine-tagged NOP56 and NOP56-like protein and N-terminal GST-tagged HD2C were cloned by Gateway cloning system using pDONR221 and pDEST17 and pDEST15 vectors. The destination vectors carrying constructs of interest were transformed into *E. coli* competent cells BL21 (DE3) cc4 for protein production. The *E. coli* competent cells were grown in ZYM-5052 auto inductive medium (Studier 2005) for 4 h at 37°C (until OD_{600} of 1 to 2) and further at 18°C overnight. The bacterial cells were then lysed and the recombinant proteins were purified using Ni-NTA agarose beads and GST sepharose beads. Production and purification of recombinant proteins were verified by immunoblot analysis (Supplementary Fig. S9). The pull down assay remained to be performed.

3. 6. Generation of complement lines in *hd2c-1* mutant background consisting of endogenous promoter and genomic DNA of *HD2C* mutated at bases coding cysteine(s)

In-vitro, it was shown that the cysteine 272 of HD2C is a target of S- nitrosylation (Fig. 14). To discover the physiological role of S-nitrosylation of individual cysteine residues *in-vivo* and at the same time to confirm the *in-vitro* result; the complement transformed lines using endogenous promoter and genomic DNA of *HD2C* mutated at bases coding cysteine(s) were generated in T-DNA insertion line *hd2c-1* (Salk_129799.19.60) background. Endogenous promoter and genomic DNA of *HD2C* were used to mimic natural production of protein with exception in the replaced cysteine residue(s) by histidine(s). The *hd2c-1* plants have already been genotyped (Supplementary Fig. S6) and homozygous lines were used for complementation. The endogenous promoter and genomic DNA of *HD2C* were amplified using appropriate primers to Gateway cloning system via touchdown PCR. The PCR products with expected sizes were amplified.

For site directed mutagenesis, histidine was chosen to be replaced by cysteine residues, because Cys269 and Cys272 of HD2C together with two histidines coordinate a zinc ion and fold as a natural zinc finger domain (C2H2 type). By replacing cysteine(s) to histidine(s), it is still possible that some unnatural zinc fingers to be produced (Negi et al., 2004), this way one could analyze the change(s) which are happening exactly because of the replacing of an aminoacid to another one without a conformational change of the protein (Fig. 22). Whereas, by replacing cysteine(s) to serine(s), formation of zinc finger domain is not possible.

```
                                                  266                       294
HD2C's natural zinc finger: C2H2 type:            AFGCKSCTRTFTSEMGLGSHTKAKHSAAA
HD2C-C269H: unnatural zinc finger: CH3 type:        H C             H     H
HD2C-C272H: unnatural zinc finger: CH3 type:        C H             H     H
HD2C-C269/272H Unnatural zinc finger: H4 type:      H H             H     H
```

Fig. 22. Comparison of natural zinc finger of HD2C with unnatural zinc fingers which might be produced by site directed mutagenesis. Marked in blue are replaced cysteine residues by histidine.

Cysteine residues of HD2C were replaced by histidine residues using the QuickChange™ site-directed mutagenesis with some modifications (Zheng et al., 2004). pDONR221- *HD2C* (genomic DNA) was used as template for site directed mutagenesis reaction. After amplification, the parental and hemiparental template DNA were digested with DpnI. The amplified plasmids were transformed into *E. coli* DH5α and the mutations were verified by sequencing. The endogenous promoter was cloned in Gateway donor vector pDONR P4-P1r. The two achieved entry clones together with pB7m24GW, 3 vector were subjected to an LR reaction to have the endogenous promoter upstream of the genomic DNA in expression clone. The pB7m24GW, 3 vector carrying whole construct was then transformed to disarmed *A. tumefaciens* strain pGV3101/pMp90 by electroporation. The entry and expression vectors were verified by sequencing. The flowered *hd2c-1* plants were infiltrated with *Agrobacterium* by floral dip method (Zhang et al., 2006). The plants were screened using Basta until T2 generation and the seeds of 4 homozygous lines were produced for each transgenic line including *hd2c/HD2C*, *hd2c/HD2C*-C269H, *hd2c/HD2C*-C272H and *hd2c/HD2C*-C269/272H.

3. 6. 1. *hd2c/HD2C-C269/272H* line shows less sensitivity to ABA

Based on literature, expression of *HD2A*, *HD2B*, *HD2C* and *HD2D* has been shown to be reduced by ABA and salt (Luo et al., 2012b). The HD2C overexpression line has shown ABA-insensitive phenotype (Sridha & Wu, 2006). On the other hand *hd2c-1* and *hd2c-3* mutant lines have shown sensitivity to ABA and salt treatments (Chen et al., 2010). Moreover, ABA can induce NO production and consequently S-nitrosylation of proteins. So, the ABA-related function of HD2C was already known; to observe the involvement/importance of cysteine residues in this function of HD2C; the 2 weeks old plants of WT, *hd2c-1/HD2C*, *hd2c-1/HD2C-C269H*, *hd2c-1/HD2C-C272H* and *hd2c-1/HD2C-C269/272H* grown in long day light condition, were treated either by 100 µM ABA or by the same volume of its solvent (ethanol) three times per week until the control plants started to flower.

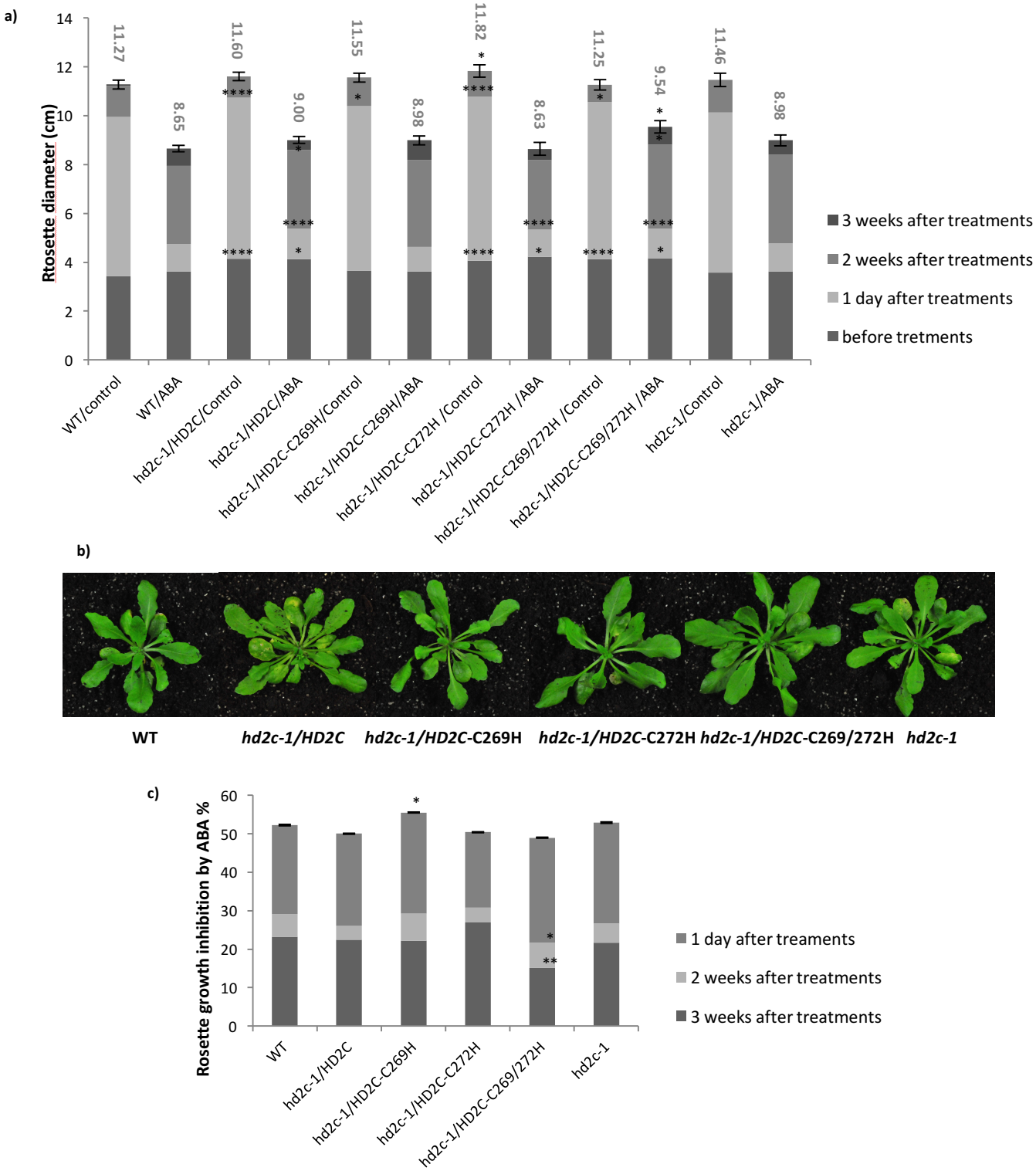

Fig. 23. Analysis of rosette diameter of ABA treated WT, *hd2c-1/HD2C*, *hd2c-1/HD2C-C269H*, *hd2c-1/HD2C-C272H* and *hd2c-1/HD2C-C269/272H* and *hd2c-1* plants. The 2 weeks old plants were sprayed with 100 µM ABA three times per week until before flowering time and a) the rosette diameter of plants were measured at 3 different time points after stopping treatments. The experiment was performed with 2 biological replicates and 24 plants for each line. The data analysis was performed by anova single factor. The results of 2 biological replicates were similar, the data analysis of one biological replicate is shown here. * and ** and **** indicate that the p-value of significance test is less than 0.05, 0.01 and 0.0001 respectively in compare to WT in each time point. b) The figure of ABA treated plants with corresponding mean rosette diameter. c) Rosette growth inhibition by ABA (%) in different lines; * and ** indicate p-value of significance test of growth inhibition by ABA in compare to that of WT.

The rosette diameter of plants was measured before treatments and at 3 different time points after stopping treatments. The experiment was performed with 2 biological replicates with 24 plants for each line (4 different homozygous lines were used for each transgenic line). The data were analyzed by anova single factor. All the ABA-treated plants showed less growth and some yellowish leaves in compare with the control plants. However, the *hd2c-1/HD2C*, *hd2c-1/HD2C-C272* and *hd2c-1/HD2C-C269/272H* lines were less affected by ABA in compare with WT according to the data of rosette diameter (Fig. 23a and b). Since the rosette diameter of those lines were significantly bigger than WT in control condition as well, then the growth inhibition by ABA was calculated for all lines 1 day, 2 weeks and 3 weeks after stopping the treatments.

Analyzing the difference of ABA treated and untreated data showed that the growth inhibition by ABA for *hd2c-1/HD2C-C272H* line in compare to WT is significantly lower at 2 and 3 weeks after stopping the treatments. However *hd2c-1/HD2C-C269H* line showed more growth inhibition by ABA which was statistically significant at 1 day after stopping the treatments (Fig. 23c). Surprisingly no significant difference was detected between WT and *hd2c-1* mutant plants, while the difference of WT and complement WT (*hd2c-1/HD2C*) in both treated and untreated conditions was significant.

Discussion

1. Identification of *Arabidopsis* nuclear candidates for S-nitrosylation

NO has appeared as a significant signaling molecule in plants, involved in many physiological processes including responses to abiotic and biotic stressors. S-nitrosylation is the most relevant reversible modification of proteins by NO, which often affects protein functions including protein–protein interaction, catalytic activity, or subcellular localization. Using biotin switch assay combined with mass spectrometry hundreds of S-nitrosylation candidates have been identified in different plants, various stress conditions and several organelles such as mitochondria (Palmieri et al., 2010, Camejo et al., 2013), peroxisome (Ortega-Galisteo et al., 2012), and apoplast (Sehrawat & Deswal, 2014).

Nucleus contains the hereditary information of the cell and its function is to maintain the probity of the genes and to regulate their expression. The nucleolus- the largest structure in nucleus- functions in the assembly of ribosome, while it involves in cell's stress response as well. Nuclear membrane separates gene expression from cytoplasmic translation, likewise cytoplasmic signaling from transcription; therefore nucleocytoplasmic transport of macromolecules is essentially important. In fact, transcriptional reprogramming, ribosome biogenesis and nuclear transport are the central nuclear events. Those events are facilitated with large number of proteins and enzymes. One way to regulate the function of those proteins could be the post-translational modification of them including S-nitrosylation. Evidences for NO accumulation in the nucleus of stomatal and epidermal cells in response to various stress conditions have been reported (Vitecek et al., 2008, Foissner et al., 2000, Gould K et al., 2003). Experimental evidence for S-nitrosylation has also been demonstrated for some nuclear-localized proteins such as AtMYB2 (Serpa et al., 2007), AtMYB30 (Tavares et al., 2014), NPR1 (Tada et al., 2008a), b-ZIP transcription factor TGA1 (Lindermayr et al., 2010), and GAPDH (Wawer et al., 2010b, Holtgrefe et al., 2008).

In this study, 50 *in-vivo* S-nitrosylated nuclear proteins could be detected, 23 of them were identified only in *Pst avr* treated cells, 2 and/or 13 h after infection and not in $MgCl_2$ treated cells (Fig. 4b and Supplementary Table. S1). These include mainly proteins involved in protein metabolism (39%), such as ribosomal proteins, translation elongation factors and also heat shock proteins. Ribosomal and heat shock proteins are known to accumulate due to pathogen attack in some other organisms and redox-reactive cysteine residues have

already characterized for some heat shock proteins in animals (Nardai et al., 2000, Ahn & Thiele, 2003, Vijayalakshmi et al., 2001). Moreover, some redox-sensitive ribosomal proteins were identified in early response to salicylic acid and flg22 in *Arabidopsis* (Liu et al., 2015). These results suggest a regulatory function of NO in protein folding, stabilization, and protein metabolism. In general, *in-vivo* S-nitrosylated proteins are not present in high amounts and one cannot exclude that some proteins identified in the water-treated samples are "background". But the fact that in some water-treated samples none or only a few proteins could be identified (e. g. 13h *Pst vir*-water, 13h $MgCl_2$-water) demonstrates that the purification background is very low under the condition that was performed. Anyway the biotin switch assay gives a list of candidates, which finally have to be verified using recombinant proteins.

Moreover, the extracted nuclear proteins of pathogen-treated *Arabidopsis* cell cultures were treated with GSNO to get a survey of possible targets for S-nitrosylation in the nucleus of these cells (Table. 2 and Supplementary Table. S1). In total, 117 nuclear proteins were identified as candidates for protein S-nitrosylation. The protein pool from the short-term (2 h) infected *Arabidopsis* cell cultures contained more candidates for S-nitrosylation than the protein pool from the long-term (13 h) infected cells. Moreover, more S-nitrosylated candidate proteins were observed after treatment with the avirulent strain than with the virulent strain. Similar results were observed in *Arabidopsis* cell cultures inoculated by virulent and avirulent *P. syringae* (Maldonado-Alconada et al., 2011b).

The number of identified S-nitrosylated candidate proteins is higher in the nucleus than in other organelles. For example in mitochondria 11 proteins were identified as targets for S-nitrosylation (Palmieri et al., 2010), 6 candidate proteins were identified in peroxisome (Ortega-Galisteo et al., 2012), and 48 candidates in apoplast (Sehrawat & Deswal, 2014). In GSNO-treated *Arabidopsis* nuclear proteins, most of candidate proteins for S-nitrosylation were identified after short-term infection (88 proteins) and only a few could be detected after long-term infection (31 proteins in incompatible interaction and 19 in compatible interaction). In previous studies, many proteins have already been identified as putative targets for S-nitrosylation after pathogen infection. Romero-Puertas *et al.* (2008) have been identified 16 S-nitrosylated proteins in *Arabidopsis* leaves under hypersensitive response.

Most of nuclear S-nitrosylation targets act in protein and RNA metabolism, stress response, and cell organization and protein transport (Fig. 4a). These data indicate that S-nitrosylation might be implicated in a various different functions of nuclear proteins. Similarly S-nitrosylation candidates have been identified from diverse classes such as signalling and stress-related proteins, or metabolic enzymes (Romero-Puertas et al., 2008). 127 candidate proteins were identified in *Arabidopsis* leaves and cell extracts treated with virulent and avirulent *P. syringae* (Maldonado-Alconada et al., 2011a). Those include structural, signalling pathogen- and stress related proteins as well as enzymes involved in carbon and nitrogen mobilization and antioxidant defense reactions. Moreover, 11 candidates were identified in tobacco cell suspensions treated with cryptogein, which were involved in amino acid biosynthetic pathways, energy and metabolism, signalling, and protein degradation (Astier et al., 2012).

1. 1. Occurrence of S-nitrosylation in various nuclear processes

This work provides a new collection of targets for protein S-nitrosylation in *Arabidopsis* and gives insight into the regulatory function of NO in the nuclear processes during plant defense response. Some of the targets of S-nitrosylation are discussed here in the context of involved nuclear events (Fig. 24).

1. 1. 1. Involvement of S-nitrosylation in regulation of gene expression

1. 1. 1. 1. S-Nitrosylation in regulation of gene transcription

Transcriptional reprogramming is a very important process in plants to cope with pathogens and environmental stresses. Chromatin modifications such as RNA-directed DNA methylation, histone modifications and ATP-dependent chromatin remodelling are the key transcriptional reprogramming mechanisms orchestrating plant abiotic and biotic responses (Luo et al., 2012a, Berr et al., 2012). Surprisingly, no transcription factor could be identified. Likewise, regarding to identifying other categories of proteins involved in transcriptional mechanisms, the S-nitrosylome was too poor. This might be due to their low abundance and due to loss of the NO-dependent modifications during nuclei preparation. Or perhaps, S-nitrosylation does not play a direct role in transcriptional level as important as it has been thought. Only 2 proteins (CCCH-type zinc finger family protein and nucleic acid-binding, OB-fold-like protein) with putative involvement in histone modifications were identified as S-nitrosylation candidates (Table. 2 and Supplementary Table. S1).

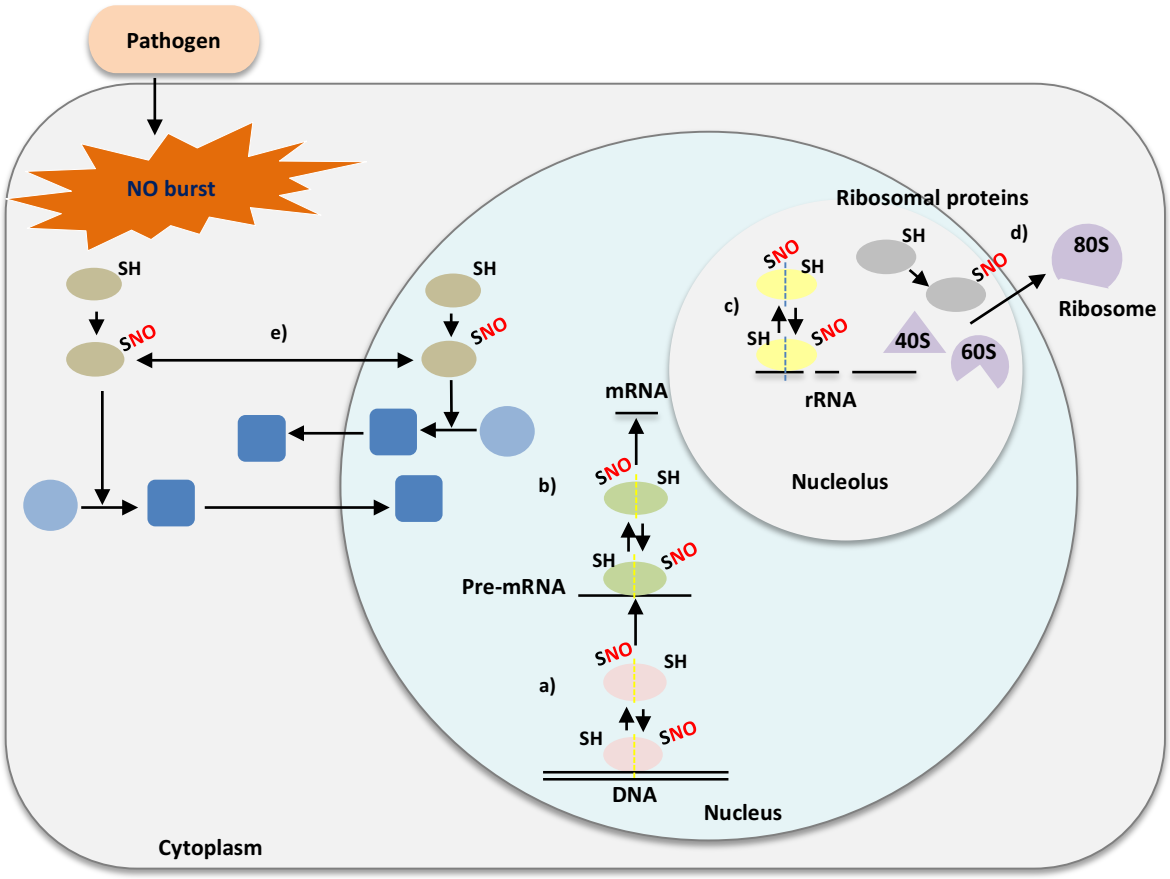

Fig. 24. S-nitrosylation targets of *Arabidopsis thaliana* are involved in various nuclear events. *Arabidopsis* S-nitrosylated nuclear proteins are involved in a) gene transcription, b) mRNA processing, c) rRNA processing, d) ribosome biogenesis and e) nuclear transport. For avoiding from complications, in cases of a, b and c, each protein is divided to two parts and shows two different possibilities of effect of S-nitrosylation. Additionally, in those processes only direct association/dissociation of proteins with DNA and RNA molecules is shown to be -possibly- regulated by S-nitrosylation. Indirect effect of S-nitrosylation by regulation of complex formation might also occur; e) which here is only shown in nuclear transport process.

CCCH-type zinc finger family protein was identified as candidate for S-nitrosylation in short-term pathogen infected *Arabidopsis* cell cultures (Table. 2 and Supplementary Table. S1). Similarly, three zinc finger proteins of *Arabidopsis* including salt-inducible zinc finger 2 (SZF 2), zinc finger protein 1 (ZFN1) and a zinc finger family protein (AT2G20280) have been identified as endogenously S-nitrosylated candidates using site-specific proteomic analysis (Hu et al., 2015). Zinc finger domains are the largest superfamily of transcription factors. They are widely various in structure, classified into nine types including: C2H2, C3HC4, C2HC, C2HC5, C4HC3, CCCH, C4, C6 and C8 (Gupta et al., 2012) and can be found between 1 and 40 numbers in a protein (Brayer & Segal, 2008). Possessing functions of DNA and RNA binding or protein-protein interactions, zinc finger proteins participate in different transcriptional and translational processes (Laity et al., 2001). Through an *in-silico* analysis 176 zinc finger

proteins have been identified in *Arabidopsis* which only a few of them are evolutionary conserved, while 81% of them are plant specific (Englbrecht et al., 2004). The majority of those non-conserved zinc finger proteins are known or believed to be involved in transcriptional regulation (Englbrecht et al., 2004). Nuclear receptors represent an important family of zinc finger transcription factors (Mangelsdorf et al., 1995). Furthermore, the nucleotide-binding site of leucine-rich repeat (NBS-LRR) disease resistance proteins represent a DNA binding zinc finger protein; this indicates the relevance of the zinc fingers in regulation of plant defense mechanisms (Gupta et al., 2012). Some of plant zinc finger proteins are involved in regulation of biotic and abiotic stress responses (Nakai et al., 2013) such as salt stress (Shi et al., 2014, Milla et al., 2006), cold stress and pathogen infection (Shi et al., 2014), water stress (Sakamoto et al., 2000), and oxidative stress (Davletova et al., 2005).

Two HD2 type histone deacetylases, HD2B and HD2C, were identified in short term and long term *Pst* avr and GSNO treated samples and in *Pst* vir and GSNO treated samples, respectively (Table. 2 and supplementary Table S1). The results of this work do not support the HDAC activity of HD2C isoform; however, since the data of our lab have shown that NO donors inhibit the total HDAC activity of *Arabidopsis* protoplast and nuclear extract (Mengel, et al; unpublished data), histone deacetylases are discussed here. Histone deacetylases together with histone acetyl transferases control the acetylation status of the chromatin which has a profound effect on gene transcription. A growing number of HDACs were characterized from different plant species like maize, *Arabidopsis*, rice, barley (Demetriou et al., 2009), potato (Lagace et al., 2003), and grape (Busconi et al., 2009). In *Arabidopsis* three HDAC families have been described: the largest family consists of twelve members - defined by a highly conserved HDAC domain with a catalytic zinc ion (Pandey et al., 2002). Homologs are also found in animals and yeast. The structurally diverse family of Sirtuins (2 members in *Arabidopsis*) is homologous to yeast SIR2 (silent information regulator 2) and has a different catalytic mechanism using NADH as a cofactor (Hollender & Liu, 2008). Current available evidences indicate that HDACs play an important role in plant growth, development, and stress responses. In the animal/human system, S-nitrosylation of HDACs has been described. In neurons, HDAC2 has been defined as a key nuclear target for S-nitrosylation (Nott et al., 2008). It has been shown that the chromatin modifier HDAC2 is S-nitrosylated on Cys262 and Cys274 after treatment of rat cortical neurons with neurotrophins. Surprisingly, S-

nitrosylation of these cysteines did not affect the enzymatic activity of HDAC2 but rather induced its release from chromatin (Nott et al., 2008). In contrast, S-nitrosylation decreases HDAC2 activity in muscle cells (Colussi et al., 2008). This difference could be as a result of S-nitrosylation of various cysteine residue(s) of HDAC2 in neurons and muscle cells (Nott & Riccio, 2009). Cys262 and Cys274 of human HDAC2 are conserved in many *Arabidopsis* HDACs (Mengel et al., 2013a). Moreover, a redox-sensitive cysteine residue has been identified recently in *Arabidopsis* HDA19 (Liu et al., 2015).

1. 1. 1. 2. S-Nitrosylation in mRNA splicing

mRNA splicing is the removal of gene introns from nascent pre-mRNA which adheres the exons to each other in mature mRNA. Splicing is an important process in regulation of gene expression of eukaryotes. Alternative splicing (AS) -in turn- is ascribed as removing or including particular exons of a gene in the final processed mRNA. AS increases transcriptome flexibility and proteome diversity and involves in different processes including biotic and abiotic stresses (Mastrangelo et al., 2012, Reddy et al., 2013, Staiger & Brown, 2013). Analysis of transcriptome of salt-treated *Arabidopsis* plants has been shown that 49% of intron-containing genes were alternatively spliced under salt stress (Ding et al., 2014). Although, large number of stress responsive genes tends to alternative splicing under stress condition; possibly, most stress-induced splicing variants does not produce functional proteins and can be described as splicing errors which is the non-specific consequence of stress damage (Ding et al., 2014). The regulating mechanisms of AS in plants are not well known. Post-translational modifications of splicing factors and spliceosomal proteins, especially phosphorylation (de la Fuente van Bentem et al., 2006) and sumoylation (Miller et al., 2013) have been demonstrated to regulate AS in plants.

RPS5/Elongation factor G/III/V (MEE5), MOS4-associated complex 3B and SAP domain containing protein are part of *Arabidopsis* spliceosome which were identified as targets of S-nitrosylation in short term *Pst* avr infected cell cultures. *Arabidopsis* modifier of snc1, 4 (MOS4), together with cell division cycle 5 (CDC5) and pleiotropic regulatory locus 1 (PRL1) are conserved across plant kingdom and seem to be essential for plant innate immunity (Palma et al., 2007). The MOS4 is a spliceosome associated complex and it has been suggested to control plant defense responses through regulation of mRNA splicing. MOS4 is important for the NPR1-independent signaling and CDC5, PRL1 and MOS4 are essential for

R-protein-mediated defense responses (Palma et al., 2007). U5 small nuclear ribonucleoprotein helicase and heat shock cognate protein 70-1 are also the nucleolus localized splicing factors (Table. 2). Moreover, some other heat shock proteins which are known to be involved in mRNA splicing were found in the list (Supplementary Table. S1), however according eFB browser they can be localized in other organelles in more amounts than nucleus. Heat shock proteins are known to be imported into the nucleus upon stress and involve in processes like mRNA splicing (Kodiha et al., 2005).

1. 1. 2. Involvement of S-nitrosylation in rRNA processing and ribosome biogenesis

Nucleolus is basically involved in transcription and processing of rRNA and assembly of ribosome. rRNA processing assigns to cleavage of transcript into precursors of the mature rRNAs in their final size and also modification of specific rRNA nucleotides. The mature rRNA then is used for ribosome assembly together with ribosomal proteins. These mechanisms and how they are regulated are not well understood in plants and lag significantly behind that of animal system which is well studied (Brown & Shaw, 2008). Some ribosomal proteins were identified as targets of S-nitrosylation (Supplementary Table. S1) and were discussed in the context of *in-vivo* S-nitrosylated proteins.

NOP56, NOP56-like pre RNA processing ribonucleoprotein and Fibrillarin 1 were identified *in-vivo* and short and long term *Pst* avr and long term *Pst* vir infected cells (Table. 2, Supplementary Table. S1). These are the core proteins or related proteins to *Arabidopsis* C/D box ribonucleoprotein complex. Small nucleolar RNAs (snoRNAs) are known to guide modifications of other RNAs, mainly ribosomal RNAs and also tRNAs and small nuclear RNAs. There are 2 main classes of snoRNAs including C/D box and H/ACA box which associate with methylation and pseudouridylation, respectively. The core proteins of the snoRNP complexes are necessary for enzymatic activity, nucleolar localization and stability of the complex (Reichow, Hamma et al. 2007). Fibrillarin has shown methylation activity in different organisms including *Arabidopsis* (Barneche et al., 2000). The Cys99 and Cys268 of fibrillarin are highly conserved in different organisms including *Arabidopsis* (Rakitina et al., 2011) and able to establish -S-S- bond. The methyl transferase domain of fibrillarin contains the Cys268, suggesting that the modification or mutation of Cys268 may affect the activity of the protein (Barygina et al., 2010). There are no published data about the redox regulation of the core proteins of snoRNP complexes in any organism.

1. 1. 3. S-Nitrosylation in protein synthesis

Occurrence of protein synthesis in nucleus is debated, since at least in one case (*Acetabularia mediterranea*), the synthesis of protein was little affected by removing of nucleus *(Brachet & Chantrenne, 1951)*. However according to a study on HeLa cells, nucleus is responsible for production of 10-15% of cell protein (Nathanson et al., 2003). One idea which supports nuclear protein synthesis is: if nucleus is the place of biosynthesis of all the machines of translation including 60S and 40S ribosomal subunits, signal recognition particles and 5S rRNA ribonucleoprotein complex and on the other hand since tRNAs, and translation initiation and elongation factors are presented in nucleus; why it would not synthesize some proteins? (Pederson, 2013). However, this hypothesis is not generally accepted because of low abundance of many translation factors and the likely inactivity of nascent ribosomes in nucleus (Dahlberg et al., 2003). Moreover, much of the claim of nuclear translation is about the existence of a functional proofreading of newly made mRNAs for presence of premature termination codons to avoid from production of deleterious proteins. But, it seems that at least in case of yeast, the translational proofreading does not occur in nucleus (Dahlberg & Lund, 2004). Although, one cannot rule out nuclear protein synthesis, in the absence of more reliable data one should be reluctant to believe it occurs. Since, some S-nitrosylated translation elongation and initiation factors can be present in high amounts in nucleus (according eFP browser, Supplementary Table. S2) -regardless of involving in nuclear protein synthesis- they are discussed here.

Elongation factors are proteins that are required for the translational elongation process during protein biosynthesis. S-nitrosylation of elongation factors has been shown in different organisms such as murine macrophages (Gao et al., 2005) and human vascular smooth muscle cells (Greco et al., 2006) and prostate epithelial cells (Lam et al., 2010). In the list of candidate proteins for S-nitrosylation, EF-G and EF-1B were identified as a candidate for S-nitrosylation after short-term avirulent infection, and EF-Tu was identified as *in-vivo* candidate of S-nitrosylation and also after avirulent and virulent infection (Table. 2 and Supplementary Table S1). Until now, several elongation factors of plants have been identified as the candidates of S-nitrosylation in different nitrosoproteom studies including eEF-1α, EF-2, EF-1Bα, EF-1Bγ, putative (Lindermayr et al., 2005), EF-1α, LOS1 (Fares et al., 2011b) several GTP binding EF-Tu family proteins, EF-1α, EF-1Bγ and EF-P from *Arabidopsis*

(Hu et al., 2015) and EF1-beta putative from potato (Kato et al., 2013). Moreover S-nitrosylation of a chloroplast localized EF-TU precursor has been identified in *Aarbidopsis* plants undergoing hypersensitive response (HR) (Romero-Puertas et al., 2008) and EF-1α, EF-2 were identified in *Arabidopsis* plants treated with *Pst avrRpt2* (Maldonado-Alconada et al., 2011b).

Eukaryotic translation initiation factors are the basic molecular key compounds regulating the process of translating the nucleic acid encoded information to the functional protein. This group of proteins is composed of at least 25 subunits precisely coordinated and regulated during mRNA translation. In *Arabidopsis* S-nitrosylated nuclear proteins, many eukaryotic translation initiation factors were identified as candidates like EIF4G that was detected after short-term infected and uninfected cells. Eukaryotic translation initiation factor 4A1 (EIF4A1) is an RNA helicase and a subunit of the eIF4F complex which is associated in cap recognition and is needed for binding mRNA to the ribosome (Graff et al., 2008, Bauer et al., 2001, Silvera et al., 2010). Furthermore, translation initiation factor SUI1, EIF-2 subunit 1, EF3G1, and EIF2 were detected in short-term infection, and EIF4A-2 was identified as *in-vivo* candidate for S-nitrosylation and after avirulent and virulent infection (13h) (Table. 2 and Supplementary Table S1). Similarly, translation initiation factors eIF-4A1 and 5A-4-related have been demonstrated as targets of S-nitrosylation in GSNO-treated *Arabidopsis* cell cultures and leaves (Lindermayr et al., 2005), and initiation factor 5A-3 was identified from GSNO-treated leaves and tuber extracts of potato (Kato et al., 2013). Additionally, some endogenously S-nitrosylated initiation factors have been identified from *gsnor1-3* mutant plants including eIF4A1 and eIFISO4G1 in Col-0 and eIF3C, EIF3E and eukaryotic initiation factor 2A family protein (Hu et al., 2015).

1. 1. 4. NO-mediated nuclear transport

Transport of RNA and protein molecules between nucleus and cytoplasm is an essential process in eukaryotes. Different families of proteins have been shown to be involved in *Arabidopsis* nuclear protein transport including importin α and β family proteins, GTP-binding nuclear proteins and nuclear transport factors. However, nucleoporins and DEAD-box proteins are involved in mRNA export. Nuclear transport factor 2, ribosomal protein L5 and importin alpha isoform 2 are involved in nuclear transport and were identified in short term *Pst* avr infected cell cultures. Importin alpha 2 has also been identified as the candidate

of endogenous S-nitrosylation in *Arabidopsis* (Hu et al., 2015). Moreover, S-nitrosylation-mediated trans-localization has been studied in case of NPR1 and GAPDH.

2. Function of S-nitrosylated HD2C

The S-nitrosylation of recombinant proteins of *Arabidopsis* HD2 isoforms (HD2A-HD2D) with GSNO as NO donor could be detected by anti-biotin antibody; GSH was used as control and did not show any band indicating that the signal from GSNO treatment is due to S-nitrosylation (Fig. 11). The confirmation of S-nitrosylation of candidates of biotin switch assay using recombinant proteins has been broadly applied (Lindermayr et al., 2005). Here the function of S-nitrosylation of HD2C is discussed.

2. 1. Releasing zinc ion as putative function of S-nitrosylation of HD2C

The classic C2H2 zinc finger domains can be found in about 0.7% of proteins of *Arabidopsis* (Englbrecht et al., 2004). HD2A and HD2C are among the conserved zinc finger proteins of *Arabidopsis* (Englbrecht et al., 2004). The zinc finger proteins which are conserved supposed to be evolutionary ancient and they have been suggested to be involved in processes such as RNA metabolism and chromatin re-modeling (Englbrecht et al., 2004). Using recombinant protein and a zinc indicator PAR, the release of zinc ion from HD2C could be measured after treating with two different NO donors (GSNO and SNAP) (Fig. 12). Releasing zinc ion can be considered as the putative function of S-nitrosylation of HD2C. In yeast, NO inhibits DNA binding of the zinc finger transcription factor LAC9 and it induces Zn^{2+}-release of the zinc storage protein metallothionein *in-vitro* via S-nitrosylation (Kroncke et al., 1994). In animals/human, S-nitrosylation regulates DNA binding activity of different zinc-finger-containing transcription factors such as egr-1 and NFκB by disrupting zinc binding (Mengel et al., 2013b, Cibelli et al., 2002, Nott & Riccio, 2009). Moreover, in animal system, releasing zinc ion from zinc-sulfur cluster protein methallothionein in a concentration-dependent manner after treating with NO (Kroncke, 2001), the nNOs/NO mediated release of zinc ion from RGSZ2 zinc finger protein which promotes regulation of zinc signaling, and cross-talk of NO and zinc signaling pathways (Rodriguez-Munoz et al., 2011) have been studied.

Since, releasing zinc ion from HD2C could be restored by adding DTT as a reducing agent; this suggests the reversibility of S-nitrosylation (Fig. 12b). Similarly, it has been shown that some of functional disruptions of zinc finger transcription factors mediated by S-nitrosylation are

reversible (Kroncke & Carlberg, 2000a, Kroncke, 2001, Berendji et al., 1999). Therefore, the following reactions occur in order: I) S-nitrosylation (which presumably causes mis-folding of protein), II) de-nitrosylation reaction and III) free folding of zinc finger domain (Fig. 25). This is theoretically possible, since zinc fingers are energetically favourable free folded domains (Gupta et al., 2012).

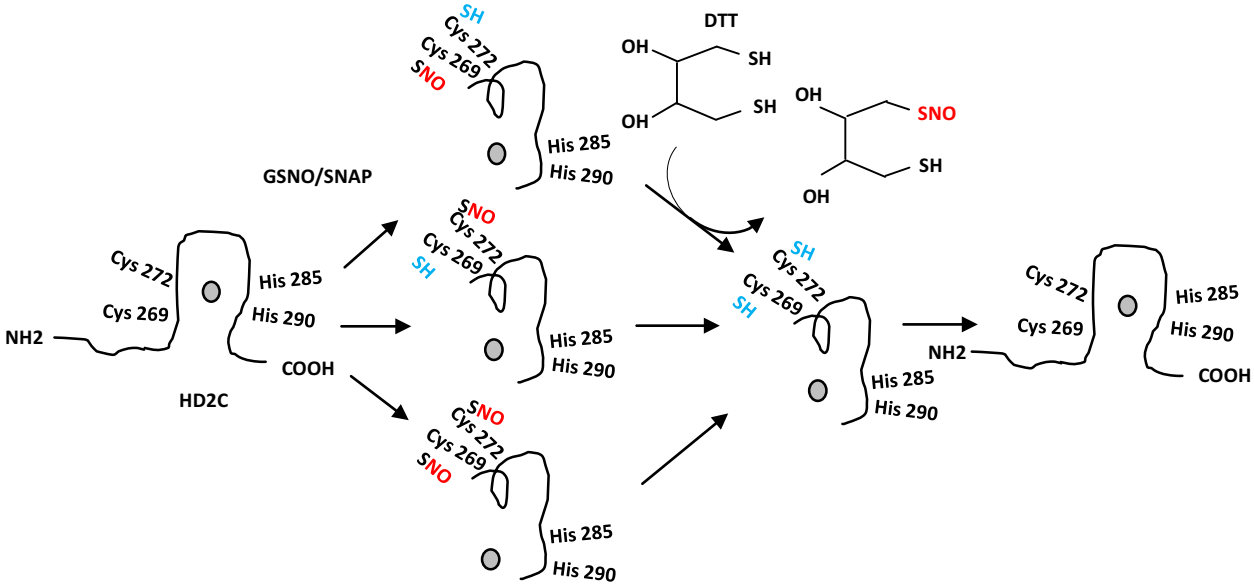

Fig. 25. Releasing zinc ion as putative function of S-nitrosylation of HD2C. In presence of NO donors, S-nitrosylation occurs and with further adding of reducing agent DTT,-SNO bond can be converted to SH. Afterward the disrupted region of protein can again be folded as a zinc finger domain, since zinc fingers are generally free folding (energetically favored) domains.

2. 2. Biochemical and physiological function of HD2C

HD2 type proteins are considered as plant specific HDACs; however, using the database of Expressed Sequence Tags (ESTs), it was found that HD2 type proteins are widespread among eukaryotes, although the absence of any vertebrate member is noticeable (Aravind, Koonin, 1998). Moreover, a phylogenetic analysis of all known plant HD2 proteins showed a considerable diversification among them; therefore, this may accompany by a functional diversity (Pandey et al., 2002).

2. 2. 1. Reluctance in HDAC terminology of HD2C

HDAC activity of recombinant HD2C was not detected in our lab. In *Arabidopsis*, although it has been demonstrated that HD2 family repress the expression of a reporter gene and may function as a transcription repressor (Wu et al., 2003), their HDAC activity have not been shown yet experimentally (Luo et al., 2012c). Moreover, the evidences related to HDAC

activity of HD2 type proteins in other plants are rather indirect. For instance, it was shown that maize HD2 accepted all core histones *in-vitro*, and it was sensitive to deacetylase inhibitors (Brosch et al., 1996). By further studies, the HDAC activity of maize HD2 protein was shown in immunoprecipitated fractions using anti-HD2 antibody; whereas, its recombinant protein failed to show any HDAC activity (Lusser et al., 1997). The evidence for association of *Arabidopsis* HD2C in an HDAC-related function is about its direct interaction with HDA6 and histone H3 (Luo et al., 2012b). The authors also demonstrated that in *hda6*, *hd2c-1*, and *hda6/hd2c-1* mutant plants, histone H3K9K14 acetylation increased and histone H3K9 dimethylation decreased in compare to WT (Luo et al., 2012b). Although, HDA6 was not identified in the Co-IP experiment; this is probably due to a temporal and/or condition-dependent complex formation of HD2C and HDA6.

A comparative analysis of amino acid sequence of HD2C and type I HDACs and its PSI-Blast analysis did not attend to support a convergence between them. HD2 type family lack an HDAC domain typical for type I HDACs, instead their N-terminal domain composes two conserved residues - His25 and an Asp75 (glutamate in HD2C) (Pandey et al., 2002) which is the strongest support for the HDAC activity of HD2 isoforms (Dangl et al., 2001). However, finding only an HDAC pfam motif for all type I HDACs in comparison with finding 11 different pfams and no HDAC pfam for HD2C suggests diverse possible non-enzymatic functions for HD2 type proteins (Fig. 16).

The first HD2 type HDAC identified in maize (ZmHD2) showed no distinct homology to yeast transcription regulators, RPD3, HDA1 and SIR2 proteins - similar to other members of the family (Lusser et al., 1997); while it was distantly related to cis-trans isomerases identified in *S. cerevisiae* and insects (Pandey et al., 2002) and a nucleolar RNA binding protein from *Trypanosoma brucei* (Dangl et al., 2001)(Aravind, Koonin, 1998). The data-based analysis of this work showed co-expression of HD2C with different chaperones, heat shock proteins and FKBPs. *Spodoptera* FK506-binding protein 46 (FKBP46) contains an acidic/basic domain with homology to the putative catalytic domain of HD2 type histone deacetylases (Dangl et al., 2001). However, the efforts for measuring the HDAC activity of FKBP46 was not successful so far (Dangl et al., 2001). In absence of experimentally shown enzymatic activity for FKBPs and HD2 isoforms; the physical associations of FKBP25 with HDAC1, HDAC2 and YY1 (a transcriptional regulator) (Yang et al., 2001) and HDA6 with HD2C (Luo et al., 2012b) can be

due to some other reasons such as diverse functions of HDACs especially that HDA6 is one of the few nucleolus-localized HDACs of *Arabidopsis*. NO type I HDAC identified in any replicate of Co-IP and the highest enrichment of any histone superfamily protein belonged to histone H2B (AT5G22880.1) which was identified only in 2 replicates with mean maximum fold change of 13 in WT in compare to *hd2c-1* samples but with only 1 spectral count and mean abundance of 200 times lower than HD2C itself. This indicates that HD2C probably has temporal interaction with histone proteins and HDACs rather than very close association - at least in condition and developmental stage which was analyzed in this work. The claim that the histone proteins and/or HDACs could not be identified because of their low amount cannot be accepted; due to the fact that some proteins with similarly low expression levels in vegetative rosette (eFP browser) could be significantly high enriched in 3 replicates of WT samples in compare with Co-IP's negative control (e. g. expression value of histone H2B (260.4) and HDA6 (108) are 2 and 1 times of that of tetratricopeptide repeat (TPR)-like protein (137.6) and RNA-metabolising metallo- lactamase (111.6), respectively (Supplementary Table. S3)).

One way of explanation of identifying highly enriched RNA methylation-related proteins in Co-IP list could be to consider them as non-histone substrates of probable deacetylation activity of HD2C. In *Arabidopsis*, a variety of proteins especially some photosynthesis-related proteins (Wu et al., 2011) and in HeLa cells and mouse liver mitochondria some RNA splicing factors, structural proteins, chaperones, signalling proteins and energy metabolic proteins (Ma et al., 2013) have been reported to be acetylated. In the Co-IP list-regardless of statistical significance-similar families of proteins were enriched (Supplementary Table. S3). However, screening literature did not show almost any information about regulation of individual highly enriched putative partner proteins of HD2C or their orthologs by acetylation and deacetylation.

Altogether, using the term ''HDAC'' for calling HD2 proteins is skeptical.

2. 2. 2. Alternative function for HD2C as an adopter protein

A tetratricopeptide repeat (TPR)-like superfamily protein (AT5G28740.1) was significantly enriched in WT samples of Co-IP (Table. 4 and Supplementary Table. S3). TPR containing proteins mediate protein-protein interactions involve in various functions; they are part of the molecular chaperone, anaphase promoting, spliceosomal, protein import and

transcription repression complexes (Blatch & Lassle, 1999). Regarding to zinc finger of HD2C (the interest of this work due to containing the only 2 cysteines of HD2C), the protein-protein interaction and with lower probability RNA binding activity have stronger evidences than DNA binding activity. The C-terminal zinc finger structure of HD2 type proteins is unique to the plants and on the base of nature and space of the zinc-chelating residues, it belongs to TFIIIA-type zinc fingers which can be part of a DNA binding domain (Dangl et al., 2001). However, they lack a conserved motif (QALGGH) which is typical of the TFIIIA-zinc fingers (Dangl et al., 2001). Moreover, one zinc finger has been described to be not enough for DNA binding activity. Likewise, analyzing the repression of reporter gene by HD2A deletions demonstrated that the deletion of C-terminal region containing zinc finger did not affect gene repression function (Wu et al., 2000). These are suggesting that zinc finger of HD2 type proteins might not have the DNA binding activity. At the same time more authors suggest the protein-protein interaction for the zinc finger of HD2 type proteins (Ma et al., 2013, Wu et al., 2000) and for C-terminal zinc fingers (McCarty et al., 2003). Additionally, HD2C contains a SKK linker (Fig. 15) which is known to be found in protein-protein interacting zinc finger proteins (Brayer & Segal, 2008). Moreover, being predicted as a highly disordered protein and containing ‘’molecular recognition features’’ (Fig. 15) which is thought to be bound to protein partners via disorder-to-order transitions suggests that HD2C could be an adopter protein which serves as a bridge between interactor proteins and assist the formation of larger complexes in a spatial and temporal manner.

One possibility could be that HD2C have both HDAC/gene repression activity and protein-protein interaction by N-terminal conserved catalytic residues and central acidic/basic domains (Wu et al., 2000) and by C-terminal zinc finger, respectively.

2. 2. 3. Proposing an rRNA processing-related function for HD2C

HD2C may function in a different way than it was previously thought; due to identifying many RNA related proteins and instead finding a few DNA binding proteins and no type I HDAC and histone proteins among highly enriched candidates of Co-IP list. However, direct association of HD2C with individual promising candidate partners such as NOP56-like pre RNA processing ribonucleoprotein and the role of S-nitrosylation on their interaction have yet to be determined. Especially, in addition to HD2C, some putative partner proteins of HD2C were identified in the context of S-nitrosylation such as HD2B, NOP56 and NOP56-like

pre RNA processing (Supplementary Table. S1). HD2C is a nucleolus-localized protein. The central alternative acidic and basic domains of HD2C are typical of nucleolar proteins such as nucleolin and Nopp44/46 which can suggest a nucleolar targeting function for HD2 proteins (Dangl et al., 2001) (Aravind, Koonin, 1998). Furthermore, according to data from *Arabidopsis* Nucleolar Protein Database (http://bioinf.scri.sari.ac.uk/cgi-bin/atnopdb/get-all-data?type=more&value=At5g03740), HD2C shows strong localization particularly in periphery of nucleolus. This can provide occurrence of trans-nitrosylation between HD2C and cytoplasmic and nucleolus-localized proteins. Moreover, the first best Co-IP candidate according statistical analysis is sks4, SKU5 similar 4 (AT4G22010.1) which has oxidoreductase activity (Supplementary Table. S3). Here, the most important highly enriched candidate partner proteins of HD2C are discussed.

2. 2. 3. 1. Highly enriched putative partners of HD2C are core proteins of C/D box snoRNP complex involved in RNA methylation

NOP56-like pre RNA processing ribonucleoprotein (AT3G05060.1), Nop56 (AT1G56110.1) and Fibrillarin 2 (AT4G25630.1) were identified among top candidates of Co-IP (Table. 4 and Supplementary Table. S3). These are the core proteins or related proteins to the C/D box snoRNP complex. Similarly, NOP56-like pre RNA processing ribonucleoprotein, NOP56 and Fibrillarin 1 were identified as targets of S-nitrosylation (Table. 2 and Supplementary Table. S3). As it mentioned before, there are no published data about S-nitrosylation of those proteins. However, by combining the promoter trap mutagenesis with a positive selection for the survival in the metabolic stress using Chinese hamster ovary cells, it has been demonstrated that the loss of three C/D box small nucleolar RNAs which are encoded in the ribosomal protein L13a are sufficient to confer the resistance to lipotoxic and oxidative stress *in-vitro*, this also inhibits generation of oxidative stress *in-vivo* (Michel et al., 2011). The C/D box small nucleolar ribonucleoproteins (snoRNPs) are characterized as abundant (noncoding) guide RNAs for sequence-specific 2'-O-ribose methylation of ribosomal (Ellis et al., 2010) and spilosomal (Xue et al., 2010a) RNAs and assembly of ribosome (Lin et al., 2011). Methyl groups of rRNA are clustered in functionally important regions of ribosome, involving in altering the RNA folds which stabilize specific structures of RNA (Watkins & Bohnsack, 2012). Those clusters of RNA modifications are crucial for cell growth, and loss of some modifications enhances cellular sensitivity to stress (Watkins & Bohnsack, 2012).

Besides RNA methylation, some snoRNPs have crucial roles in pre-RNA folding and function as chaperones of rRNAs for the assembly of the ribosome (Ellis et al., 2010) and rRNA processing (Watkins & Bohnsack, 2012). Recent studies have shown a broad range of roles for snoRNPs including mediating metabolic stress, regulating alternative splicing, editing RNA and repression of gene expression (Watkins & Bohnsack, 2012).

Eukaryotic C/D snoRNA contains four proteins including Snu13, NOP56, NOP58 and Fibrillarin (Ellis et al., 2010). The RNA component of the complex is responsible for the sequence specificity of the target RNA (Ellis et al., 2010). The core proteins are necessary for enzymatic activity, nucleolar localization and stability of the complex (Reichow et al., 2007). Fibrillarin is an evolutionary conserved nucleolar protein which is required for viability of pro- and eukaryotic cells (Barygina et al., 2010). Fibrillarin transfers a methyl group from S-adenosylmethionine (SAM) to RNA ribose; it binds to the guide-substrate duplex at the minor groove and also loads the target ribose specifically to its active site (Lin et al., 2011). The methylation activity of *Arabidopsis* fibrillarin has been demonstrated as well (Barneche et al., 2000). NOP family proteins play important roles in pre-RNA processing and Pre-mRNA splicing (Aittaleb et al., 2003). C-terminal domain of NOP5 binds to RNA and NOP5-fibrillarin interaction is required for methylation activity of fibrillarin (Aittaleb et al., 2003); since fibrillarin itself has no affinity to s-RNA-target duplex, NOP5 provides as a bridge between the targeting and catalytic function of C/D box complex (Hardin et al., 2009). NOP56/58 play a role in methylation cofactor (SAM) binding by fibrillarin (Oruganti et al., 2007). In *Arabidopsis*, 2 genes *Fib1* and *Fib2* encode closely identical proteins conserved with other eukaryotic fibrillarins. It has been demonstrated that *Arabidopsis* Fib2 directly interacts with methyltransferases of Histone H2A, H3 and H4, AtPRMT1a and AtPRMT1b and is a potential substrate of those enzymes; suggesting a collaboration between protein methyltransferases and RNA methyltransferases (Yan et al., 2007). Figure 26 describes a prospected model for the function of HD2C in rRNA processing.

Additionaly, high enrichment of some very lowly expressed proteins in vegetative rosette (according e-FP browser) involved in RNA processing - regardless of their statistical significance - reinforce this hypothesis that HD2C might have close association with RNA rather than DNA (Table. 4 and Supplementary Table. S3). Interestingly, on the first studies related to HD2 type proteins Lusser et al suggested that HD2 type HDACs - due to their

nucleolar localization - may be involved in regulation of ribosomal chromatin structure and mediate deacetylating nucleolar histones (Lusser et al., 1997). Since rRNA genes have special localization, different subset of transcription regulators and a distinct RNA polymerase, then it is not surprising if they associate with special histone deacetylases (Lusser et al., 1997). It seems that their hypothesis about rRNA-related function of HD2 isoforms was partially true, since apparently HD2C involves in post-transcription rather than transcriptional mechanisms of rRNA genes.

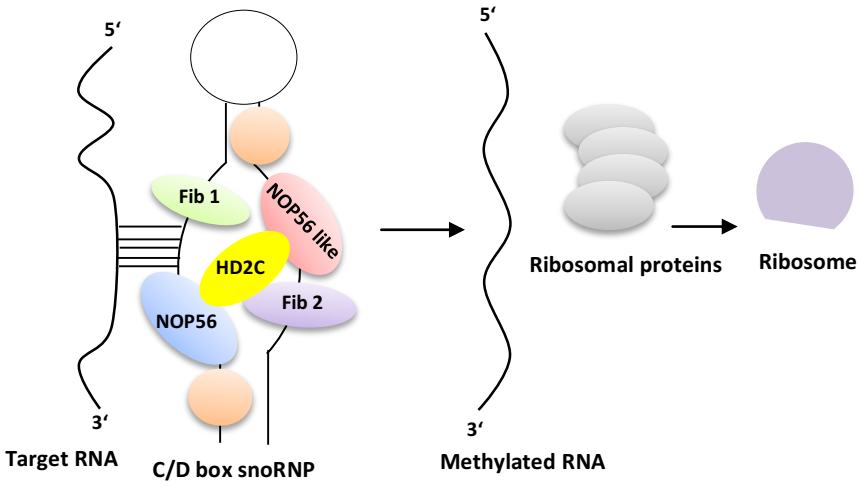

Fig. 26. Prospected function of HD2C in rRNA processing (methylation). NOP56-like pre RNA processing ribonucleoprotein, NOP 56 and Fib2 are the highly enriched putative partners of HD2C; therefore HD2C is shown in the center of those three proteins. The structure of *Arabidopsis* C/D box has not been solved yet; the C/D box snoRNP complex that is shown in this figure is a mimicked version from animal system.

Except snoRNP complexes, DEAD box RNA helicase (RH3) and HD2B are also important putative partner proteins of HD2C and may involve in RNA processing; therefore they are discussed here.

2. 2. 3. 2. DEAD box RNA helicases are other RNA-related important putative partners of HD2C

It has been demonstrated that HD2C involves in stress-induced re-localization of STRESS RESPONSE SUPPRESSOR DEAD-box RNA helicases (STRS1). STRS1 and STRS2 are negative regulators of abiotic stress responses, since their overexpression decreased tolerance to abiotic stresses such as salt and heat in ABA-dependent and -independent manner (Khan et al., 2014). In control condition STRS proteins are localized in nucleolus. The STRS proteins showed a stress-mediated nucleolar–nucleoplasmic re-localization which was reversible due to removing the stress agent or condition. Using FRAP studies, a fast re-localization was due

to salt stress (2 min) and a delayed one was due to ABA treatment or osmotic stress (40 min). The kinetics of those re-localizations was faster than the stress-mediated down-regulation of STRS gene expression which suggests the importance of immediate inactivation of STRS proteins via re-localization upon abiotic stress. STRS1 displayed mis-localization in the *hd2c* mutant. STRS2 was mis-localized in several mutants of RNA-directed methylation. Both STRS1 and STRS2 also displayed aberrant localization in the *cbf5* mutant, a core protein of H/ACA box snoRNP complex. Altogether, the authors concluded that STRS1 and STRS2 are involved in gene silencing via methylation and deacetylation (Khan et al., 2014). The authors suggested that STRS proteins are important for preventing constitutive activation of stress responsive genes which captures the plant growth (Khan et al., 2014). SRTS1 was not identified in the Co-IP list. Instead, another DEAD box RNA helicase (RH3) was enriched in WT samples in compare to *hd2c-1* samples (Supplementary Table. S3); RH3 governs RNA chaperone activity and plays important roles in intron splicing, ribosome biogenesis, and seedling growth.

2. 2. 3. 3. HD2B, putative partner of HD2C, is involved in RNA-related mechanisms

HD2B another HD2 isoform was highly enriched in WT samples of Co-IP list (Supplementary Table. S3). Similar to C/D box core proteins, HD2B was identified as target of S-nitrosylation (Table. 2 and Supplementary Table. S1) and S-nitrosylation of recombinant protein of HD2B was demonstrated (Fig. 11 and Supplementary Fig. S4). HD2B has been shown to interact with ribosomal protein S6 (RPS6) which is a downstream component of TOR (target of rapamaycin) kinase pathway (Kim et al., 2014). TOR kinase signaling pathway regulates several biological processes including translation, ribosome biogenesis and rRNA transcription (Kim et al., 2014). The chip analysis suggested that RPS6 directly interacts with promoter regions of rRNA genes. Moreover, overexpression of HD2C and RPS6 induced down-regulation of pre-18 S rRNA synthesis which consequently decreased the transcription of some ribosomal proteins. They suggested that HD2B involves in regulation of rDNA transcription, since it interacts with RPS6 and RPS6 in turn interacts with the rDNA promoter. Since the authors did not verify the enzymatic activity of HD2B, they proposed that HD2B can function through a mechanism not involved in the chromatin modification (Kim et al., 2014). Binding of TOR to rDNA promoter probably controls the optimum transcription of rRNA genes according variable environmental conditions; since TOR signaling counterpart

many cellular metabolic activities under diverse energy and stress conditions (Kim et al., 2014).

The data about the importance and various functions of HD2 proteins in plants are expanding and at the same time almost no significant phenotype has been reported for the mutants of these proteins. This arises the question that whether there is a functional redundancy among them. In case of HD2C and HD2B, there might be such a functional redundancy which has to be investigated.

2. 3. S-Nitrosylation might inhibit the putative positive function of HD2C in an ABA-induced pathway

2. 3. 1. Less ABA-induced inhibition of rosette diameter of *hd2c-1/HD2C-C269/272H line* might correlated with loss of S-nitrosylation

Treating *Arabidopsis* plants with ABA showed that complemented *hd2c-1/HD2C-C269/272H* line has less sensitivity to ABA in compare to WT and *hd2c-1* mutant (Fig. 23). However, WT and *hd2c-1* mutant showed no difference in rosette diameter. This is explainable by published data about the contradictory role of HD2C in ABA context which can be negative or positive and it is mostly like a modulation. Expression of *HD2C* has been shown to be repressed by ABA and *HD2C* overexpression line showed an ABA insensitive phenotype according germination rate and the root length of seedlings (Sridha & Wu, 2006). Besides, *HD2C* overexpression line exhibited decreased transpiration and enhanced tolerance to salt and drought stresses in compare to WT. The expression of several ABA responsive genes such as ABI2, KAT1 and KAT2 was repressed in *HD2C* overexpression line (Sridha & Wu, 2006). ABI2 is a regulator of transduction signals upstream of the activation of Ca^{2+}-induced anion channel whereby K^+ efflux is formed in the guard cells leading to stomatal closure (Sridha & Wu, 2006). While, KAT1 and KAT2 are the ion channel proteins mediating K^+ influx in stomatal opening; this suggests that HD2C plays a role in modulating ABA responses (Sridha & Wu, 2006). Although, according to data-based tool GENEVESTIGATOR, high number of putative partner proteins of HD2C is only downregulated – not upregulated - by various ABA treatments similar to HD2C (Supplementary Table. S3).

hd2c-1/HD2C-C269H line showed the most growth inhibition by ABA among all transgenic lines and WT *hd2c-1/HD2C-C272H* showed lower growth in compare to *hd2c-1/HD2C-C269/272H* line and better growth in compare to WT and *hd2c-1* mutant. This is consistent

with the result from recombinant proteins which showed much stronger signal of S-nitrosylation for HD2C-C269S in compare to HD2C-C272S and confirming that Cys272 is the main target of S-nitrosylation. However, the results of WT and complement WT questionize this conclusion. This remains to be determined together with investigation about the transcription and translation level of different cysteine mutated transgenic lines, besides the treatment of those plants with NO to observe the direct effect of NO.

Although WT and *hd2c-1* plant did not show significant difference after treating with ABA, the phenotype of complemented transgenic line with *HD2C* mutated at both cysteines (*hd2c-1/HD2C-C269/272H*) in ABA-treated condition can be due to loss of S-nitrosylation; this way protein can function perfectly with a 4 histidine zinc finger which cannot be disturbed by S-nitrosylation. Similarly, the distrubtion of zinc finger doamins in examples from animal system has been shown to deactivate their function - which was discussed before.

2. 4. Hypothetical model for physiological role of S-nitrosylated HD2C

Enrichment of rRNA processing-related proteins in Co-IP list, which several of them are targets of S-nitrosylation and also are known to be down-regulated by ABA (similar to HD2C) (Supplementary Table. S3) suggests that HD2C and its putative complex may involve in an ABA/NO induced signaling pathway which leads to regulation of post transcriptional events that finally is associated with cell protein synthesis (Fig. 27). Figure 27 describes a hypothetical model for physiological role of S-nitrosylation in the putative protein complex which HD2C is involved. ABA represses the gene expression of *HD2C* and core proteins of C/D box. Since, ABA is known to induce NO formation in *Arabidopsis*, this way ABA also can regulate the function of those proteins via S-nitrosylation. This can lead to the regulation of ribosome biogenesis. HD2C protein plays a modulatory role in ABA related pathways, since it represses the expression of various genes which either lead to stomatal opening or stomatal closure. Better growth of the transgenic line mutated at the bases coding both cysteines of *HD2C* under - ABA-treated condition - suggests that S-nitrosylation of cysteines inhibits the putative positive function of HD2C (Fig. 27). This is a hypothetical model which needs to be further experimentally examined.

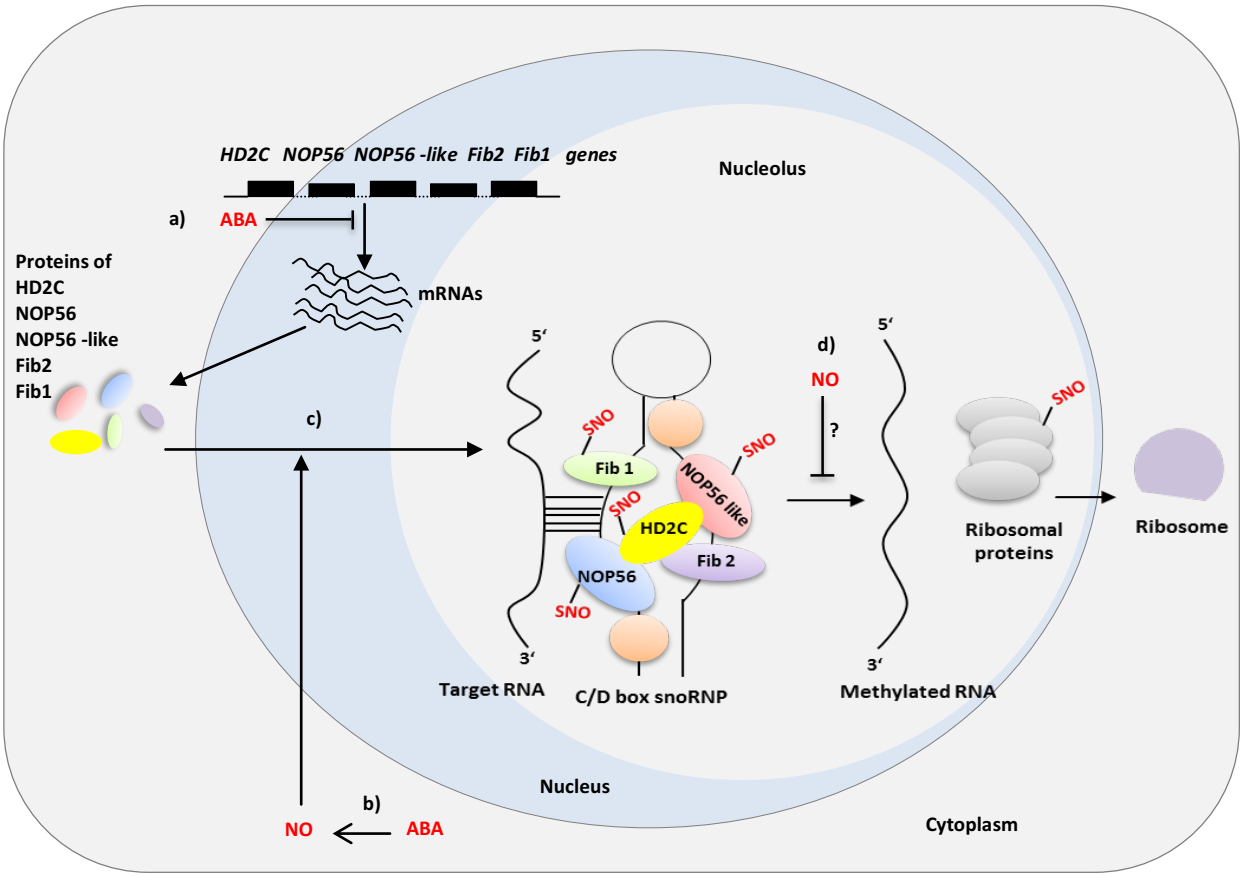

Fig. 27. Hypothetical model for physiological role of S-nitrosylated HD2C. a) ABA represses the gene expression of *HD2C* and core proteins of C/D box. Since, ABA is known to b) induce NO formation in *Arabidopsis*, this way ABA can also regulate the function of those proteins c) via S-nitrosylation (S-Nitrosylation target proteins are shown by -SNO group (Supplementary Table. S3). This can lead to regulation of ribosome biogenesis and consequently protein synthesis. Better growth of the transgenic line mutated at the bases coding both cysteines of *HD2C* under ABA treated condition suggests that d) S-nitrosylation of cysteines inhibits the putative positive part of function of HD2C.

According to GENEVESTIGATOR many putative partner proteins of HD2C are upregulated by glucose (Supplementary Table. S3). Along with, the most highlighted studies related to snoRNP complexes and some other RNA processing candidate partners of HD2C are related to metabolic/sugar stress. Fibrillarin 2 has been identified as glucose responsive gene (Kojima et al., 2007). Sucrose enhanced the Fibrillarin 2 mRNA level up to 10 fold and Nap57, Nhp2 and Nop10 (members of H/ACA snoRNP complex) from 3 to 10 fold in compare to control (Kojima et al., 2007). However, this is far from the interest of this work, since it can be interesting it is mentioned here.

Outlook

The results of this work highlighted the importance of NO in nuclear post-transcriptional mechanisms; although at starting point it was predicted to identify more S-nitrosylation candidates that are involved in gene regulation. Among the candidates, HD2 proteins were - purposely - selected to verification of function of S-nitrosylation; since they were known as HDACs and supposed to be involved in regulation of gene expression. However, results of this work demonstrated the convergence of HD2C's function with post-transcriptional mechanisms. In one side, this indicates the - often underestimated - importance of NO in post-transcriptional level and in another side; this may indicate the inefficiency of BST to identify all targets of S-nitrosylation. Therefore, I) a study especially about the role of S-nitrosylation on rRNA processing is recommended; since three core proteins of C/D box were identified as target of S-nitrosylation. However, studying those proteins is challenging, because they function within a complex and their mutation often is lethal. II) It is suggested to use some alternative approaches to identify S-nitrosylation candidates in regulation of gene expression.

Regarding biochemical function of S-nitrosylation on HD2C, an *in-vitro* pull-down of HD2C with core proteins of C/D box (Supplementary Table. S9), besides an *in-vivo* approach (e. g. bimolecular fluorescence complementation (BiFC)) is recommended. Applying NO and using HD2C with replaced cysteines in those approaches can reveal the effect of S-nitrosylation and similarly prove putative involvement of zinc finger domain in protein-protein interaction. Due to identifying HD2C in context of RNA methylation according results of Co-IP, investigating putative RNA binding and methyltransferase-related function of HD2C can be interesting.

Regarding physiological function of S-nitrosylation on HD2C, an experiment similar to ABA treatment of this work is suggested to be performed using fumigation of plants with NO or spraying them with NO donors. This way one can observe the direct effect of NO on mutant lines transformed by *HD2C* mutated at the bases coding cysteine(s).

It seems that HD2 isoforms of *Arabidopsis* are functionally redundant. Therefore, for deeper analysis of effect of S-nitrosylation on their physiological function, generation of double and triple mutants of HD2 proteins is necessary.

Materials and methods

1. Materials

1. 1. Plant material

1. 1. 1. Plants generally used in this work

Wild type (WT) plants that were used in this work were *Arabidopsis thaliana* ecotype Columbia (Col-0). The *hd2c* mutant line which was used in this work was a T-DNA insertion line (*hd2c-1* SALK_129799.19.60.n) in Col-0 background.

1. 1. 2. Transgenic lines generated in this work

Construct	Mutant background
HD2C (Endogenous promoter-Genomic DNA): *hd2c-1/HD2C*	*hd2c-1* (SALK_1297 99.19.60.n)
HD2C (Endogenous promoter-Genomic DNA) -C269H: *hd2c-1/HD2C-C269H*	
HD2C (Endogenous promoter-Genomic DNA) -C272H: *hd2c-1/HD2C-C269H*	
HD2C (Endogenous promoter-Genomic DNA) -C269/272H: *hd2c-1/HD2C-C269/272H*	

1. 2. Suspension cell culture material

1. 2. 1. Suspension cell culture

Suspension cell cultures used in this work were *Arabidopsis thaliana* ecotype Col-0.

1. 2. 2. Suspension cell culture medium

AS medium (1000 ml) pH 5.7	
Component	**Concentration/Amount**
MS (Murashige & Skoog)-Medium (MS-Fertigmedium)	3.7275 g
2,4-D	2 mg/ml
sucrose	0.03 % (w/v)
MS-Vitamin	1% (v/v)
MS-Vitamin (500 ml)	
nicotin acid	25 mg
pyridoxin-HCl	25 mg
thiamin-HClxH_2o	5.3 mg
M-Inositol	5000 mg

1. 3. Bacterial material

1. 3. 1. Bacterial strains

The bacterial strains which were used in this work were including: *Pseudomonas syringae* pv. tomato DC3000 (vir), *Pseudomonas syringae* pv. tomato DC3000 (avrRpm1), *Agrobacterium tumefaciens* GV3101 (pMP90), *Escherichia coli* DH-5α, *Escherichia coli* DB-3.1, *Escherichia coli* BL21 (DE3) cc4.

1. 3. 2. Bacterial media

Medium	Component	Concentration
King's B medium (1000 ml)	peptone	20 g
pH 7.2 -7.4	glycerol	16 ml
	K_2HPO_4	1.5 g
	$MgSO_4.7H_2O$	1.5 g
	agar for solid media	15 g
LB medium	tryptone	1% (w/v)
pH 7.0	yeast extract	0.5% (w/v)
	NaCl	0.5% (w/v)
	agar for solid media	1.5% (w/v)

ZYM-5052 medium for auto-induction of *E. coli* competent cells (BL21 (DE3) cc4) (1000 ml)			
Medium/stock solution	**Component**	**Concentration**	**Volume**
ZY medium	tryptone	1% (w/v)	958 ml
	yeast extract	0.5% (w/v)	
50X M stock solution	Na_2HPO_4	25 mM	20 ml
	KH_2PO_4	25 mM	
	NH_4Cl	50 mM	
	Na_2SO_4	5 mM	
50X 5052 stock solution	glycerol	0.5% (v/v)	20 ml
	glucose	0.05% (w/v)	
	A-lactose	0.2% (v/v)	
1 M $MgSO_4$	$MgSO_4$	2mM	2 ml
1000X trace elements	$FeCl_3$	50 mM	0.2 ml
	$CaCl_2$	20 mM	
	$MnCl_2$	10 mM	
	$ZnSO_4$	10 mM	
	$CoCl_2$	2 mM	
	$CuCl_2$	2 mM	
	$NiCl_2$	2 mM	
	Na_2MoO_4	2 mM	
	Na_2SeO_3	2 mM	
	H_3BO_3	2 mM	

1. 3. 3. Antibiotics

Name	Dilution reagent	Concentration (µl/ml)	Company
Ampicillin	ddH_2O	100	Roche, Mannheim, Germany
Kanamycin	ddH_2O	50	Sigma, Deisenhofen, Germany
Spectinomycin	ddH_2O	50	Sigma, Deisenhofen, Germany
Gentamycin	ddH_2O	25	Sigma, Deisenhofen, Germany
Rifampicin	DMF	50	Sigma, Deisenhofen, Germany

1. 3. 4. Bacterial storage solution

Component	Concentration
glycerol	65% (v/v)
1M $MgSO_4$	10% (v/v)
1M Tris-HCl	2.5% (v/v)
pH 8.0	

1. 4. DNA material

1. 4. 1. Oligonucleotide primers

Lyophilized oligonucleotides were purchased from Eurofins MWG Operon, Germany. 100 µM stock solutions of oligonucleotides were prepared in sterile ddH_2O and stored at -20°C.

Primers used for cloning cDNAs of HD2 type isoforms in Gateway system

Gene	Primer	Sequence
HD2A	B1-TEV-*HD2A*-f	5’gcaggcttcgagaatctttattttcagggcgagttctggggaattgaagttaaatcagga 3’
	B2-*HD2A*-r	5’ggggaccactttgtacaagaaagctgggtctcacttggcagcagcgtgcttg 3’
HD2B	B1-TEV-*HD2B*-f	5’gcaggcttcgagaatctttattttcagggcgagttctggggagttgcggtg 3’
	B2-*HD2B*-r	5’ggggaccactttgtacaagaaagctgggtcttaagctctacccttttcccttgccc 3’
HD2C	*HD2C*-f	5’ggggacaagtttgtacaaaaaagcaggcttcatggagttctggggtgttgaagttaagaatg 3’
	HD2C-r	5’ggggaccactttgtacaagaaagctgggtctcaagcagctgcactgtgtttgg 3’
HD2D	B1-TEV-*HD2D*-f	5'gcaggcttcgagaatctttattttcagggcgtccatgcctctcaggttaccctt 3’
	B2-*HD2D*-r	5'ggggaccactttgtacaagaaagctgggtcctacttttgcaagagggaccacaagg 3’
HD2A-*HD2D*	B1-TEV-f	5’ggggacaagtttgtacaaaaaagcaggcttcgagaatctttattttcag 3’

Primers used for cloning endogenous promoter and genomic DNA of *HD2C* in Gateway system

Primer	Sequence
B4-*HD2C*-promoter-f	5’ggggacaactttgtatagaaaagttgtcggtgataagcaactgaaattggaagataaaaagtag 3’
B1r-*HD2C*-promoter-r	5’ggggactgctttttgtacaaacttcgtgttgtgcgaggtagtgtgatctt 3’
B1-*HD2C*-genomic-f	5’ggggacaagtttgtacaaaaaagcaggcttcatggagttctggggtaaaaaacatctcctatct 3’
B2-*HD2C*-genomic-r	5’ggggaccactttgtacaagaaagctgggtctcaagcagctgcactgtgtttgg 3’

Primers used for sequencing

Primer	Sequence
M13 Forward (−20) primer	5’gtaaaacgacggccag 3’
M13 Reverse primer	5’caggaaacagctatgac 3
Mp-*HD2C*-P	5’gatcaagtacttatcaacgcagcttggg 3’
Mp-*HD2C*-G	5’cagctgtctacggagattgtcttgg 3’
AT3G05060.1	5’-gctgctaagctagacttctccg 3’
AT3G05060.1	5‘-aaaagatgggatcaggcggtc 3'
AT3G05060.1	5‘-aagctaaagtttagttctga 3‘
AT5G52470.1	5‘-aagagaactaacgttattccaa 3‘
AT1G56110.1	5‘ agagtcagggaatggtattcgtg 3‘
AT1G56110.1	5‘ actactgcttttggtgagaagc 3‘

Primers used for the characterization of *hd2c-1* mutant (HD2CT99, Salk_129799.19.60N)	
Primer	**Sequence**
LBa1 of pBIN-pROK2 for SALK lines	5'tggttcacgtagtgggccatcg 3'
HD2C-LP	5'gcgctgtctcatacttggaag 3'
HD2C-RP	5'atgaggagttgcaacatggac 3'

Primers used for site directed mutagenesis of bases coding cysteine(s) of *HD2C* to serine(s) (for protein production in *E.coil*) and to histidine (for complement transformation in *Arabidopsis*)	
Primer	**Sequence**
HD2C-C269S-f	5'gcgtttgggtccaagtcgtgcaccagaacctttacttcgg 3'
HD2C-C269S-r	5'gcacgacttggacccaaacgctcctgcagacttcggtgtc 3'
HD2C-C269H-f	5'gcgtttgggcacaagtcgtgcaccagaacctttacttcgg 3'
HD2C-C269H-r	5'gcacgacttgtgcccaaacgctcctgcagacttcggtg 3'
HD2C-C272S-f	5'gggtgcaagtcgtccaccagaacctttacttcggaaatgg 3'
HD2C-C272S-r	5'ggttctggtggacgacttgcacccaaacgctcctgcagac 3'
HD2C-C272H-f	5'gggtgcaagtcgcacaccagaacctttacttcggaaatgg 3'
HD2C-C272H-r	5'ggttctggtgtgcgacttgcacccaaacgctcctgcagac 3'
HD2C-C269/272S-f	5'caggagcgtttgggtccaagtcgtccaccagaacctttacttcggaaatggg 3'
HD2C-C269/272S-r	5'gtaaaggttctggtggacgacttggacccaaacgctcctgcagacttcggtg 3'
HD2C-C269/272H-f	5'caggagcgtttgggcacaagtcgcacaccagaacctttacttcggaaatggg 3'
HD2C-C269/272H-r	5'gtaaaggttctggtgtgcgacttgtgcccaaacgctcctgcagacttcggtg

Primers used for cloning cDNAs of C/D box proteins in Gateway system		
Gene	**Primer**	**Sequence**
AT3G05060.1	B1-NOP56-like-f (N-terminal tag)	5'ggggacaagtttgtacaaaaaagcaggcttcatggtcttagtgctatacgagacag 3'
AT3G05060.1	NOP56-like-B2-r (N-terminal tag)	5'ggggaccactttgtacaagaaagctgggtctcagtccttactcttcttttttcttctct 3'
AT3G05060.1	B1-NOP56-like-f (C-terminal tag)	5'ggggacaagtttgtacaaaaaagcaggcttcgaaggagatagaaccatggtcttagtgctatacgagacag 3'
AT3G05060.1	NOP56-like-B2-r (C-terminal tag)	5'ggggaccactttgtacaagaaagctgggtcgtccttactcttcttttttcttctctttctt 3'
AT5G52470.1	B1-Fib1-f (N-terminal tag)	5'ggggacaagtttgtacaaaaaagcaggcttcatgagacccccagttacaggagga 3'
AT5G52470.1	Fib1-B2-r (N-terminal tag)	5'ggggaccactttgtacaagaaagctgggtcctatgaggctggggtcttttgtttcttcg 3'
AT5G52470.1	B1-Fib1-f (C-terminal tag)	5'ggggacaagtttgtacaaaaaagcaggcttcgaaggagatagaaccatgagacccccagttacaggagga 3'
AT5G52470.1	Fib1-B2-r (C-terminal tag)	5'ggggaccactttgtacaagaaagctgggtctgaggctggggtcttttgtttcttcg 3'
AT1G56110.1	B1-NOP56-f (N-terminal tag)	5'ggggacaagtttgtacaaaaaagcaggcttcatggcgatgtatgttatctacgagtct 3'
AT1G56110.1	NOP56-B2-r (N-terminal tag)	5'ggggaccactttgtacaagaaagctgggtcctattcagcgctcttagacttcttcttctt 3'
AT1G56110.1	B1-NOP56-f (C-terminal tag)	5'ggggacaagtttgtacaaaaaagcaggcttcgaaggagatagaaccatggcgatgtatgttatctacgagtct 3'
AT1G56110.1	NOP56-B2-r (C-terminal tag)	5'ggggaccactttgtacaagaaagctgggtcttcagcgctcttagacttcttcttctt 3'

1. 4. 2. Plasmids

1. 4. 2. 1. Plasmids generally used in this work

Vector	Selection	Description/Use	Company
pDONR 221	Kan/Cm	Gateway entry cloning by BP recombination	Invitrogen
pDONR P4-P1R	Kan/Cm	Multi-fragment GATEWAY	Invitrogen
pDEST17	Amp	Protein expression in *E.coli*, N-terminal 6X His tag	Invitrogen
pDEST15	Amp	Protein expression in *E.coli*, N-terminal GST tag	Invitrogen
pDEST42	Amp	Protein expression in *E.coli*, C-terminal 6X His tag	Invitrogen
pB27m24GW,3	Basta	2- fragment multisite cloning vector	Invitrogen

1. 4. 2. 2. Plasmids generated in this work

Construct	AGI code	Vector
TEV-*HD2A* (cDNA)	AT3G44750	pDONR 221, pDEST17
TEV-*HD2B* (cDNA)	AT5G22650	pDONR 221, pDEST17
HD2C (cDNA)	AT5G03740	pDONR 221, pDEST17,pDEST15
TEV-*HD2D* (cDNA)	AT2G27840	pDONR 221, pDEST17
HD2C (cDNA)-C269S	AT5G03740	pDONR 221, pDEST17
HD2C (cDNA)-C272S	AT5G03740	pDONR 221, pDEST17
HD2C (cDNA) -C269/272S	AT5G03740	pDONR 221, pDEST17
HD2C (Endogenous promoter)	AT5G03740	pDONR P4-P1R
HD2C (Genomic DNA)	AT5G03740	pDONR 221
HD2C (Genomic DNA)-C269H	AT5G03740	pDONR 221
HD2C (Genomic DNA)-C272H	AT5G03740	pDONR 221
HD2C (Genomic DNA)-C269/272H	AT5G03740	pDONR 221
HD2C (Endogenous promoter -Genomic DNA)	AT5G03740	pB27m24GW,3
HD2C (Endogenous promoter- Genomic DNA)-C269H	AT5G03740	pB27m24GW,3
HD2C (Endogenous promoter- Genomic DNA)-C272H	AT5G03740	pB27m24GW,3
HD2C (Endogenous promoter- Genomic DNA)-C269/272H	AT5G03740	pB27m24GW,3
NOP56-like	AT3G05060	pDONR221, pDEST17
Fibrillarin1	AT5G52470	pDONR221, pDEST17, pDEST15, PDEST42
NOP56	AT1G56110	pDONR221, pDEST42

1. 5. Recombinanit proteins produced in this work

Construct	AGI code of gene (construct)	MW (kDa)
N-terminal 6X His-TEV-HD2A	AT3G44750	~26+(2)
N-terminal 6X His-TEV-HD2B	AT5G22650	~32+(2)
N-terminal 6X His- HD2C	AT5G03740	~31+(1)
N-terminal GST- HD2C	AT5G03740	~31+(26)
N-terminal 6X His-TEV- HD2D	AT2G27840	~22.5+(2)
N-terminal 6X His- HD2C-C269S	AT5G03740	~31+(1)
N-terminal 6X His- HD2C-C272S	AT5G03740	~31+(1)
N-terminal 6X His- HD2C-C269/272S	AT5G03740	~31+(1)
N-terminal 6X His-NOP56 like	AT3G05060	~59+(1)
N-terminal 6X-His-Fibrillarin1	AT5G52470	~33+(1)
C-terminal 6X-His-Fibrillarin1	AT5G52470	~33+(1)
C-terminal 6X His-NOP56	AT1G56110	~59+(1)

1. 6. Buffers, reagents and solutions

For total RNA extraction from *Arabidopsis* cell cultures		
	Component	**Concentration**
Tri-reagent	phenol	38% (v/v)
	guanidine thiocyanate	0.8 M
	ammonium thiocyanate	0.4 M
	sodium acetate and	0.1 M
	glycerol	5% (v/v)

For extraction and detection of nucleic acids		
Genomic DNA extraction from *Arabidopsis* plant by CTAB method		
	Component	**Concentration**
CTAB buffer	Tris-HCl	100 mM
pH 8	NaCl	1.4 M
	CTAB	2% (w/v)
	EDTA	20 mM
	β- mercaptoethanol	0.2 % (v/v)
DNA gel electrophoresis		
50x TAE running buffer	Tris base	2.0 M
	glacial acetic acid	5.71% (v/v)
	EDTA	50 mM
6x DNA loading buffer	50X TAE buffer	1X
	glycerol	30% (v/v)
	Orange G	0.25% (w/v)

For production and purification of recombinant proteins		
	Component	**Concentration**
Bacteria lysis buffer	Tris-HCl	50 mM
pH 8.0	NaCl	300 mM
	imidazole	20 mM
	β-mercaptoethanol	10 mM
	$MgSO_4$	10 mM
	protease inhibitor cocktail	1X
Buffer A	Tris-HCl	50 mM
pH 8.0	NaCl	300 mM
	imidazole	20 mM
	β-mercaptoethanol	10 mM

For nuclear protein extraction from *Arabidopsis* plants		
Nuclei isolation		
	Component	**Concentration**
Nuclear extraction buffer I (NEB I)	sucrose	0.4 M
pH 8.0	HEPES	10 mM
	$MgCl_2$	10 mM
	DTT	1 mM
	EDTA	2 mM
	PMSF	0.1 mM
	protease inhibitor cocktail	1% (w/v)
Nuclear extraction buffer II (NEB II)	sucrose	0.25 M
pH 8.0	HEPES	10 mM
	$MgCl_2$	10 mM
	PMSF	0.1 mM
	triton X-100	1% (v/v)
	protease inhibitor cocktail	1% (w/v)
Nuclear extraction buffer III (NEB III)	sucrose	1.7 M
pH 8.0	HEPES	10 mM
	$MgCl_2$	2 mM
	PMSF	0.1 mM
	triton X-100	0.15% (v/v)
	protease inhibitor cocktail	1% (w/v)
Nuclear protein extraction		
Nuclear lysis buffer (NLB-A)	Tris-HCl	100mM
pH7.4	SDS	0.05% (w/v)
	NaCl	75 mM
	triton X-100	0.1% (v/v)
	EDTA	1mM
	glycerol	10% (v/v)
	protease inhibitor cocktail	1% (w/v)
Nuclear lysis buffer (NLB-B)	Tris-HCl	50 mM
pH 7.5	KCl	150 mM
	NP-40	0.5 % (v/v)
	EDTA	0.5 mM
	DTT	1 mM
	SDS	0.05 % (w/v)
	$Na_4O_7P_2.10\ H_2O$	2.5 mM
	beta- glycerophosphate	1 mM
	Na_3VO_4	1 mM
	protease inhibitor cocktail	1% (w/v)
Nuclear lysis buffer (NLB-C)	5X IP buffer from Dynabeads® Co-IP Kit	1X
Nuclear lysis buffer (NLB-D)	5X IP buffer from Dynabeads® Co-IP Kit	1X
	NaCl	100 mM
	$MgCl_2$	2 mM
	DTT	2 mM
	protease inhibitor cocktail	1% (w/v)
Nuclear lysis buffer (NLB-E)	5X IP buffer from Dynabeads® Co-IP Kit	1X
	NaCl	75 mM
	$MgCl_2$	2 mM
	DTT	1 mM
	protease inhibitor cocktail	1% (w/v)

For nuclear protein extraction from suspension cell cultures		
	Component	**Concentration**
Protoplast isolation		
Washing buffer I	MES	20 mM
pH 5.5	mannitol	0.4 M
Nuclear protein extraction		
Washing buffer II	mannitol	0.4 M
Nuclear isolation buffer (NIB I)	HEPES	20 mM
pH 7.4	KCl	20 mM
	triton X-100	1% (v/v)
	hexylon glycol	13.8% (v/v)
	spermine	50 µM
	spermidine	125 µM
Nuclear lysis buffer	Tris-HCl	10 mM
pH 7.5	NaCl	500 mM
	triton X-100	1% (v/v)
	glycerol	10% (v/v)
	$Na_4P_2O_7$. 10 H_2O	1 mM
	protease inhibitor cocktail	1% (w/v)
For nuclear protein extraction from suspension cell cultures (Dr. Mounira Chaki)		
Extraction buffer	PIPES-KOH	20 mM
pH 7.0	hexylene glycol	2 M
	$MgCl_2$	10 mM
	β-mercaptoethanol	5 mM
	protease inhibitor cocktail	1% (w/v)
Gradient buffer	PIPES-KOH	5 mM
pH 7.0	hexylene glycol	0.5 M
	$MgCl_2$	10 mM
	triton X-100	1% (v/v)
	protease inhibitor cocktail	1% (w/v)
Lysis buffer	Tris-HCl	10 mM
pH 7.5	NaCl	500 mM
	triton X-100	1% (v/v)
	glycerol	10% (v/v)
	tetrasodium diphosphate	1 mM
	protease inhibitor cocktail	1% (w/v)

For biotin switch assay and purification of biotinylated proteins		
	Component	**Concentration**
HEN buffer	HEPES	25 mM
pH 7.7	EDTA	1 mM
	neocuproine	0.1 mM
Neutralization buffer	HEPES	20 mM
pH 7.7	NaCl	100 mM
	EDTA	1 mM
	triton X-100	0.5% (v/v)
Washing buffer	HEPES	20 mM
pH 7.7	NaCl	600 mM
	EDTA	1 mM
	triton X-100	0.5% (v/v)

For detection of released zinc ion from recombinant proteins		
	Component	**Concentration**
HS buffer	HEPES-KOH	50mM
pH 7.5	NaCl	200 mM

For Glycine-SDS polyacrylamide gel electrophoresis		
SDS-PAGE	**Component**	**Concentration/Volume**
Running gel (12%) (7.5 ml)	running gel buffer	1.87 ml
	30% Acrylamide	3 ml
	10% SDS	75 µl
	TEMED	3.75 µl
	10% APS	37.5 µl
	ddH_2O	2.51 ml
Stacking gel (~1.5 ml)	stacking gel buffer	390 µl
	30% Acrylamide	313 µl
	10% SDS	15.6 µl
	TEMED	6.25 µl
	10% APS	12.5 µl
	ddH_2O	781 µl
Running gel buffer	Tris-HCl	1.5 M
pH 8.8	SDS	0.4% (w/v)
Stacking gel buffer	Tris-HCl	0.5 M
pH 6.2	SDS	0.4% (w/v)
10X Running buffer	Tris base	250 mM
	glycine	2 M
	SDS	1% (w/v)
5X reducing loading buffer	Tris-HCl	250 mM
pH 6.8	SDS	10% (w/v)
	glycerol	50% (w/v)
	bromophenol blue	0.05% (w/v)
	DTT	1 mM
Coomassie staining solution	methanol	40% (v/v)
	acetic Acid	10% (v/v)
	brilliant blue R-250	0.1% (w/v)
Coomassie destaining solution	methanol	40% (v/v)
	acetic Acid	10% (v/v)
Silver staining		
Fixation solution	methanol	50% (v/v)
	acetic acid	12% (v/v)
	formaldehyde (37%)	0.05% (v/v)
Sensitizer	$NA_2S_2O_3$	0.2 g/l
Staining solution	$AgNO_3$	2 g/l
	formaldehyd (37%)	0.075% (v/v)
Developing solution	Na_2CO_3	60 g/l
	$NA_2S_2O_3$	5 mg/l
	formaldehyd (37%)	0.05% (v/v)
Stopping solution	methanol	50% (v/v)
	acetic acid	12% (v/v)
Storage solution	ethanol	20% (v/v)
	glycerol	2% (v/v)

For transferring and immunodetection of proteins		
	Component	**Concentration**
Transfer buffer	1X running buffer methanol	80% (v/v) 20% (v/v)
Blocking buffer	BSA milk powder tween 20	1% (w/v) 1% (w/v) 0.05% (v/v) in TBS buffer
TBS buffer pH 7.5	Tris-HCl NaCl $MgCl_2.6H_20$	10 mM 0.9% (w/v) 1 mM
TBS-T buffer	tween 20	0.05% (w/v) in TBS buffer
Antibody incubation Buffer	BSA	1% (w/v) in TBS-T buffer
Alkaline phosphatase (AP)- buffer pH 9.5	Tris-HCl NaCl $MgCl_2.6H_2O$	100mM 100mM 5mM
BCIP solution	BCIP	5% (w/v) in 100% DMF
NBT solution	NBT	5% (w/v) in 70% DMF

1. 7. Kits, reaction systems and enzymes

Name	**Company**
AccuPrime™ Taq DNA Polymerase High Fidelity	Invitrogen, Life technologies
Epigenase™ HDAC Activity/Inhibition Direct Assay Kit	Epigentek, Farmingdale, USA
Extract-N-AmpTM plant PCR kit	Sigma, Germany
Dynabeads® Co-Immunoprecipitation Kit	Novex, Life technologies
iProof™ High-Fidelity DNA Polymerase	Bio-Rad, Germany
MinElute® PCR Purification Kit	Qiagen GmbH, Hilden
QIAprep® Spin Miniprep Kit	Qiagen GmbH, Hilden
Qiagen MinElute Gel Extraction Kit	Qiagen GmbH, Hilden
Taq DNA Polymerase	Agrobiogen GmbH, Germany

All restriction endonucleases and their reaction buffers were purchased from New England Biolabs (Frankfurt, Germany) or MBI Fermentas (St. Leon-Rot, Germany).

1. 8. Chemicals and consumed material

All commonly used chemicals used were of high purity grade and purchased from Amersham Pharmacia (Freiburg), Bio-Rad Lab GmbH (München), Gibco-BRL (Eggenstein), Merck (Darmstadt), Roche (Mannheim), Roth (Karlsruhe), Serva (Heidelberg) and Sigma (Deisenhofen). Handling was performed following standard protocols and the manufacturer's instructions. If any application required chemicals from specific suppliers this

is mentioned in the text, otherwise replacement with any chemical of equal purity of any supplier should be possible. Standard laboratory material was used for all experiments and was not restricted to a specific provider.

1. 8. 1. Antibodies

Antibody	Company
Primary antibodies	
Antibiotin alkaline phosphatase antibody mAb	Sigma, Steinheim, Germany
HDT3 histone deacetylase rabbit pAb	Agrisera, Sweden
Anti-Histidine-tagged protein mouse mAb	Merck KGaA, Darmstadt, Germany
Anti-H3ac pAb	Millipore, Darmstadt, Germany
Anti-H4ac pAb	Millipore, Darmstadt, Germany
Secondary antibodies	
Anti-mouse IgG (H&L), AP conjugate	Promega, Mannheim, Germany
Anti-rabbit IgG (Fc), AP conjugate	Promega, Mannheim, Germany
Anti-rabbit-IgG-horseradish peroxidase	Promega, Medison, USA

1. 8. 2. Specific chemicals/materials

Specific chemicals/materials	
Name	**Company**
10 kDa biospin column	Biovision, California, USA
10 kD Spin column	Abcam, UK
ABA	Acros organics, Pittsburgh, USA
Biotin-HPDP	Thermo Scientific, Darmstadt, Germany
cPTIO	Invitrogen, Germany
DAF-FM	Sigma, Steinheim, Germany
DAPI	Sigma, Steinheim, Germany
Dynabeads Protein A	Thermo Scientific, Darmstadt, Germany
GSH	Sigma, Steinheim, Germany
GSNO	Enzo life science, Lörrach, Germany
High capacity neutravidin agarose resin	Thermo Scientific, Darmstadt, Germany
Micro Biospin column	Bio-Rad, Germany
Miracloth	Merck, Germany
MMTS	Sigma, Steinheim, Germany
Neocuproine	Sigma, Steinheim, Germany
Ni-NTA agarose	Qiagen, Hilden, Germany
Nylon filters	Millipore, Ireland
PAR	Sigma, Steinheim, Germany
PD-10 column	GE health care life sciences, Freiburg, Germany
PMSF	Sigma, Steinheim, Germany
Protease inhibitor cocktail	Roche, Mannheim, Germany
Protein A agarose beads	Thermo Scientific, Darmstadt, Germany
Spermidine	Sigma, Switzerland
Spermine	Sigma, Switzerland
SNAP	Sigma, Steinheim, Germany
Zinc chloride 0.1 M solution	Sigma, Steinheim, Germany
Zincon monosodium salt	Sigma, Steinheim, Germany

1. 9. Instruments and accessories

General instruments such as centrifuges, thermo blockers, PCR termal cyclers, water bathes, shakers and incubators which were used in this work, were supplied from different companies such as Thermo Life Sciences, Eppendorf, Beckmann Coulter, Heraeus and *etc*. Those instruments can be replaced with other standard qualified equipment from different companies.

Specific instruments	
Name	**Company**
Magnetic rack	Life technology, Germany
Nanodrop ND-1000 spectrophotometer	Kisker-biotech, Germany
Sonopuls HD 2070 tip sonicator system	Bandelin, Berlin, Germany
Tecan infinite M1000 pro plate reader	Tecan, Austria GmbH
Gene Pulser™ Electroporation System	Bio-Rad, Germany

1. 10. Bioinformatics tools

Description	**Webserver/Software/Online tool**
Subcellular localization	*Arabidopsis* eFP Browser (http://bar.utoronto.ca/efp/cgi-bin/efpWeb.cgi)
Nucleolar localization	*Arabidopsis* Nucleolar Protein Database (bioinf.scri.sari.ac.uk/cgi-bin/atnopdb/home)
Functional classification	MapMan Ontology of *Arabidopsis* proteins, version 3.5.1R2 (http://mapman.gabipd.org/web/guest/mapman)
Prediction of *S*-nitrosylation sites	Group-based Prediction System (GPS-SNO 1.0) software (Xue et al., 2010b)(http://sno.biocuckoo.org/)
Prediction of *S*-nitrosylation motifs	Motif-X algorithm (Chou & Schwartz, 2011) (http://motif-x.med.harvard.edu)
Aminoacid sequence alignment	Clustal2.1 (http://www.ebi.ac.uk/Tools/msa/clustalw2/)
Protein phylogenetic tree	phylogeny.fr online tool (http://www.phylogeny.fr/)
Prediction of secondary structure	PROFsec (Rost & Sander, 1993) from Predict protein webserver (https://www.predictprotein.org/)
PSI-Blast of aminoacid sequences	Predict protein webserver (https://www.predictprotein.org/)
Prediction of protein-protein interaction	SPPIDER (Porollo & Meller, 2007) (http://sppider.cchmc.org/)
Prediction of RNA binding sites	pPRINT (Kumar et al., 2008) (http://www.imtech.res.in/raghava/pprint/submit.html)

Prediction of DNA binding sites	DP-bind was used (Kuznetsov et al., 2006) (http://lcg.rit.albany.edu/dp-bind/)
Prediction of disordered regions	PONDR (Romero et al., 2001) (http://www.pondr.com/cgi-bin/PONDR/pondr.cgi)
Prediction of Molecular Recognition Features	MoRFpred (Disfani et al., 2012) (http://biomine.ece.ualberta.ca/MoRFpred/)
Prediction of motifs	MOTIF search (http://www.genome.jp/tools/motif/)
Expression and co-expression data-based tools	GENEVESTIGATOR (https://genevestigator.com/gv/index.jsp) ATTED II (http://atted.jp/)
Protein-protein interaction network analysis	*Arabidopsis* Interactions Viewer (http://bar.utoronto.ca/interactions/cgi-bin/arabidopsis_interactions_viewer.cgi)

2. Methods

2. 1. Plant methods

2. 1. 1. Growing *Arabidopsis* plants

Arabidopsis seeds were sterilized with 80% ethanol, dried then on a filter paper and grown in pots containing 2:1 ratio of soil: sand. The trays containing the pots were incubated for 2-3 days in 4°C room and then transferred to a growth chamber with ~100 µE m-2 s-1 light intensity with either long day or short day condition. Long day condition was consisting of 8 h dark and 16 h light, humidity of 65-68%, and night and day temperature of 18 and 20°C, respectively. Short day condition was consisting of 10 h light, 14 h dark, temperature and humidity of 16°C and 80% for day and 20°C and 65% for night, respectively.

2. 1. 2. Total genomic DNA extraction from *Arabidopsis* plants by CTAB method

1 to 3 leaves of 2 weeks old *Arabidopsis* plants were ground in liquid nitrogen shortly and then mixed with 250 µl of 2% CTAB buffer (1. 6). The sample was incubated at 65°C for at least 10 min and after cooling down, 200 µl of chloroform/isoamyl alcohol 24:1 was mixed with the sample by vortexing for 1 min. Sample was centrifuged for 2 min and the supernatant was transferred to a new micro tube. 1 µl of 1 % linear polyacrylamide (LPA) was added to the sample and mixed very well; three phases appeared; the upper phase was taken carefully. The sample was mixed with 600 µl of 100 % ethanol, incubated then at -20°C for at least 20 min and centrifuged at 17,000 xg for 10 min at 4°C. Afterward the pellet was

washed with 70% ethanol and dried at RT. The pellet was solved in 50 µl of ddH_2O and stored at -20°C.

2. 1. 3. *A. tumefaciens* mediated *Arabidopsis* transformation

The transformation of *Arabidopsis* was carried out by the floral dip method (Zhang et al., 2006). The *Arabidopsis* plants were grown in light day condition for 3-4 weeks and then transferred to long day condition to induce flowering. The plants with good closed flower buds were chosen for transformation and for an effective transformation the siliques were cut. A single colony of *A. tumefaciens* strain GV3101 containing Ti plasmid (pMP90) with inserted construct of interest (1. 4. 2. 2) was pre-cultured in 2 ml LB medium (1. 3. 2) with appropriate antibiotics at 28°C and 200 rpm overnight. The bacteria were centrifuged at 4,000 xg for 5 min and the pellet was re-cultured in 1000 ml flask containing 300 ml selective LB medium containing rifampicin and gentamicin for *A. tumefaciens* and appropriate antibiotic(s) for T-DNA vector at 28°C and 200 rpm until reaching its stationary phase (OD_{600} 1.5-1.6). The bacterial culture were then centrifuged at 4,000 xg for 10 min at RT and re-suspended in 5% (w/v) sucrose solution to a final OD_{600} of approximately 0.8. Silwet L-77 was freshly added to the suspension to a final concentration of 0.02-0.05%. Inflorescence shoots from 10-15 *Arabidopsis* plants were dipped into the bacterial suspension and soaked for 45 sec. Infiltrated plants were covered with transparent plastic covers for 24 h to maintain the humidity, and then they were transferred to long day condition. The seeds of T_0 generation were harvested and grown on soil. Since the vector (pB27m24GW,3) which was used in this work contained basta resistance, the 7-10 days old seedlings were sprayed with basta and the seeds of resistant T_1 generation were collected separately. The seeds of 8 individual plants were grown and sprayed by basta, the seedlings of T_2 generation which showed approximately 3:1 ratio of survival and not more were from a heterozygous parental plant with only one insertion and not multiple insertions. 30 to 50 seeds from 16 individual plants from those survived seedlings with 3:1 ratio which theoretically contained 1:2 ratio of homozygous: heterozygous lines were grown and sprayed then by basta. Afterward the seedlings which 100% survived applying basta were from a homozygous parent. The seed from at least 4 homozygous lines of each construct of interest were collected.

2. 1. 4. Nuclear protein extraction from *Arabidopsis* plants for Co-IP

2. 1. 4. 1. Nuclei isolation from *Arabidopsis* plants

The nuclei isolation for Co-IP was performed using a published protocol specifically for Co-Immunoprecipitation of nuclear proteins and chromatin immunoprecipitation (ChIP) with some modifications (Fiil et al., 2008). 10 g of 4 weeks old *Arabidopsis* rosettes were harvested from soil very carefully without injuring the plants, and then the roots were rinsed very well by floating rosettes on the water and shaking them slowly to wash the soil particles. The rosettes were dried on a tissue paper for 1-2 min and immediately were ground in liquid nitrogen until achieving a fine powder. The ground plant powder was then transferred into a 50 ml falcon tube (3.3 g per each falcon tube) and kept in ice for 5 min to let the liquid nitrogen be evaporated. 50 ml of clod nuclear extraction buffer I (NEB I) (1. 6) was added to the sample in each falcon tube and the samples were then mixed gently with a spatula and put in ice for 15 min. The samples were filtered through 4 layers of Miracloth (Merck, Germany) into a new falcon tube on ice and centrifuged at 3,000 xg for 10 min at 4℃. The supernatant was removed slowly and the tube was put upside-down on a tissue paper to remove the rest of the supernatant, this step was done also after all further washing steps. The pellet was re-suspended with 2 ml cold nuclear extraction buffer II (NEB II) (1. 6), transferred into a 2 ml tube and centrifuged at 12,000 xg for 10 min at 4℃. After this step the pellet had to look white; if it was still greenish, the last step was repeated 1 to 3 times by washing with NEB II with half concentration of triton X-100 (0.05%). Afterward, the pellet was re-suspended in 300 µl of cold extraction buffer III (NEBIII) (1. 6). Then, 500 µl of cold NEB III was added into a new 1.5 ml tube and the re-suspended pellet was layered carefully over the NEB III and centrifuged at 16,000 xg for 45 min at 4℃. The yielded pellet was the nuclei enriched fraction.

2. 1. 4. 2. Nuclear protein extraction from isolated nuclei

For finding optimum nuclear lysis buffer for Co-IP experiment, 5 variations of nuclear lysis buffers were tested: NLB-A, NLB-B, NLB-C, NLB-D and NLB-E (1. 6). Finally, the NLB-E was chosen due to optimum amount of yielded protein and no protein degradation after sonification which both was checked by SDS-PAGE and also successful subsequent Co-IP experiment without losing the interacting proteins and at the same time with lowest background proteins.

The nuclei enriched fraction (2. 1. 4. 1) was re-suspended in 300 µl nuclei lysis buffer (NLB-E) and sonicated for 25 s with 20% power and 3 cycles for 7 times with 1 min intervals using 2 mm sonicator tip of Sonopuls HD 2070 tip sonicator system (Bendalin, Germany). The sonicated sample was centrifuged at 12,000 xg for 15 min at 4℃. The supernatant containing nuclear proteins either was used immediately for Co-IP or was frozen in liquid nitrogen and stored at -80°C.

2. 1. 5. Treating *Arabidopsis* plants with ABA

Arabidopsis plants were grown in long day condition. The 2 weeks old plants were sprayed 3 times per week with 100 µM ABA and the control plants were treated with the same concentration of ABA solvent (ethanol). The treatment was stopped before control plants start to flower, the rosette diameter was measured for control and treated plants. The data were analyzed by Anova single factor. 24 plants for each line were used for each biological replicate. Plants from 4 different homozygous lines were used for each transgenic line.

2. 2. Cell culture methods

2. 2. 1. Growing and maintenance of *Arabidopsis* suspension cell cultures

2.2-2.4 g of *Arabidopsis* suspension cell cultures were transferred into 200 ml flasks containing 40 ml of AS medium (1. 2. 2). The cell cultures were maintained at 25-26°C on a rotary shaker (120 rpm) in darkness and sub-cultured into fresh medium every 7 days.

2. 2. 2. Inoculation of *Arabidopsis* suspension cell cultures by *P.syringae*

Arabidopsis cell suspension cultures were grown in dark at 26°C (126 rpm) in AS medium (1. 2. 2). The 6-days old cell cultures were inoculated with 1×10^6 CFU/ml of *Pseudomonas syringae pv. tomato (Pst)* DC3000 containing avirulent *Pst* DC3000 *avrRpm1* (*Pst avr*) and the virulent *Pst* DC3000 (*Pst vir*), and were incubated for 2 and 13 h, and only 13 h, respectively. Afterward, the cell cultures were washed through a 150 µm pore size membrane (Merck, Germany) to filter the bacteria. The control samples were treated with 10 mM $MgCl_2$.

2. 2. 3. Detection of NO in pathogen-treated *Arabidopsis* cell cultures

To monitor the NO accumulation in *Arabidopsis* suspension cell cultures after infection with pathogen, the DAF-fluorescence was measured by Tecan reader (1. 9). Cell cultures were incubated with 5 µM DAF-FM for 1 h at 26°C (200 rpm) in darkness. Afterward, samples were washed three times with AS medium (1. 2. 2) and inoculated with 1×10^6 CFU/ml *Pst avr* for

28 h. As a control, cell cultures were incubated with 5 mM $MgCl_2$. NO production was estimated by measuring fluorescence intensity every 10 min for 28 h. Fluorescence was expressed as relative fluorescence units.

2. 2. 4. Total RNA extraction from *Arabidopsis* cell cultures

100-150 mg of *Arabidopsis* cell suspension cultures were ground in liquid nitrogen and transferred to cold 2 ml micro tubes. 1 ml of Tri-reagent (1. 6) was added to the sample under the hood and the sample was rotated in 1,400 rpm at RT for 5 min. 200 µl ice cold chloroform was added to the sample and it was shaken overhead for 15 sec. Then, the sample was incubated at RT for 2-3 min and centrifuged at 18,800 xg for 20 min at 4 °C. Then the upper phase was transferred slowly to a new 2 ml micro tube. Subsequently, 500 µl ice cold isopropanol was added to the sample and it was shaken overhead for 15 sec. The sample was then incubated at 4°C for 30-60 min and centrifuged at 17,500 xg for 10 min at 4 °C. The pellet was washed twice using 1 ml ice cold 70% ethanol at 17,500 xg for 10 min at 4 °C. The pellet was floated in the ethanol between last two washing steps. The pellet was dried for 30 min at RT and afterward dissolved in 25-50 µl sterile ddH_2O. The RNA sample was stored at -80°C.

2. 2. 5. Nuclear protein extraction from *Arabidopsis* suspension cell cultures

2. 2. 5. 1. Protoplast isolation from *Arabidopsis* cell cultures

6 days old *Arabidopsis* suspension cell cultures grown in 40 ml AS medium (1. 2. 2) (from 2.2-2.4 g starting cell culture) were transferred to a 50 ml falcon tube and washed twice with washing buffer I (1. 6) by centrifuging at 300 xg for 12 min at 23°C. The cells were re-suspended in washing buffer I (1. 6) containing 0.5 % cellulase and 0.5% macerozyme, transferred to 200 ml flasks and incubated then at 25-26°C in darkness with gentle agitation (150 rpm) for 5 h. The isolation of protoplasts was observed every 1 h under microscope.

2. 2. 5. 2. Nuclei isolation from isolated protoplasts

The isolated protoplasts (2. 2. 5. 1) were transferred to a 50 ml falcon tube, centrifuged at 300 xg and 4°C for 12 min and then washed twice with washing buffer II (1. 6) at 300 xg for 12 min at 4°C. The protoplasts then were re-suspended by 40 ml NIB I buffer (1. 6), filtered by a 30 µm nylon membrane (Merck, Germany) and centrifuged at 1,000 xg for 12 min at 4°C. Afterward, the pellet was re-suspended in 1ml NIBA (NIB I containing 1% protease

inhibitor cocktail), layered on 1.5 M sucrose (2.3 M sucrose in NIB I) which its level in a 30 ml tube of ultracentrifuge was corresponded to level of 800 µl liquid in a 1.5 ml tube and centrifuged at 10,000 xg and 4°C for 20 min. The nuclei enriched fraction was re-suspended in 1 ml NIBA and transferred to a 1.5 ml tube. Nuclei were visualized by DAPI staining and washed 3 times with NIBA at 10,000 xg for 5 min at 4°C.

2. 2. 5. 3. Nuclear protein extraction from isolated nuclei

The nuclei enriched fraction (2. 2. 5. 2) was re-suspended in 340 µl nuclear lysis buffer (1. 6) and sonicated using 5 mm sonicator tip of Sonopuls HD 2070 tip sonicator system (Bendalin, Germany) with 10 % power and 5 cycles for 25 s with 1 min intervals for 7 times. The lysate was centrifuged at 12,000 xg for 15 min at 4°C. The supernatant (nuclear proteins) was taken and stored at -80°C.

2. 2. 5. 4. Isolation of *Arabidopsis* nuclei and extraction of proteins from nuclear enriched fractions

Nuclei were extracted using the method described by Folta and Kaufman, 2006 [34] with some modifications. 7 g of *Arabidopsis* cell suspension cultures were washed and resuspended in two volumes of cold extraction buffer (1. 6). Afterward, the cell cultures were homogenized gently and filtered through filter mesh 80 µm. The lysate was diluted to a total volume of 30 ml by extraction buffer. 1% triton X-100 was added to the lysate and incubated for 30 min. The percoll density gradient was prepared in gradient buffer (1. 6) by layering 80% percoll (6 ml) on 30% percoll (6 ml). The lysate was layered onto the top of the 30% percoll layer and centrifugated at 2000 xg for 30 min at 4 ^{o}C. The nuclear fraction presented as a white band at the interface between the 30% and 80% fractions was gently pipetted on the top of 30% percoll (6 ml), and centrifuged at 2000 xg for 10 min at 4 ^{o}C to wash the nuclei. The pellet contained multiple layers; the nuclei reside in the top layer, which was resuspended in 1.5 ml of gradient buffer and centrifuged at 800 xg for 10 min at 4 ^{o}C. The nuclei were again reside in the top of the pellet, were gently resuspended in 350 µl of lysis buffer (1. 6). The intactness of the nuclei was analysedby DAPI staining. The lysate was sonicated and centrifuged at 12000 xg for 15 min at 4 °C. The supernatant containing nuclear enriched fraction was used freshly for the biotin switch assay (Dr. Mounira Chaki).

2. 3. Molecular biology methods

2. 3. 1. Bacterial methods

2. 3. 1. 1. Growing and storage of bacterial strains

Virulent (vir) and avirulent (avrRpm1) strains of *P.syringae.* pv. tomato Pst. DC3000 (1. 3. 1) were grown in King's B medium (1. 3. 2) containing 50µg/ml Rifampicin and 50µg/ml Kanamycin at 28°C overnight (liquid culture) or up to 2 days (solid culture). *A. tumefaciens* strains (1. 3. 1) were grown in LB medium (1. 3. 2) containing 50µg/ml Rifampicin and 50µg/ml Gentamycin at 28°C overnight (liquid culture) or up to 2 days (solid culture). *E.coli* strains (1. 3. 1) were grown in LB medium containing appropriate antibiotics at 37°C. The duration of incubation was dependent of the aim of experiment up to 18 h.

For long term storage, the bacteria (*P. syringae*, *E. coli* and *A. tumefaciens*) were grown in liquid media consisting of the appropriate antibiotics. 1 volume of glycerol storage solution (1. 3. 4) was mixed with bacterial suspension. The samples were then frozen in liquid nitrogen and incubated at -80°C.

2. 3. 1. 2. Heat shock transformation of *E. coli*

An aliquot of competent *E. coli* cells (DH5α or DB3.1) and competent *E.coli* expression cells (BL21 (DE3) cc4) was thawed on ice, mixed with approximately 100-200 ng plasmid DNA (1-2 µl), incubated for 10 min on ice and then incubated in a 42°C water bath for 45 sec and subsequently cooled on ice for 2 min. After addition of 500 µl LB medium (1. 3. 2), cells were incubated for 1 h at 37°C with gentle agitation. Cells were then centrifuged at 4,000 xg for 2 min at RT. The pellets were re-suspended with 50-100 µl of LB medium and plated on the selective LB medium containing corresponding antibiotics.

2. 3. 1. 3. Electroporation of competent *A. tumefaciens* cells

An aliquot of electro competent cells of *A. tumefaciens* GV3101 containing the helper Ti plasmid (pMP90) was thawed on ice and mixed with 80-100 ng (~1 µl) of plasmid DNA. The mixture was then transferred to a dry, pre-chilled 0.1 cm electroporation cuvette. Electroporation was performed with the Gene-Pulser electroporation system (Bio-Rad, Germany) using the following conditions: Capacitance 25 µF, Voltage 1.25 kV and Resistance 400 Ω. 700 µl of LB medium (1. 3. 2) was immediately added to the cuvette and the bacterial suspension transferred to a new 1.5 ml micro tube. The culture was incubated at 28°C for 1 h with gentle agitation. The cells were centrifuged at 4,000 xg for 2 min at RT and the pellet

then re-suspended in 50 to 100 µl LB medium and cultured on selective LB medium containing rifampicin and gentamicin for *A. tumefaciens* and appropriate antibiotic for T-DNA vector. The cultures were incubated at 28°C for 2 days and the grown colonies were verified for the insertion of the DNA fragment via colony PCR (2. 3. 3. 4) or enzyme digestion (2. 3. 3. 3) and further sequencing (2. 3. 3. 5).

2. 3. 1. 4. Recombinant protein production in *E.coli*

The destination vectors from Gateway cloning technology which carried the gene of interest (expression clones) were heat shock transformed to *E. coli* BL21 (DE3) cc4 competent expression cells (2. 3. 1. 2). An aliquot of transformed cells was pre-cultured in LB medium (1. 3. 2) with appropriate antibiotics for 4 h at 37°C. The cells were then centrifuged at 4,000 xg at 4 °C for 5 min. The pellet was re-suspended in 1 ml fresh LB medium and cultured in 250 ml of ZYM-5052 auto inductive medium (Studier, 2005) (1. 3. 2) containing corresponding antibiotic(s), incubated then at 37 °C (230 rpm) until achieving optimal growth at $O.D_{600}$ nm of 1 to 2, and further incubated at 18 °C (230 rpm) overnight. The cells were then centrifuged at 8,000 xg for 20 min at 4 °C and the pellet was re-suspended with 4 volumes of bacterial lysis buffer (1. 6). The sample was sonicated using 5mm sonicator tip of Sonopuls HD 2070 tip sonicator system (Bendalin, Germany) with 60% power, 3 cycles for 3 min and 3 times with 1 min intervals and then centrifuged at 17,000 x g for 1 h at 4°C. The supernatant was taken and the recombinant proteins were purified using affinity chromatography (2. 4. 3).

2. 3. 2. DNA methods

2. 3. 2. 1. Determination of nucleic acids concentration

The concentrations of DNA and RNA samples were determined by measuring the absorption using Nanodrop ND-1000 spectrophotometer (Kisker-biotech, Germany) at 260 and 280 nm, respectively. The corresponding buffer or ddH_2O was used as the blank. The purity of total DNA or RNA was evaluated by the ratio of A260/A280 which yields information about the contaminants which could be absorbed at 280 nm. A ratio of approximately 1.8 and 2.0 is considered to be an indication of high quality of DNA and RNA, respectively. The purity was further controlled by the ratio of A260/A230, which had to be in the range of 2.0 to 2.2 in the loss of contaminants absorbing at 230 nm.

2. 3. 2. 2. Designing oligonucleotide primers

Specific primers suitable for Gateway cloning system were designed according to the strategy of cloning and using the Gateway® Technology manual (https://tools.lifetechnologies.com/content/sfs/manuals/gatewayman.pdf) (1. 4. 1). The primers for site-directed mutagenesis were designed using QuickChange™ site-directed mutagenesis with some modifications (Zheng et al., 2004) (1. 4. 1). The primers for characterization of *hd2c-1* mutant (SALK_129799.19.60.n) were downloaded from the website of SIGnal Salk Institute Genomic Analysis Laboratory (http://signal.salk.edu/cgi-bin/tdnaexpress) (1. 4. 1).

2. 3. 2. 3. Polymerase chain reaction (PCR)

To amplify DNA sequences (with approximate sizes between 700bp and 3Kb) from template double-stranded DNA, PCR was performed by repeated cycles of denaturation, primer annealing and elongation. The annealing temperature and the duration of elongation step were dependent on the melting temperature of primers and the size of the DNA fragment of interest, respectively. The elongation *in- vitro* was catalyzed by Taq DNA Polymerase (6805-P, Agrobiogen GmbH, Germany), AccuPrime™ Taq DNA Polymerase High Fidelity (12346-086, Invitrogen by life technologies, Germany) and iProof™ High-Fidelity DNA Polymerase (1725300, Bio-Rad, Germany) to decrease the mismatch rate. PCR reaction was carried out using an automated Multicycler with the standard programs of the different DNA polymerases with some adjustments for optimizing each reaction according to different properties. The PCR mixtures for the different polymerases were employed using their manuals as follow:

The PCR mixtures using different DNA polymerases

Component	**Concentration**		
	Agrobiogen Taq polymeras	**AccuPrime™ Taq DNA Polymerase**	**iProof™ DNA Polymerase**
Template DNA	~2 ng - 20 ng	~2 ng - 20 ng	~2 ng - 20 ng
Reaction buffer	1X	1X	1X
25 mM $MgCl_2$	1.5 mM	-	-
20 mM dNTPs	0.2 mM	0.2 mM	0.2 mM
10 µM forward primer	0.5 µM	0.5 µM	0.5 µM
10 µM reverse primer	0.5 µM	0.5 µM	0.5 µM
DNA polymerase	1 unit	0.4 unit	0.4 unit
Sterile ddH_2O	-	-	-

The PCR reactions using different DNA polymerases						
Step	**Temperature (°C)**			**Time**		
	Agrobiogen Taq polymeras	**AccuPrime™ Taq DNA Polymerase**	**iProof™ DNA Polymerase**	**Agrobiogen Taq polymeras**	**AccuPrime™ Taq DNA Polymerase**	**iProof™ DNA Polymerase**
1 (Denaturing)	94	94	98	1-2 min	2 min	30 sec
2 (Denaturing)	94	94	98	15-30 sec	30 sec	10 sec
3 (annealing)	X	X	X	15-30 sec	30 sec	1 min
4 (Elongation)	72	68	72	1 min/ kb	1 min/ kb	1 min/ kb
5 (Elongation)	72	68	72	10 min	10 min	10 min
6 (Storage)	4	4	4	-	-	-
* The steps 2-4 were performed between 25-35 cycles.						

2. 3. 2. 3. 1. Touch-down PCR

For the amplification of endogenous promoter and genomic DNA of HD2C, touch-down PCR was performed.

The touch-down PCR reaction using iProof™ High-Fidelity DNA Polymerase		
Step	**Temperature (°C)**	**Time**
1 (Denaturing)	98	3 min
2 (Denaturing)	98	15 sec
3 (annealing)	68 -53	45 sec
4 (Elongation)	72	2 min
5 (Elongation)	72	10 min
6 (Storage)	4	-
*In touch-down PCR, at first 16 cycles the annealing temperature was reduced 1 °C per cycle (from 68 to 53°C). The steps 2 to 4 were performed 35 cycles.		

2. 3. 2. 3. 2. PCR-based site directed mutagenesis of cysteine residue(s) of HD2C

Site directed mutagenesis of cDNA and genomic DNA of *HD2C* was performed at Cys269, Cys272 and Cys269/272 to serine and histidine, respectively. The mutated primers were designed based on the QuickChange™ site-directed mutagenesis with some modifications (Zheng et al., 2004) (1. 4. 1). For amplification, 50 ng of plasmid DNA (*HD2C* in pDONR 221) was used in a total volume of 15 µl, including 1 µM of each primer, 0.4 µl of 20 mM dNTPs, and 1 unit of i-Proof DNA polymerase (Bio-RAD, Germany). After denaturation (30 s at 98°C), 20 cycles were conducted, consisting of 25 s at 98°C, 25 s at 60°C, and 10 min at 72°C which followed by a final extension step at 72°C for 10 min. Subsequently, the parental and hemiparental template DNA was digested with 1 unit DpnI by incubating at 37°C for 2 h. The mutation was verified by sequencing (2. 3. 3. 5).

2. 3. 2. 3. 3. PCR-based genotyping of mutant plants

To verify the homozygous mutants, the PCR-based genotyping was performed using specific primers (LBa1 of pBIN-pROK2 for SALK lines, HD2C-LP, HD2C-RP) (1. 4. 1) from the website of SIGnal Salk Institute Genomic Analysis Laboratory (http://signal.salk.edu/cgi-bin/tdnaexpress) and Extract-N-AmpTM plant PCR kit (sigma, Germany) following the manufacturer's instructions. According to the Salk institute website (Fig. 28), by using the three primers (LBb1.3+LP+RP) for SALK lines, WT (no insertion) should yield a product of about 900-1100 bps (from LP to RP), homozygous lines (insertions in both chromosomes) will produce a band of 410+N bps (from RP to insertion site 300+N bases, plus 110 bases from LBb1.3 to the left border of the vector), and heterozygous lines (one of the pair chromosomes with insertion) will yield both bands.

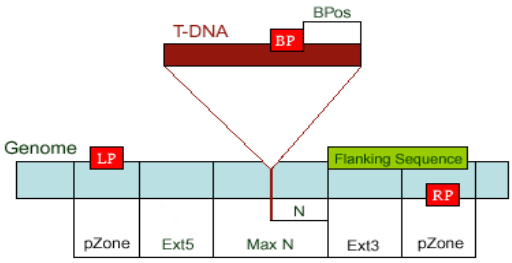

Fig. 28. SALK T-DNA verification. According to the Salk institute website (http://signal.salk.edu/cgi-bin/tdnaexpress) by using the three primers (LBb1.3+LP+RP) for SALK lines, WT should yield a product of about 900-1100 bps (from LP to RP), homozygous lines will produce a band of 410+N bps (from RP to insertion site 300+N bases, plus 110 bases from LBb1.3 to the left border of the vector), and heterozygous lines will yield both bands.

The product size should be 200 bases larger if LBa1 is used instead of LBb1.3 (http://signal.salk.edu/cgi-bin/tdnaexpress).

2. 3. 2. 4. DNA gel electrophoresis

Nucleic acids were separated in 1% agarose gels and their sizes were determined by loading an appropriate standard size marker. Agarose was dissolved in 1X Tris-acetate-EDTA [TAE] buffer (1. 6) containing 0.5 µg/mL ethidium bromide. The samples were mixed with 6x DNA loading buffer (1. 6) and loaded on the gels. Then gels were run in 1x TAE buffer at 5-10 V/cm for 30 min to 1 h. The DNA fragments were visualized under UV light and recorded with Gel Doc 2000 (Bio-Rad, Munich, Germany).

2. 3. 2. 5. Purification of PCR products

To purify PCR products from the agarose gels, target DNA bands were cut from the gel under UV light and transferred into a sterile micro tube. The extraction was carried out with the Qiaquick^{R} Gel Extraction Kit (Qiagen, Hilden, Germany) following the manufacturer's manual.

The purification of the target DNA fragments from the primers, nucleotides and salts of the previous enzymatic reactions, was performed using the QIAquick^{R} PCR Purification Kit (Qiagen, Hilden, Germany) following manufacturer's instructions.

2. 3. 2. 6. Total cDNA synthesis from total RNA

250 ng/ µl Random Hexamer Primer and 2.5 µg of total RNA were transferred into 0.5 ml micro tube and the volume was reached to 15 µl by sterile ddH_2O and centrifuged briefly. The sample was incubated at 65°C for 5 min, then incubated in ice for 1 min and centrifuged shortly. The following reagents were added to the sample in volume of 10 µl: 5 µl 5x First Strand Buffer, 2.5mM dNTPs, 0.1M DTT and 1 µl RNaseOUT and centrifuged briefly. Afterward, sample was incubated at 25°C for 10 min and then at 42°C for 2 min. 1 µl of Superscript II was added to the sample and was incubated in 42°C for 60 to 75 min and in 70°C for 15 min. The sample was mixed and incubated in ice for 1 min. The total cDNA sample was stored at -20°C.

2. 3. 3. Gateway cloning

2. 3. 3. 1. Molecular cloning using single fragment or multisites two fragment Gateway^{TM} recombination technology

The Gateway^{TM} recombination technology was employed for cloning of all constructs of this work. The cloning of the target DNA to the destination vector was achieved by two steps of site-specific recombination reactions, BP and LR cloning following manufacturer's instructions. Via BP cloning, an attB-flanked DNA fragment and an attP containing donor vector generated an entry clone. And LR cloning was employed to generate an expression clone from an attL-contaning entry clone and an attR-containing destination vector.

For single fragment cloning, the full-length cDNAs encoding *HD2A*, *HD2B*, *HD2C*, and *HD2D* were amplified by PCR from total cDNA (2. 3. 2. 6) using primers containing specific attachment sites allowing recombination reactions (1. 4. 1). TEV cleavage site also was

included in the primers to be able to cleave the produced proteins from the tag (1. 4. 1) (in case that it was necessary). PCR fragments were recombined into the pDONR221 vector (1. 4. 2. 1) via BP cloning and further recombined via LR cloning into the pDEST17 destination vector (1. 4. 2. 1) which represents a 6X-His-tag in N-terminal region of the produced proteins. The same procedure of LR cloning was done using the entry vector containing cDNA of *HD2C* which had already been subjected to site directed mutagenesis at Cys269, Cys272 and Cys269/272 to serine (2. 3. 2. 3. 2).

For the multisite two fragments cloning, the endogenous promoter and genomic DNA of *HD2C* were amplified via touch-down PCR (2. 3. 2. 3. 1) from total genomic DNA (2. 1. 2) using primers containing specific attachment sites allowing recombination reactions (1. 4. 1). The endogenous promoter and genomic DNA were inserted into pDONR P4-P1R (1. 4. 2. 1) and pDONR 221 via BP cloning, respectively (Fig. 29). Those two entry clones containing the desired fragments were then recombined via an LR cloning with the destination vector pB27m24GW,3 (1. 4. 2. 1) to generate the final expression clone. The same procedure was performed for generation of expression clones in destination vector pB27m24GW,3 using endogenous promoter of *HD2C* and its genomic DNA which has been site directed mutated at Cys269, Cys272 and Cys269/272 to histidine (2. 3. 2. 3. 2).

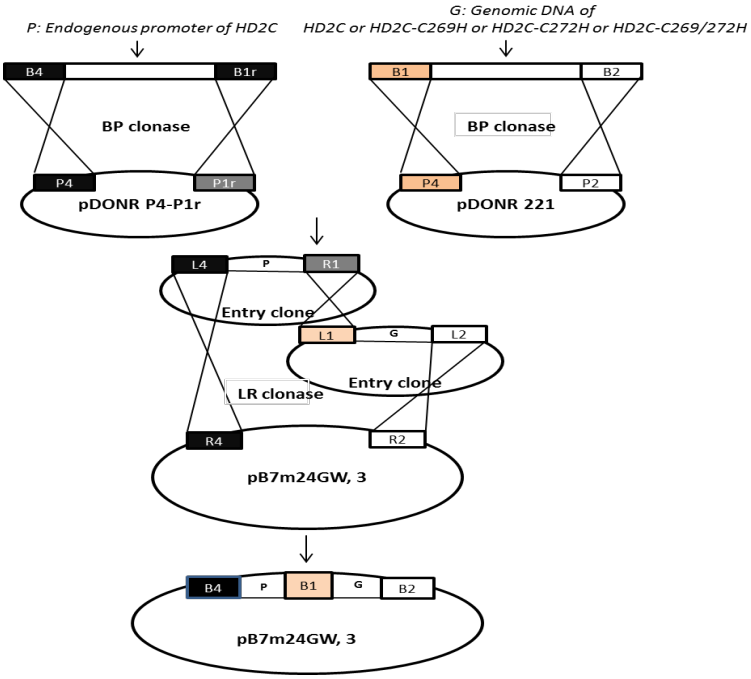

Fig. 29. Illustration of the GATEWAY™ two-fragment vector recombination method. This method was used for production of constructs for transformation of endogenous promoter of *HD2C* and its genomic DNA (and also its genomic DNA mutated at cysteine(s)) to *hd2c- 1* mutant background (1. 1. 2).

2. 3. 3. 2. Miniprep plasmid DNA preparation

Plasmid DNA from *E. coli* or *A. tumefaciens* was isolated with Qiaprep^{R} Spin Miniprep Kit (Qiagen, Hilden, Germany), following the manufacturer's instructions.

2. 3. 3. 3. Plasmid DNA digestion by restriction endonucleases

The insertion of target DNA fragments into the vectors was verified by restriction digestions performed with restriction enzymes from New England Biolabs (Frankfurt am Main, Germany) or Fermentas (Thermo Scientific, Germany) using the appropriate buffer and temperature according to the manufacturer's recommendations. 400-600ng of plasmid DNA or PCR products were digested in a mixture containing 1 x reaction buffer and 5 units of restriction endonuclease (s). The mixture was incubated at 37°C for about 2-4 h in a thermoblock. After digestion, the enzymes were deactivated for 10 min at 65°C and the fragment(s) sizes were checked by agarose gel electrophoresis.

2. 3. 3. 4. Colony PCR

Colony PCR was performed, to determine the presence or absence of a target DNA fragment in vectors which were transformed in the *E. coli* or *A. tumefaciens* competent cells. A Single colony which was cultured on the LB (1. 3. 2) plates containing appropriate antibiotics was picked using a sterile toothpick and transferred into PCR reaction tubes. Samples were supplied with PCR reaction mixture for taq polymerase and PCR was carried out (2. 3. 2. 3).

2. 3. 3. 5. DNA Sequencing

To get to know about the order of sequence of isolated plasmid DNA or the purified DNA fragments, the samples were prepared by mixing the DNA fragments and appropriate oligonucleotide primer according to the manufacturer's instructions and processed by Eurofins MWG GmbH (Ebersberg, Germany).

The required cDNA, promoter and genomic DNA sequences of the genes were downloaded either from The Arabidopsis Information Resource (TAIR) database (https://www.arabidopsis.org/) or National Center for Biotechnology Information (NCBI) database (http://www.ncbi.nlm.nih.gov/). The sequences of all PCR products were aligned with those from the original databases and their complete similarity was proved.

2. 4. Protein biochemical methods

2. 4. 1. Determination of protein concentration by Bradford assay

Nine serial dilutions of bovine serum albumin (BSA) standard with a range of 1 µg protein were prepared in 800 µl of ddH_2O, then 200 µl of 5x Bradford reagent was added to the samples and mixed very well. The samples incubated for 10 min at RT. The absorbance was measured at 595 nm and the data of 3 replications were used for drawing the standard curve. The equation of the standard curve was used for estimating the concentration of protein extracts and recombinant proteins.

2. 4. 2. Protein separation and immunodetection

2. 4. 2. 1. SDS polyacrylamide gel electrophoresis

Separation of proteins on polyacrylamide gels was carried out with a Mini-PROTEAN Tetra Cell system (Bio-Rad, Germany). Proteins were separated according to their molecular weight with 12% resolving gels. Gels were prepared as described by Sambrook and Russell (2006) according to Laemmli (1970) (Sambrook & Russell, 2006, Laemmli, 1970) (1. 6). Protein samples were mixed 1:2 with 2x reducing sample buffer (1. 6) and boiled for 5 min at 95°C before loading into the gel pockets. The gels were casted according to the manufacturer´s handbook. Gels were run at a constant current of 25 mA per gel with an Electrophoresis Power Supply EPS 601 (GE Healthcare, Freiburg, Germany). All gels were run until the bromophenol blue dye front reached the bottom of the gel. The samples were separated together with Page Ruler Pre-stained protein ladder (10-170 kDa, Thermo Scientific, Germany) for estimation of molecular masses of the separated proteins.

2. 4. 2. 1. 1. Coomassie staining

The SDS-PAGE gels were stained in coomassie staining solution (1. 6) for 1 to 2h at RT and destained with coomassie destaining solution (1. 6) for a few h or overnight until the background color was completely cleared.

2. 4. 2. 1. 2. Silver staining

The SDS-PAGE gels were silver stained at RT. The gels were fixed in fixation solution (1. 6) for 30 min and washed in 50% ethanol for 30 min. The gels were then sensitized with 0.2g/L

$Na_2S_2O_3$ for 1 min and washed shortly with ddH_2O. The gels were stained by staining solution (1. 6) for 20 min and washed shortly. Then, the gels were developed using developing solution (1. 6) up to 10 min until sufficient coloring. The developing was terminated using stop solution (1. 6) for 10 min. The gels were kept in storage solution (1. 6) at 4°C.

2. 4. 2. 1. 3. Western blot analysis

Separated proteins in an SDS gel were transferred to Hybond-LFP PVDF membranes with 0.2 µm pore size (GE Healthcare, Freiburg, Germany) using Hoefer SemiPhor semidry transfer unit (GE Healthcare, Freiburg, Germany). The membrane was activated by transfer buffer (1. 6) containing 20% methanol. A blotting unit consisted of 3 sheets of Whatman 3 MM paper, the activated membrane, the polyacrylamide gel and again 3 sheets of Whatman 3 MM paper. The gel and Whatman papers were soaked in transfer buffer for a few min. The transfer was performed based on the size of the membrane (2.5 MA per cm2) for 45 min. After transfer, the membrane was stained for 5 min with Ponceau-S, documented and then destained by water. The membrane was then blocked in blocking buffer (1. 6) with gentle shaking for 30 min at RT, and subsequently incubated with the primary antibody in the required dilution in TBST buffer (1. 6) with gentle shaking at 4°C overnight. The unbound primary antibody was washed using 2 washing steps of TBST buffer and 1 washing step by TBS buffer (1. 6) for 10 min with gentle shaking at 4°C. If the first antibody was not conjugated with AP, the membrane was incubated with an appropriate secondary antibody conjugated with AP with gentle shaking at 4°C for 2h. The similar washing steps with TBST and TBS was performed for removing the extra secondary antibody. Colorimetric detection of marked proteins was performed by incubating the membrane in 3 ml AP-buffer (1. 6) supplemented with 10 µl of NBT solution (1. 6) and 10 µl of BCIP solution (1. 6) and the stained membrane was documented.

2. 4. 2. 1. 1. Dot blot analysis

To find the optimum working concentration of antibodies, and get to know if the antibody is sensitive enough to detect low amounts of protein, a dot blot analysis was performed. A serial dilution of HD2C recombinant protein was prepared, afterward 5 µl of each dilution was put on small circles which already were marked on the Hybond-LFP PVDF membranes with 0.2 µm pore size (GE Healthcare, Freiburg, Germany) and the membranes then dried. The membranes were blocked with 5% BSA with gentle shaking for 30 min at RT. Then, they

were incubated in different dilutions of antibody in TBST (1. 6) with gentle shaking at RT for 1 h. After washing membranes 2 times in TBST buffer and 1 time in TBS buffer for 10 min with gentle shaking at 4°C, they were incubated with secondary antibody with gentle shaking for 30 min at RT and the same washing steps were performed. Colorimetric detection was done using AP-buffer (1. 6) supplemented with NBT and BCIP solutions (1. 6) similar to western blot analysis (2. 4. 2. 1. 4).

2. 4. 3. Purification of His-tagged recombinant proteins by Ni^{2+}-affinity chromatography

All the recombinant proteins produced in this work (HD2A, HD2B, HD2C, HD2D and HD2C-C269S, HD2C-C272S and HD2C-C269/272S) contained an N-terminal 6X-histidine tag which represents high affinity to metals such as Nickel. To purify the recombinant proteins produced in *E. coli* from the bacterial lysate (2. 3. 1. 4), the Ni^{2+}-affinity chromatography was used. The supernatant sample containing soluble recombinant proteins yielded from lysing bacteria (2. 3. 1. 4) was loaded in a column containing 250 µl of Ni-NTA agarose which has already been equilibrated with buffer A (1. 6). The column containing the sample was incubated at 4 °C for 30 min with overhead mixing with 5 min intervals. The column was then washed 3 times with 30 ml of buffer A and once in between with buffer A and 1 M NaCl. The bound proteins were eluted by adding 1 ml of buffer B (300 mM imidazole in buffer A) to the column and waiting for 5 min. The eluted sample was transferred to a micro tube containing 50 µl of glycerol 100%, mixed very well, then was frozen in liquid nitrogen and stored at -80°C. An aliquot of the eluted sample was loaded on SDS gel. The target protein was detected by coomassie stained SDS-PAGE and the presence of the histidine tag on the recombinant protein was detected via western blot analysis using anti-histidine antibody. Before doing biotin switch assay and detection of released zinc ion from recombinant proteins, β-mercaptoethanol was removed from the protein samples by gel filtration using Micro Biospin columns (BioRad, Munich, Germany).

2. 4. 4. Biotin labeling of S-nitrosothiols and purification of biotin-labeled proteins

2. 4. 4. 1. Biotin switch assay

Generation of S-nitrosylated proteins and biotin switch assay were performed as described by Lindermayr *et al*, 2005 (Lindermayr et al., 2005). The recombinant proteins re-buffered before starting the assay for removing the reducing agents which was used during their purification procedure. The Nuclear enriched fractions or recombinant purified proteins

were adjust to a maximum concentration of 0.8 µg/µl in HEN buffer (1. 6) and treated with 250 µM GSNO for 20 min in darkness at room temperature for trans-nitrosylating of its redox-sensitive cysteine residues. Control samples were treated with ddH_2O. 1 mM GSH was used as a negative control. Afterwards, the samples were treated with 20 mM MMTS and 2.5% SDS at 50 °C for 20 min with frequent vortexing for blocking of the free thiols. Residual MMTS was discarded by precipitation with 2 volumes of ice cold acetone. Then, the samples were treated with 1 mM ascorbate and 2 mM biotin-HPDP at room temperature for 1 h in which theoretically the S-nitrosylated cysteine residues reduce selectively with ascorbate and the freshly generated free thiols S-biotinylate by biotin-HPDP. This labelling allows the detection of SNO proteins by anti-biotin antibody and their isolation by affinity chromatography.

2. 4. 4. 2. Purification of biotinylated proteins

Purification of biotin-labelled proteins were done as described by Sell *et al*, 2008 (Sell et al., 2008) with a few modifications. Biotin-HPDP was removed by precipitation with 2 volumes of ice cold acetone and the proteins were re-suspended in 50 µl of HENS (1. 6) buffer/mg of protein and at least 2 volumes of neutralization buffer (1. 6). The protein fraction was added to 30 µl of equilibrated neutravidin agarose slurry and incubated at 25 °C for 1-2 h with gentle shaking. The matrix was washed 5 times with 10 volumes of washing buffer (1. 6) and bound proteins were eluted by incubating for 20 min with 100 mM β-mercaptoethanol in neutralization buffer which had boiled at 95 °C for 5 min.

2. 4. 5. Histone deacetylase activity assay of recombinant proteins

HDAC activity in protein extracts was measured using the EpigenaseTM HDAC Activity/Inhibition Direct Assay Kit (Fluorimetric, cat. # P-4035) according to the manufacturer´s instructions. Briefly, 0.5 – 10 µg of protein extract per well were incubated with 50 ng of substrate for 90 min at room temperature. Deacetylated product was immuno-detected and fluorescence at Ex/Em = 530/590 nm was measured on a fluorescence microplate reader (Tecan infinite 1000). (Alexnader Mengel).

2. 4. 6. Detection of released zinc ion from recombinant proteins

Releasing of zinc ion from recombinant HD2C after treatment with NO donors (GSNO and SNAP), GSH and H_2O_2 (with and without adding DTT) was studied. HD2A and HD2D were

used as positive (zinc finger protein) and negative (non-zinc finger protein) controls, respectively. The displaced zinc was detected with the metallochromic indicator PAR, which binds Zn^{2+} in a 2:1 complex and turns its color from yellow to orange with strong absorbance at 490 nm (Atanassova & Zamble, 2005).

100 µg of HD2C (around 3.22 nanomole) and control recombinant proteins in 500 µl HS buffer was used for each replicate, 20% (100 µl) of each sample was used for measuring zinc ion before treatment. Since, each molecule of HD2C contains 1 zinc ion and if all zinc ions of a protein sample is released due to a treatment, it cannot be more than 2.57 nanomole (80% of 3.22). Therefore, for measuring/estimation of zinc ion, a serial dilution from 500nM to 50µM of $ZnCl_2$ (stock solution was prepared from 0.1 M $ZnCl_2$ solution (Sigma, Germany)) in 100 µl HS buffer (1. 6) was prepared in 3 replicates. This serial dilution contained from 0 to 5 nanomole zinc ion in 100 µl which was in an appropriate range for measuring released zinc ion from the recombinant protein. The absorption of the serial dilutions was measured by tecan reader after adding 0.1 mM PAR and a standard curve was created. The equation of the standard curve was used for reversing absorption values to concentration/amount values in untreated condition. Since, NO donors, GSH, H_2O_2 and DTT, can complex with zinc ion and reduce the absorption by PAR, a separate standard curve was created for each single reagent and its equation was used for calculation of concentration/amount of corresponding samples.

The recombinant proteins re-buffered in HS buffer using PD-10 column (GE health care life sciences, Freiburg, Germany). Zn^{2+} was loaded on protein samples by incubating the recombinant proteins with 0.1 mM $ZnSO_4$ in HS buffer for 1 h at RT. Protein samples were washed 5-7 times with 10kD Spin Column (Abcam, UK) until the follow through had low and similar amount of zinc ion with HS buffer using PAR. 100 µg of protein samples in 500 µl HS buffer was used for each replicate. 100 µl of each sample was used to measure the absorption before treatment. The protein samples were treated with different concentrations of SNAP, GSNO, GSH and H_2O_2 in 3 replicates and incubated for 10 min in darkness at RT (with or without further adding 1 mM DTT for 5 min). 100 µl of each sample was loaded in a well of a 96 well plate. PAR (stock solution, 1mM) was added to the samples to reach a final concentration of 0.1 mM. The absorption was detected at 490 nm by tecan reader. The amount of released zinc ion (nanomole) for 500 µl was calculated using

corresponding standard curve for before and after treatments. The released zinc ion was calculated in treated samples relative to the untreated corresponding samples (%). Data analysis was performed by anova single factor.

2. 4. 7. Co-Immunoprecipitation (Co-IP)

The nuclear lysate extracted from 4 weeks old WT *Arabidopsis* plants were used for studying the protein-protein interaction of HD2C via Co-IP using its specific antibody (Agrisera, Sweden). *hd2c-1* mutant line (SALK_129799.19.60.n) was used as negative control.
The Co-IP was optimized with testing the incubation of nuclear protein sample (2. 1. 4) with specific antibody to HD2C with 3 different protocols using: I) protein A agarose beads, in which the lysate was incubated with protein A dynabeads and then with the antibody, II) Protein A dynabeads, in which first the lysate was incubated with antibody and then with protein A dynabeads and III) using direct coupling of antibody to dynabeads by Dynabeads® Co-Immunoprecipitation Kit manual (Novex, Life technologies). For all 3 methods, the lysate was first pre-cleared with the beads. The protein A agarose beads showed the highest background bands in both WT and *hd2c-1* mutant, protein A Dynabeads showed medium background bands and the direct coupling of the antibody to Dynabeads (third method) showed the lowest background; So, it was established for Co-IP experiment and it is explained here in details.

In this method, first Antibody coupled dynabeads were prepared using Dynabeads® Co-Immunoprecipitation Kit manual. Briefly, 100 µl (25 µg) of antibody was mixed with 4 mg dynabeads, 300 µl buffer C1 and 400 µl buffer C2 from the kit and incubated at 37°C overnight with gentle shaking. During shaking time, to achieve high efficiency of binding, the tubes were fixed in a way that it prevents from the precipitation of dynabeads. Afterward the beads were washed with 800 µl HB, LB and SB buffers from the kit according the manufacture's manual, respectively. The supernatant was removed using magnetic rack after each washing step. Then antibody coupled dynabeads were then blocked with 0.1 % BSA for 5 min and washed with 900 µl NLB-E buffer (1. 6). Afterward, the antibody coupled dynabeads were incubated for 2.5 h with the nuclear lysate (1. 6) and then were washed 10 times with 200 µl of NLB-E and once with last wash buffer (LW) from the kit for 5 min at RT with gentle rotation. To observe the interacting bands clearly and without disturbing by heavy and light chains of antibody, the complex was eluted with 60 µl of elution buffer from

the kit for 5 min at RT with gentle rotation; since the elution buffer from the kit did not elute the antibody. The sample was then concentrated using 10kD Spin columns (Abcam, UK) and visualized by silver stained SDS-PAGE. After observing the similar pattern of pull-downed proteins for HD2C in WT samples in 3 different biological replicates, the Co-IP experiment was performed with 3 other biological replicates in which the elution of the complex was done by 2X reducing SDS loading buffer (1. 6) which was compatible with further mass spectrometry analysis (2. 4. 8).

2. 4. 8. nano LC-MS/MS analyses

Sample preparation and mass spectrometric analyses were done according to protocols described previously (Merl et al., 2012, von Toerne et al., 2013). 1D-gel clean-up of samples was performed to purify the proteins. The protein content of samples was measured using the BCA protein assay (Thermo Scientific Pierce). 30 µg of each sample were loaded on a 12% self-cast gel. After a total separation distance of 1 cm, the gel was fixed and stained using coomassie brilliant blue. The complete lanes were subjected to in-gel digest.

Excised bands of the pre-fractionation gel were cut in cubes of 1 mm3 and transferred into tubes (Eppendorf). For de-staining the gel pieces were washed for 10 min with 200 µl 60% acetonitrile (ACN) followed by a 10 min-wash using 200 µl H_2O. For subsequent dehydration, the gel cubes were incubated for 10 min with 200 µl 100% ACN. For protein reduction, 100 µl of 5 mM DTT was added to the dehydrated gel pieces and incubated for 15 minutes at 60 °C. After removal of DTT and an additional dehydration step using 100% ACN, 100 µl of freshly prepared 25 mM iodacetamide solution was added for 15 min at room temperature in the dark. The gel cubes were washed for 5 min with 100 µl H_2O and again dehydrated by incubation in 100% ACN for 10 min in order to remove remaining DTT and IAA. After three wash steps of 10 minutes with 50 mM ammoniumbicarbonate (ABC), 60% ACN and 100% ACN, the gel cubes were air-dried for 15 min at 37 °C. 100 µl of a 0.01 µg/µl trypsin solution (Sigma) in 50 mM ABC was added. After incubation for 10 minutes, 25 mM ABC was added to cover the gel pieces completely during digest at 37°C over night. For elution, 100 µl of 60% ACN/0.1% TFA were added to the gel cubes and incubated for 15 min shaking. The supernatant was transferred to a new tube and 100 µl of 99.9% ACN/0.1% TFA were added to the gel pieces. After additional 30 minutes of incubation, the supernatants were pooled.

The supernatants containing the eluted peptides were dried in a speedvac (UniEquip) and stored at -20 °C.

For mass spectrometric analyses dried pre-fractionated samples were thawed and dissolved in 45 µl of 2% ACN/0.5% trifluoroacetic acid by incubation for 30 min at RT under agitation. Before loading, the samples were centrifuged for 5 min at 4 °C. LC-MS/MS analysis was performed as described previously on a LTQ-Orbitrap XL (Thermo Scientific). Briefly, samples were automatically injected and loaded onto the trap column and after 5 min, the peptides were eluted and separated on the analytical column separation by reversed phase chromatography operated on a nano-HPLC (Ultimate 3000, Dionex) with a nonlinear 170 min gradient using 35 % ACN in 0.1 % formic acid in water (A) and 0.1 % formic acid in 98 % ACN (B) at a flow rate of 300 nl/min. The gradient settings were: 5–140 min: 14.5-90 % A, 140–145 min: 90% A - 95 % B, 145–150 min: 95 % B and followed by equilibration for 15 min to starting conditions. From the MS prescan, the 10 most abundant peptide ions were selected for fragmentation in the linear ion trap if they exceeded an intensity of at least 200 counts and were at least doubly charged. During fragment analysis a high-resolution (60,000 full-width half maximum) MS spectrum was acquired in the Orbitrap with a mass range from 200 to 1500 Da.

For peptide identification, Mascot (Matrix Science, version 2.3) was set up to search with one missed cleavage allowed, a fragment ion mass tolerance of 0.6 Da and a parent ion tolerance of 10 ppm. Carbamidomethylation was set as fixed modification, methionine oxidation and asparagine or glutamine deamidation were allowed as variable modifications. Spectra were searched against the TAIR database (Release 10; 35386 sequences). The Scaffold software (version 3_00_03, Proteome Software Inc.) was used to display results.

Abat J, Saigal P, Deswal R, 2008a. S-Nitrosylation — another biological switch like phosphorylation? *Physiology and Molecular Biology of Plants* **14**, 119-30.
Abat JK, Mattoo AK, Deswal R, 2008b. S-nitrosylated proteins of a medicinal CAM plant Kalanchoe pinnata-ribulose-1,5-bisphosphate carboxylase/oxygenase activity targeted for inhibition. *FEBS J* **275**, 2862-72.
Ahn SG, Thiele DJ, 2003. Redox regulation of mammalian heat shock factor 1 is essential for Hsp gene activation and protection from stress. *Genes Dev* **17**, 516-28.
Airaki M, Leterrier M, Valderrama R*, et al.*, 2015. Spatial and temporal regulation of the metabolism of reactive oxygen and nitrogen species during the early development of pepper (Capsicum annuum) seedlings. *Ann Bot*.
Aittaleb M, Rashid R, Chen Q, Palmer JR, Daniels CJ, Li H, 2003. Structure and function of archaeal box C/D sRNP core proteins. *Nature Structural Biology* **10**, 256-63.
Astier J, Besson-Bard A, Lamotte O*, et al.*, 2012. Nitric oxide inhibits the ATPase activity of the chaperone-like AAA+ ATPase CDC48, a target for S-nitrosylation in cryptogein signalling in tobacco cells. *Biochem J* **447**, 249-60.
Atanassova A, Zamble DB, 2005. Escherichia coli HypA is a zinc metalloprotein with a weak affinity for nickel. *J Bacteriol* **187**, 4689-97.
Bannister AJ, Kouzarides T, 2011. Regulation of chromatin by histone modifications. *Cell Research* **21**, 381-95.
Barneche F, Steinmetz F, Echeverria M, 2000. Fibrillarin genes encode both a conserved nucleolar protein and a novel small nucleolar RNA involved in ribosomal RNA methylation in Arabidopsis thaliana. *J Biol Chem* **275**, 27212-20.
Barygina VV, Veiko VP, Zatsepina OV, 2010. Analysis of nucleolar protein fibrillarin mobility and functional state in living HeLa cells. *Biochemistry* **75**, 979-88.
Bauer C, Diesinger I, Brass N, Steinhart H, Iro H, Meese EU, 2001. Translation initiation factor eIF-4G is immunogenic, overexpressed, and amplified in patients with squamous cell lung carcinoma. *Cancer* **92**, 822-9.
Benhar M, Forrester MT, Hess DT, Stamler JS, 2008. Regulated protein denitrosylation by cytosolic and mitochondrial thioredoxins. *Science* **320**, 1050-4.
Benhar M, Forrester MT, Stamler JS, 2009. Protein denitrosylation: enzymatic mechanisms and cellular functions. *Nat Rev Mol Cell Biol* **10**, 721-32.
Berendji D, Kolb-Bachofen V, Zipfel PF, Skerka C, Carlberg C, Kroncke KD, 1999. Zinc finger transcription factors as molecular targets for nitric oxide-mediated immunosuppression: inhibition of IL-2 gene expression in murine lymphocytes. *Molecular Medicine* **5**, 721-30.
Berr A, Menard R, Heitz T, Shen WH, 2012. Chromatin modification and remodelling: a regulatory landscape for the control of Arabidopsis defence responses upon pathogen attack. *Cell Microbiol* **14**, 829-39.
Besson-Bard A, Pugin A, Wendehenne D, 2008. New insights into nitric oxide signaling in plants. *Annu Rev Plant Biol* **59**, 21-39.
Bethke PC, Badger MR, Jones RL, 2004. Apoplastic synthesis of nitric oxide by plant tissues. *Plant Cell* **16**, 332-41.
Blatch GL, Lassle M, 1999. The tetratricopeptide repeat: a structural motif mediating protein-protein interactions. *Bioessays* **21**, 932-9.
Bourque S, Dutartre A, Hammoudi V*, et al.*, 2011. Type-2 histone deacetylases as new regulators of elicitor-induced cell death in plants. *New Phytol* **192**, 127-39.
Brachet J, Chantrenne H, 1951. Protein synthesis in nucleated and non-nucleated halves of Acetabularia mediterranea studied with carbon-14 dioxide. *Nature* **168**, 950.
Brayer KJ, Segal DJ, 2008. Keep your fingers off my DNA: protein-protein interactions mediated by C2H2 zinc finger domains. *Cell Biochemistry and Biophysics* **50**, 111-31.
Brendeford EM, Andersson KB, Gabrielsen OS, 1998. Nitric oxide (NO) disrupts specific DNA binding of the transcription factor c-Myb in vitro. *FEBS Lett* **425**, 52-6.
Brosch G, Lusser A, Goralik-Schramel M, Loidl P, 1996. Purification and characterization of a high molecular weight histone deacetylase complex (HD2) of maize embryos. *Biochemistry* **35**, 15907-14.
Brown JW, Shaw PJ, 2008. The role of the plant nucleolus in pre-mRNA processing. *Current Topics in Microbiology and Immunology* **326**, 291-311.
Busconi M, Reggi S, Fogher C, Bavaresco L, 2009. Evidence of a sirtuin gene family in grapevine (Vitis vinifera L.). *Plant Physiol Biochem* **47**, 650-2.
Camejo D, Romero-Puertas Mdel C, Rodriguez-Serrano M*, et al.*, 2013. Salinity-induced changes in S-nitrosylation of pea mitochondrial proteins. *J Proteomics* **79**, 87-99.
Chaki M, Kovacs I, Spannagl M, Lindermayr C, 2014. Computational prediction of candidate proteins for S-nitrosylation in Arabidopsis thaliana. *PLoS ONE* **9**, e110232.
Chen LT, Luo M, Wang YY, Wu K, 2010. Involvement of Arabidopsis histone deacetylase HDA6 in ABA and salt stress response. *J Exp Bot* **61**, 3345-53.

Chen YJ, Ching WC, Lin YP, Chen YJ, 2013. Methods for detection and characterization of protein S-nitrosylation. *Methods* **62**, 138-50.
Chen YJ, Lu CT, Su MG*, et al.*, 2015. dbSNO 2.0: a resource for exploring structural environment, functional and disease association and regulatory network of protein S-nitrosylation. *Nucleic Acids Res* **43**, D503-11.
Chou MF, Schwartz D, 2011. Biological sequence motif discovery using motif-x. *Curr Protoc Bioinformatics* **Chapter 13**, Unit 13 5-24.
Cibelli G, Policastro V, Rossler OG, Thiel G, 2002. Nitric oxide-induced programmed cell death in human neuroblastoma cells is accompanied by the synthesis of Egr-1, a zinc finger transcription factor. *J Neurosci Res* **67**, 450-60.
Citiulo F, Jacobsen ID, Miramon P*, et al.*, 2012. Candida albicans scavenges host zinc via Pra1 during endothelial invasion. *PLoS Pathog* **8**, e1002777.
Colussi C, Mozzetta C, Gurtner A*, et al.*, 2008. HDAC2 blockade by nitric oxide and histone deacetylase inhibitors reveals a common target in Duchenne muscular dystrophy treatment. *Proc Natl Acad Sci U S A* **105**, 19183-7.
Corpas F, Barroso J, 2015. Functions of Nitric Oxide (NO) in Roots during Development and under Adverse Stress Conditions. *Plants* **4**, 240.
Corpas FJ, Barroso JB, Carreras A*, et al.*, 2006. Constitutive arginine-dependent nitric oxide synthase activity in different organs of pea seedlings during plant development. *Planta* **224**, 246-54.
Corpas FJ, Hayashi M, Mano S, Nishimura M, Barroso JB, 2009a. Peroxisomes are required for in vivo nitric oxide accumulation in the cytosol following salinity stress of Arabidopsis plants. *Plant Physiol* **151**, 2083-94.
Corpas FJ, Palma JM, Del Rio LA, Barroso JB, 2009b. Evidence supporting the existence of L-arginine-dependent nitric oxide synthase activity in plants. *New Phytol* **184**, 9-14.
Crawford NM, 2006. Mechanisms for nitric oxide synthesis in plants. *J Exp Bot* **57**, 471-8.
Dahlberg JE, Lund E, 2004. Does protein synthesis occur in the nucleus? *Current Opinion in Cell Biology* **16**, 335-8.
Dahlberg JE, Lund E, Goodwin EB, 2003. Nuclear translation: What is the evidence? *RNA* **9**, 1-8.
Dalle-Donne I, Rossi R, Colombo G, Giustarini D, Milzani A, 2009. Protein S-glutathionylation: a regulatory device from bacteria to humans. *Trends in Biochemical Sciences* **34**, 85-96.
Dangl M, Brosch G, Haas H, Loidl P, Lusser A, 2001. Comparative analysis of HD2 type histone deacetylases in higher plants. *Planta* **213**, 280-5.
Davletova S, Schlauch K, Coutu J, Mittler R, 2005. The zinc-finger protein Zat12 plays a central role in reactive oxygen and abiotic stress signaling in Arabidopsis. *Plant Physiol* **139**, 847-56.
De La Fuente Van Bentem S, Anrather D, Roitinger E*, et al.*, 2006. Phosphoproteomics reveals extensive in vivo phosphorylation of Arabidopsis proteins involved in RNA metabolism. *Nucleic Acids Res* **34**, 3267-78.
Delledonne M, Xia Y, Dixon RA, Lamb C, 1998. Nitric oxide functions as a signal in plant disease resistance. *Nature* **394**, 585-8.
Demetriou K, Kapazoglou A, Tondelli A*, et al.*, 2009. Epigenetic chromatin modifiers in barley: I. Cloning, mapping and expression analysis of the plant specific HD2 family of histone deacetylases from barley, during seed development and after hormonal treatment. *Physiologia Plantarum* **136**, 358-68.
Desikan R, Griffiths R, Hancock J, Neill S, 2002. A new role for an old enzyme: nitrate reductase-mediated nitric oxide generation is required for abscisic acid-induced stomatal closure in Arabidopsis thaliana. *Proc Natl Acad Sci U S A* **99**, 16314-8.
Ding F, Cui P, Wang Z, Zhang S, Ali S, Xiong L, 2014. Genome-wide analysis of alternative splicing of pre-mRNA under salt stress in Arabidopsis. *BMC Genomics* **15**, 431.
Disfani FM, Hsu WL, Mizianty MJ*, et al.*, 2012. MoRFpred, a computational tool for sequence-based prediction and characterization of short disorder-to-order transitioning binding regions in proteins. *Bioinformatics* **28**, i75-83.
Donaldson L, Ludidi N, Knight MR, Gehring C, Denby K, 2004. Salt and osmotic stress cause rapid increases in Arabidopsis thaliana cGMP levels. *FEBS Lett* **569**, 317-20.
Durner J, Wendehenne D, Klessig DF, 1998. Defense gene induction in tobacco by nitric oxide, cyclic GMP, and cyclic ADP-ribose. *Proc Natl Acad Sci U S A* **95**, 10328-33.
Ellis JC, Brown DD, Brown JW, 2010. The small nucleolar ribonucleoprotein (snoRNP) database. *RNA* **16**, 664-6.
Englbrecht CC, Schoof H, Bohm S, 2004. Conservation, diversification and expansion of C2H2 zinc finger proteins in the Arabidopsis thaliana genome. *BMC Genomics* **5**, 39.
Fares A, Rossignol M, Peltier JB, 2011a. Proteomics investigation of endogenous S-nitrosylation in Arabidopsis. *Biochemical and Biophysical Research Communications* **416**, 331-6.
Fares A, Rossignol M, Peltier JB, 2011b. Proteomics investigation of endogenous S-nitrosylation in Arabidopsis. *Biochem Biophys Res Commun* **416**, 331-6.

Fiil BK, Qiu JL, Petersen K, Petersen M, Mundy J, 2008. Coimmunoprecipitation (co-IP) of Nuclear Proteins and Chromatin Immunoprecipitation (ChIP) from Arabidopsis. *CSH Protoc* **2008**, pdb prot5049.
Foissner I, Wendehenne D, Langebartels C, Durner J, 2000. In vivo imaging of an elicitor-induced nitric oxide burst in tobacco. *Plant J* **23**, 817-24.
Forrester MT, Foster MW, Benhar M, Stamler JS, 2009. Detection of protein S-nitrosylation with the biotin-switch technique. *Free Radic Biol Med* **46**, 119-26.
Francis SH, Busch JL, Corbin JD, Sibley D, 2010. cGMP-dependent protein kinases and cGMP phosphodiesterases in nitric oxide and cGMP action. *Pharmacological Reviews* **62**, 525-63.
Freschi L, 2013. Nitric oxide and phytohormone interactions: current status and perspectives. *Front Plant Sci* **4**, 398.
Gao C, Guo H, Wei J, Mi Z, Wai PY, Kuo PC, 2005. Identification of S-nitrosylated proteins in endotoxin-stimulated RAW264.7 murine macrophages. *Nitric Oxide* **12**, 121-6.
Gaupels F, Furch AC, Will T, Mur LA, Kogel KH, Van Bel AJ, 2008. Nitric oxide generation in Vicia faba phloem cells reveals them to be sensitive detectors as well as possible systemic transducers of stress signals. *New Phytol* **178**, 634-46.
Gould K, Lamotte O, Klinguer A, A P, D AW, 2003. Nitric oxide production in tobacco leaf cells: a generalized stress response? *Plant Cell Environment* **16**.
Graff JR, Konicek BW, Carter JH, Marcusson EG, 2008. Targeting the eukaryotic translation initiation factor 4E for cancer therapy. *Cancer Research* **68**, 631-4.
Greco TM, Hodara R, Parastatidis I*, et al.*, 2006. Identification of S-nitrosylation motifs by site-specific mapping of the S-nitrosocysteine proteome in human vascular smooth muscle cells. *Proc Natl Acad Sci U S A* **103**, 7420-5.
Guo F-Q, 2006. Response to Zemojtel et al: Plant nitric oxide synthase: AtNOS1 is just the beginning. *Trends Plant Sci* **11**, 527-8.
Guo FQ, Okamoto M, Crawford NM, 2003. Identification of a plant nitric oxide synthase gene involved in hormonal signaling. *Science* **302**, 100-3.
Gupta KJ, Zabalza A, Van Dongen JT, 2009. Regulation of respiration when the oxygen availability changes. *Physiol Plant* **137**, 383-91.
Gupta SK, Rai AK, Kanwar SS, Sharma TR, 2012. Comparative Analysis of Zinc Finger Proteins Involved in Plant Disease Resistance. *PLoS ONE* **7**, e42578.
Hara MR, Agrawal N, Kim SF*, et al.*, 2005. S-nitrosylated GAPDH initiates apoptotic cell death by nuclear translocation following Siah1 binding. *Nat Cell Biol* **7**, 665-74.
Hardin JW, Reyes FE, Batey RT, 2009. Analysis of a critical interaction within the archaeal box C/D small ribonucleoprotein complex. *J Biol Chem* **284**, 15317-24.
Hess DT, Matsumoto A, Kim SO, Marshall HE, Stamler JS, 2005. Protein S-nitrosylation: purview and parameters. *Nat Rev Mol Cell Biol* **6**, 150-66.
Hollender C, Liu Z, 2008. Histone deacetylase genes in Arabidopsis development. *J Integr Plant Biol* **50**, 875-85.
Holtgrefe S, Gohlke J, Starmann J*, et al.*, 2008. Regulation of plant cytosolic glyceraldehyde 3-phosphate dehydrogenase isoforms by thiol modifications. *Physiol Plant* **133**, 211-28.
Holzmeister C, Frohlich A, Sarioglu H, Bauer N, Durner J, Lindermayr C, 2011. Proteomic analysis of defense response of wildtype Arabidopsis thaliana and plants with impaired NO- homeostasis. *Proteomics* **11**, 1664-83.
Hu J, Huang X, Chen L*, et al.*, 2015. Site-specific nitrosoproteomic identification of endogenously S-nitrosylated proteins in Arabidopsis. *Plant Physiol* **167**, 1731-46.
Huang B, Chen SC, Wang DL, 2009. Shear flow increases S-nitrosylation of proteins in endothelial cells. *Cardiovascular Research* **83**, 536-46.
Huang X, Von Rad U, Durner J, 2002. Nitric oxide induces transcriptional activation of the nitric oxide-tolerant alternative oxidase in Arabidopsis suspension cells. *Planta* **215**, 914-23.
Isner JC, Maathuis FJ, 2011. Measurement of cellular cGMP in plant cells and tissues using the endogenous fluorescent reporter FlincG. *Plant J* **65**, 329-34.
Jaffrey SR, Erdjument-Bromage H, Ferris CD, Tempst P, Snyder SH, 2001. Protein S-nitrosylation: a physiological signal for neuronal nitric oxide. *Nat Cell Biol* **3**, 193-7.
Jasid S, Simontacchi M, Bartoli CG, Puntarulo S, 2006. Chloroplasts as a Nitric Oxide Cellular Source. Effect of Reactive Nitrogen Species on Chloroplastic Lipids and Proteins. *Plant Physiology* **142**, 1246-55.
Jones JD, Dangl JL, 2006. The plant immune system. *Nature* **444**, 323-9.
Kaiser WM, Weiner H, Kandlbinder A*, et al.*, 2002. Modulation of nitrate reductase: some new insights, an unusual case and a potentially important side reaction. *J Exp Bot* **53**, 875-82.
Kato H, Takemoto D, Kawakita K, 2013. Proteomic analysis of S-nitrosylated proteins in potato plant. *Physiol Plant* **148**, 371-86.

Keller A, Nesvizhskii AI, Kolker E, Aebersold R, 2002. Empirical statistical model to estimate the accuracy of peptide identifications made by MS/MS and database search. *Analytical Chemistry* **74**, 5383-92.
Khan A, Garbelli A, Grossi S*, et al.*, 2014. The Arabidopsis STRESS RESPONSE SUPPRESSOR DEAD-box RNA helicases are nucleolar- and chromocenter-localized proteins that undergo stress-mediated relocalization and are involved in epigenetic gene silencing. *Plant J* **79**, 28-43.
Kim YK, Kim S, Shin YJ*, et al.*, 2014. Ribosomal protein S6, a target of rapamycin, is involved in the regulation of rRNA genes by possible epigenetic changes in Arabidopsis. *J Biol Chem* **289**, 3901-12.
Kodiha M, Chu A, Lazrak O, Stochaj U, 2005. Stress inhibits nucleocytoplasmic shuttling of heat shock protein hsc70. *Am J Physiol Cell Physiol* **289**, C1034-41.
Kojima H, Suzuki T, Kato T*, et al.*, 2007. Sugar-inducible expression of the nucleolin-1 gene of Arabidopsis thaliana and its role in ribosome synthesis, growth and development. *Plant J* **49**, 1053-63.
Kornberg MD, Sen N, Hara MR*, et al.*, 2010. GAPDH mediates nitrosylation of nuclear proteins. *Nat Cell Biol* **12**, 1094-100.
Kovacs I, Lindermayr C, 2013. Nitric oxide-based protein modification: formation and site-specificity of protein S-nitrosylation. *Front Plant Sci* **4**, 137.
Kroncke KD, 2001. Zinc finger proteins as molecular targets for nitric oxide-mediated gene regulation. *Antioxid Redox Signal* **3**, 565-75.
Kroncke KD, Carlberg C, 2000a. Inactivation of zinc finger transcription factors provides a mechanism for a gene regulatory role of nitric oxide. *FASEB J* **14**, 166-73.
Kroncke KD, Carlberg C, 2000b. Inactivation of zinc finger transcription factors provides a mechanism for a gene regulatory role of nitric oxide. *Faseb Journal* **14**, 166-73.
Kroncke KD, Fehsel K, Schmidt T*, et al.*, 1994. Nitric oxide destroys zinc-sulfur clusters inducing zinc release from metallothionein and inhibition of the zinc finger-type yeast transcription activator LAC9. *Biochem Biophys Res Commun* **200**, 1105-10.
Kumar M, Gromiha MM, Raghava GP, 2008. Prediction of RNA binding sites in a protein using SVM and PSSM profile. *Proteins* **71**, 189-94.
Kuznetsov IB, Gou Z, Li R, Hwang S, 2006. Using evolutionary and structural information to predict DNA-binding sites on DNA-binding proteins. *Proteins* **64**, 19-27.
Laemmli UK, 1970. Cleavage of structural proteins during the assembly of the head of bacteriophage T4. *Nature* **227**, 680-5.
Lagace M, Chantha SC, Major G, Matton DP, 2003. Fertilization induces strong accumulation of a histone deacetylase (HD2) and of other chromatin-remodeling proteins in restricted areas of the ovules. *Plant Molecular Biology* **53**, 759-69.
Laity JH, Lee BM, Wright PE, 2001. Zinc finger proteins: new insights into structural and functional diversity. *Current Opinion in Structural Biology* **11**, 39-46.
Lam YW, Yuan Y, Isaac J, Babu CV, Meller J, Ho SM, 2010. Comprehensive identification and modified-site mapping of S-nitrosylated targets in prostate epithelial cells. *PLoS One* **5**, e9075.
Lamotte O, Bertoldo JB, Besson-Bard A*, et al.*, 2014. Protein S-nitrosylation: specificity and identification strategies in plants. *Frontiers in Chemistry* **2**, 114.
Lin A, Wang Y, Tang J*, et al.*, 2012. Nitric oxide and protein S-nitrosylation are integral to hydrogen peroxide-induced leaf cell death in rice. *Plant Physiol* **158**, 451-64.
Lin J, Lai S, Jia R*, et al.*, 2011. Structural basis for site-specific ribose methylation by box C/D RNA protein complexes. *Nature* **469**, 559-63.
Lindermayr C, Durner J, 2007. S-Nitrosylation in Plants – Spectrum and Selectivity. In: Lamattina L, Polacco J, eds. *Nitric Oxide in Plant Growth, Development and Stress Physiology.* Springer Berlin Heidelberg, 53-71. (Plant Cell Monographs; vol. 5.)
Lindermayr C, Saalbach G, Durner J, 2005. Proteomic identification of S-nitrosylated proteins in Arabidopsis. *Plant Physiol* **137**, 921-30.
Lindermayr C, Sell S, Durner J, 2008. Generation and detection of S-nitrosothiols. *Methods in Molecular Biology* **476**, 217-29.
Lindermayr C, Sell S, Muller B, Leister D, Durner J, 2010. Redox regulation of the NPR1-TGA1 system of Arabidopsis thaliana by nitric oxide. *Plant Cell* **22**, 2894-907.
Liu L, Hausladen A, Zeng M, Que L, Heitman J, Stamler JS, 2001. A metabolic enzyme for S-nitrosothiol conserved from bacteria to humans. *Nature* **410**, 490-4.
Liu P, Zhang H, Yu B, Xiong L, Xia Y, 2015. Proteomic identification of early salicylate- and flg22-responsive redox-sensitive proteins in Arabidopsis. *Scientific reports* **5**, 8625.

Liu X, Yang S, Zhao M*, et al.*, 2014. Transcriptional repression by histone deacetylases in plants. *Mol Plant* **7**, 764-72.
Lozano-Juste J, Colom-Moreno R, Leon J, 2011. In vivo protein tyrosine nitration in Arabidopsis thaliana. *J Exp Bot* **62**, 3501-17.
Lundgren DH, Hwang SI, Wu L, Han DK, 2010. Role of spectral counting in quantitative proteomics. *Expert Rev Proteomics* **7**, 39-53.
Luo M, Liu X, Singh P, Cui Y, Zimmerli L, Wu K, 2012a. Chromatin modifications and remodeling in plant abiotic stress responses. *Biochim Biophys Acta* **1819**, 129-36.
Luo M, Wang YY, Liu X*, et al.*, 2012b. HD2C interacts with HDA6 and is involved in ABA and salt stress response in Arabidopsis. *J Exp Bot* **63**, 3297-306.
Luo M, Wang YY, Liu X, Yang S, Wu K, 2012c. HD2 proteins interact with RPD3-type histone deacetylases. *Plant Signal Behav* **7**, 608-10.
Lusser A, Brosch G, Loidl A, Haas H, Loidl P, 1997. Identification of maize histone deacetylase HD2 as an acidic nucleolar phosphoprotein. *Science* **277**, 88-91.
Ma X, Lv S, Zhang C, Yang C, 2013. Histone deacetylases and their functions in plants. *Plant Cell Rep* **32**, 465-78.
Maldonado-Alconada AM, Echevarria-Zomeno S, Lindermayr C, Redondo-Lopez I, Durner J, Jorrin-Novo JV, 2011a. Proteomic analysis of *Arabidopsis* protein S-nitrosylation in response to inoculation with *Pseudomonas syringae*. *Acta Physiologiae Plantarum* **33**, 1493-514.
Maldonado-Alconada AM, Echevarría-Zomeño S, Lindermayr C, Redondo-López I, Durner J, Jorrín-Novo JV, 2011b. Proteomic analysis of Arabidopsis protein S-nitrosylation in response to inoculation with Pseudomonas syringae. *Acta Physiol Plant* **33**, 1493–514.
Mangelsdorf DJ, Thummel C, Beato M*, et al.*, 1995. The nuclear receptor superfamily: the second decade. *Cell* **83**, 835-9.
Marino SM, Gladyshev VN, 2010a. Cysteine function governs its conservation and degeneration and restricts its utilization on protein surfaces. *J Mol Biol* **404**, 902-16.
Marino SM, Gladyshev VN, 2010b. Structural analysis of cysteine S-nitrosylation: a modified acid-based motif and the emerging role of trans-nitrosylation. *J Mol Biol* **395**, 844-59.
Marino SM, Gladyshev VN, 2012. Analysis and functional prediction of reactive cysteine residues. *J Biol Chem* **287**, 4419-25.
Martinez MC, Andriantsitohaina R, 2009. Reactive nitrogen species: molecular mechanisms and potential significance in health and disease. *Antioxid Redox Signal* **11**, 669-702.
Mastrangelo AM, Marone D, Laido G, De Leonardis AM, De Vita P, 2012. Alternative splicing: enhancing ability to cope with stress via transcriptome plasticity. *Plant Sci* **185-186**, 40-9.
Mccarty AS, Kleiger G, Eisenberg D, Smale ST, 2003. Selective dimerization of a C2H2 zinc finger subfamily. *Molecular Cell* **11**, 459-70.
Mengel A, Chaki M, Shekariesfahlan A, Lindermayr C, 2013a. Effect of nitric oxide on gene transcription - S-nitrosylation of nuclear proteins. *Frontiers in plant science* **4**, 293.
Mengel A, Chaki M, Shekariesfahlan A, Lindermayr C, 2013b. Effect of nitric oxide on gene transcription - S-nitrosylation of nuclear proteins. *Front Plant Sci* **4**, 293.
Merl J, Ueffing M, Hauck SM, Von Toerne C, 2012. Direct comparison of MS-based label-free and SILAC quantitative proteome profiling strategies in primary retinal Muller cells. *Proteomics* **12**, 1902-11.
Michel CI, Holley CL, Scruggs BS*, et al.*, 2011. Small nucleolar RNAs U32a, U33, and U35a are critical mediators of metabolic stress. *Cell Metab* **14**, 33-44.
Milla MA, Townsend J, Chang IF, Cushman JC, 2006. The Arabidopsis AtDi19 gene family encodes a novel type of Cys2/His2 zinc-finger protein implicated in ABA-independent dehydration, high-salinity stress and light signaling pathways. *Plant Molecular Biology* **61**, 13-30.
Miller MJ, Scalf M, Rytz TC, Hubler SL, Smith LM, Vierstra RD, 2013. Quantitative proteomics reveals factors regulating RNA biology as dynamic targets of stress-induced SUMOylation in Arabidopsis. *Mol Cell Proteomics* **12**, 449-63.
Moreau M, Lindermayr C, Durner J, Klessig DF, 2010. NO synthesis and signaling in plants--where do we stand? *Physiol Plant* **138**, 372-83.
Mur LA, Carver TL, Prats E, 2006. NO way to live; the various roles of nitric oxide in plant-pathogen interactions. *J Exp Bot* **57**, 489-505.
Mur LA, Mandon J, Persijn S*, et al.*, 2013. Nitric oxide in plants: an assessment of the current state of knowledge. *AoB Plants* **5**, pls052.
Nakai Y, Nakahira Y, Sumida H*, et al.*, 2013. Vascular plant one-zinc-finger protein 1/2 transcription factors regulate abiotic and biotic stress responses in Arabidopsis. *Plant Journal* **73**, 761-75.

Nardai G, Sass B, Eber J, Orosz G, Csermely P, 2000. Reactive cysteines of the 90-kDa heat shock protein, Hsp90. *Arch Biochem Biophys* **384**, 59-67.
Nathanson L, Xia T, Deutscher MP, 2003. Nuclear protein synthesis: a re-evaluation. *RNA* **9**, 9-13.
Negi S, Itazu M, Imanishi M, Nomura A, Sugiura Y, 2004. Creation and characteristics of unnatural CysHis(3)-type zinc finger protein. *Biochem Biophys Res Commun* **325**, 421-5.
Neill S, Barros R, Bright J*, et al.*, 2008. Nitric oxide, stomatal closure, and abiotic stress. *J Exp Bot* **59**, 165-76.
Nott A, Riccio A, 2009. Nitric oxide-mediated epigenetic mechanisms in developing neurons. *Cell Cycle* **8**, 725-30.
Nott A, Watson PM, Robinson JD, Crepaldi L, Riccio A, 2008. S-Nitrosylation of histone deacetylase 2 induces chromatin remodelling in neurons. *Nature* **455**, 411-5.
Ortega-Galisteo AP, Rodriguez-Serrano M, Pazmino DM, Gupta DK, Sandalio LM, Romero-Puertas MC, 2012. S-Nitrosylated proteins in pea (Pisum sativum L.) leaf peroxisomes: changes under abiotic stress. *J Exp Bot* **63**, 2089-103.
Oruganti S, Zhang Y, Li H*, et al.*, 2007. Alternative conformations of the archaeal Nop56/58-fibrillarin complex imply flexibility in box C/D RNPs. *J Mol Biol* **371**, 1141-50.
Palma K, Zhao Q, Cheng YT*, et al.*, 2007. Regulation of plant innate immunity by three proteins in a complex conserved across the plant and animal kingdoms. *Genes and Development* **21**, 1484-93.
Palmieri MC, Lindermayr C, Bauwe H, Steinhauser C, Durner J, 2010. Regulation of plant glycine decarboxylase by s-nitrosylation and glutathionylation. *Plant Physiol* **152**, 1514-28.
Palmieri MC, Sell S, Huang X*, et al.*, 2008. Nitric oxide-responsive genes and promoters in Arabidopsis thaliana: a bioinformatics approach. *J Exp Bot* **59**, 177-86.
Pandey R, Muller A, Napoli CA*, et al.*, 2002. Analysis of histone acetyltransferase and histone deacetylase families of Arabidopsis thaliana suggests functional diversification of chromatin modification among multicellular eukaryotes. *Nucleic Acids Res* **30**, 5036-55.
Parani MR, S; Myers, R; Weirich, H; Smith, B; Leaman, Dw; Goldman, Sl, 2004. Microarray analysis of nitric oxide responsive transcripts in Arabidopsis. *Plant Biotechnology Journal* **2**, 359-66.
Pederson T, 2013. The persistent plausibility of protein synthesis in the nucleus: process, palimpsest or pitfall? *Current Opinion in Cell Biology* **25**, 520-1.
Penson SP, Schuurink RC, Fath A, Gubler F, Jacobsen JV, Jones RL, 1996. cGMP Is Required for Gibberellic Acid-Induced Gene Expression in Barley Aleurone. *Plant Cell* **8**, 2325-33.
Polverari A, Molesini B, Pezzotti M, Buonaurio R, Marte M, Delledonne M, 2003. Nitric oxide-mediated transcriptional changes in Arabidopsis thaliana. *Mol Plant Microbe Interact* **16**, 1094-105.
Porollo A, Meller J, 2007. Prediction-based fingerprints of protein-protein interactions. *Proteins* **66**, 630-45.
Puyaubert J, Fares A, Reze N, Peltier JB, Baudouin E, 2014. Identification of endogenously S-nitrosylated proteins in Arabidopsis plantlets: effect of cold stress on cysteine nitrosylation level. *Plant Sci* **215-216**, 150-6.
Rakitina DV, Taliansky M, Brown JWS, Kalinina NO, 2011. Two RNA-binding sites in plant fibrillarin provide interactions with various RNA substrates. *Nucleic Acids Research* **39**, 8869-80.
Ravi K, Brennan LA, Levic S, Ross PA, Black SM, 2004. S-nitrosylation of endothelial nitric oxide synthase is associated with monomerization and decreased enzyme activity. *Proceedings of the National Academy of Sciences of the United States of America* **101**, 2619-24.
Reddy AS, Marquez Y, Kalyna M, Barta A, 2013. Complexity of the alternative splicing landscape in plants. *Plant Cell* **25**, 3657-83.
Reichow SL, Hamma T, Ferre-D'amare AR, Varani G, 2007. The structure and function of small nucleolar ribonucleoproteins. *Nucleic Acids Res* **35**, 1452-64.
Requejo R, Hurd TR, Costa NJ, Murphy MP, 2010. Cysteine residues exposed on protein surfaces are the dominant intramitochondrial thiol and may protect against oxidative damage. *FEBS J* **277**, 1465-80.
Riccio A, Alvania RS, Lonze BE*, et al.*, 2006. A nitric oxide signaling pathway controls CREB-mediated gene expression in neurons. *Molecular Cell* **21**, 283-94.
Rodriguez-Munoz M, De La Torre-Madrid E, Sanchez-Blazquez P, Garzon J, 2011. NO-released zinc supports the simultaneous binding of Raf-1 and PKCgamma cysteine-rich domains to HINT1 protein at the mu-opioid receptor. *Antioxid Redox Signal* **14**, 2413-25.
Romero-Puertas MC, Campostrini N, Matte A*, et al.*, 2008. Proteomic analysis of S-nitrosylated proteins in Arabidopsis thaliana undergoing hypersensitive response. *Proteomics* **8**, 1459-69.
Romero P, Obradovic Z, Li X, Garner EC, Brown CJ, Dunker AK, 2001. Sequence complexity of disordered protein. *Proteins* **42**, 38-48.
Rost B, Sander C, 1993. Prediction of protein secondary structure at better than 70% accuracy. *J Mol Biol* **232**, 584-99.

Sakamoto H, Araki T, Meshi T, Iwabuchi M, 2000. Expression of a subset of the Arabidopsis Cys(2)/His(2)-type zinc-finger protein gene family under water stress. *Gene* **248**, 23-32.
Sakihama Y, Nakamura S, Yamasaki H, 2002. Nitric oxide production mediated by nitrate reductase in the green alga Chlamydomonas reinhardtii: an alternative NO production pathway in photosynthetic organisms. *Plant Cell Physiol* **43**, 290-7.
Sambrook J, Russell DW, 2006. SDS-Polyacrylamide Gel Electrophoresis of Proteins. *CSH Protoc* **2006**.
Sanchez-Blazquez P, Rodriguez-Munoz M, Bailon C, Garzon J, 2012. GPCRs promote the release of zinc ions mediated by nNOS/NO and the redox transducer RGSZ2 protein. *Antioxid Redox Signal* **17**, 1163-77.
Sehrawat A, Deswal R, 2014. S-Nitrosylation Analysis in Brassica juncea Apoplast Highlights the Importance of Nitric Oxide in Cold-Stress Signaling. *Journal of Proteome Research*.
Sell S, Lindermayr C, Durner J, 2008. Identification of S-nitrosylated proteins in plants. *Methods in Enzymology* **440**, 283-93.
Serpa V, Vernal J, Lamattina L, Grotewold E, Cassia R, Terenzi H, 2007. Inhibition of AtMYB2 DNA-binding by nitric oxide involves cysteine S-nitrosylation. *Biochem Biophys Res Commun* **361**, 1048-53.
Shi H, Wang X, Ye T*, et al.*, 2014. The Cysteine2/Histidine2-Type Transcription Factor ZINC FINGER OF ARABIDOPSIS THALIANA6 Modulates Biotic and Abiotic Stress Responses by Activating Salicylic Acid-Related Genes and C-REPEAT-BINDING FACTOR Genes in Arabidopsis. *Plant Physiol* **165**, 1367-79.
Silvera D, Formenti SC, Schneider RJ, 2010. Translational control in cancer. *Nature Reviews Cancer* **10**, 254-66.
Sridha S, Wu K, 2006. Identification of AtHD2C as a novel regulator of abscisic acid responses in Arabidopsis. *Plant J* **46**, 124-33.
Staiger D, Brown JW, 2013. Alternative splicing at the intersection of biological timing, development, and stress responses. *Plant Cell* **25**, 3640-56.
Stamler JS, Lamas S, Fang FC, 2001. Nitrosylation. the prototypic redox-based signaling mechanism. *Cell* **106**, 675-83.
Stamler JS, Toone EJ, Lipton SA, Sucher NJ, 1997. (S)NO signals: translocation, regulation, and a consensus motif. *Neuron* **18**, 691-6.
Stohr C, Stremlau S, 2006. Formation and possible roles of nitric oxide in plant roots. *J Exp Bot* **57**, 463-70.
Studier FW, 2005. Protein production by auto-induction in high density shaking cultures. *Protein Expression and Purification* **41**, 207-34.
Sun J, Steenbergen C, Murphy E, 2006. S-nitrosylation: NO-related redox signaling to protect against oxidative stress. *Antioxid Redox Signal* **8**, 1693-705.
Tada Y, Spoel SH, Pajerowska-Mukhtar K*, et al.*, 2008a. Plant immunity requires conformational changes [corrected] of NPR1 via S-nitrosylation and thioredoxins. *Science* **321**, 952-6.
Tada Y, Spoel SH, Pajerowska-Mukhtar K*, et al.*, 2008b. Plant immunity requires conformational charges of NPR1 via S-nitrosylation and thioredoxins. *Science* **321**, 952-6.
Taldone FS, Tummala M, Goldstein EJ, Ryzhov V, Ravi K, Black SM, 2005. Studying the S-nitrosylation of model peptides and eNOS protein by mass spectrometry. *Nitric Oxide* **13**, 176-87.
Tan YF, O'toole N, Taylor NL, Millar AH, 2010. Divalent metal ions in plant mitochondria and their role in interactions with proteins and oxidative stress-induced damage to respiratory function. *Plant Physiol* **152**, 747-61.
Tavares CP, Vernal J, Delena RA, Lamattina L, Cassia R, Terenzi H, 2014. S-nitrosylation influences the structure and DNA binding activity of AtMYB30 transcription factor from Arabidopsis thaliana. *Biochim Biophys Acta* **1844**, 810-7.
Tun NN, Santa-Catarina C, Begum T*, et al.*, 2006. Polyamines induce rapid biosynthesis of nitric oxide (NO) in Arabidopsis thaliana seedlings. *Plant Cell Physiol* **47**, 346-54.
Van Der Linde K, Gutsche N, Leffers HM*, et al.*, 2011. Regulation of plant cytosolic aldolase functions by redox-modifications. *Plant Physiol Biochem* **49**, 946-57.
Vijayalakshmi J, Mukhergee MK, Graumann J, Jakob U, Saper MA, 2001. The 2.2 A crystal structure of Hsp33: a heat shock protein with redox-regulated chaperone activity. *Structure* **9**, 367-75.
Vitecek J, Reinohl V, Jones RL, 2008. Measuring NO production by plant tissues and suspension cultured cells. *Mol Plant* **1**, 270-84.
Von Toerne C, Kahle M, Schafer A*, et al.*, 2013. Apoe, Mbl2, and Psp plasma protein levels correlate with diabetic phenotype in NZO mice--an optimized rapid workflow for SRM-based quantification. *J Proteome Res* **12**, 1331-43.
Wang YQ, Feechan A, Yun BW*, et al.*, 2009. S-nitrosylation of AtSABP3 antagonizes the expression of plant immunity. *J Biol Chem* **284**, 2131-7.
Watkins NJ, Bohnsack MT, 2012. The box C/D and H/ACA snoRNPs: key players in the modification, processing and the dynamic folding of ribosomal RNA. *Wiley Interdiscip Rev RNA* **3**, 397-414.

Wawer I, Bucholc M, Astier J*, et al.*, 2010a. Regulation of Nicotiana tabacum osmotic stress-activated protein kinase and its cellular partner GAPDH by nitric oxide in response to salinity. *Biochemical Journal* **429**, 73-83.
Wawer I, Bucholc M, Astier J*, et al.*, 2010b. Regulation of Nicotiana tabacum osmotic stress-activated protein kinase and its cellular partner GAPDH by nitric oxide in response to salinity. *Biochemical Journal* **429**, 73-83.
Wu K, Tian L, Malik K, Brown D, Miki B, 2000. Functional analysis of HD2 histone deacetylase homologues in Arabidopsis thaliana. *Plant J* **22**, 19-27.
Wu K, Tian L, Zhou C, Brown D, Miki B, 2003. Repression of gene expression by Arabidopsis HD2 histone deacetylases. *Plant J* **34**, 241-7.
Wu X, Oh MH, Schwarz EM*, et al.*, 2011. Lysine acetylation is a widespread protein modification for diverse proteins in Arabidopsis. *Plant Physiol* **155**, 1769-78.
Xu Y, Shao XJ, Wu LY, Deng NY, Chou KC, 2013. iSNO-AAPair: incorporating amino acid pairwise coupling into PseAAC for predicting cysteine S-nitrosylation sites in proteins. *PeerJ* **1**, e171.
Xue S, Wang R, Yang F*, et al.*, 2010a. Structural basis for substrate placement by an archaeal box C/D ribonucleoprotein particle. *Molecular Cell* **39**, 939-49.
Xue Y, Liu Z, Gao X*, et al.*, 2010b. GPS-SNO: computational prediction of protein S-nitrosylation sites with a modified GPS algorithm. *PLoS ONE* **5**, e11290.
Yan D, Zhang Y, Niu L, Yuan Y, Cao X, 2007. Identification and characterization of two closely related histone H4 arginine 3 methyltransferases in Arabidopsis thaliana. *Biochemical Journal* **408**, 113-21.
Yang WM, Yao YL, Seto E, 2001. The FK506-binding protein 25 functionally associates with histone deacetylases and with transcription factor YY1. *EMBO Journal* **20**, 4814-25.
Yun BW, Feechan A, Yin M*, et al.*, 2011. S-nitrosylation of NADPH oxidase regulates cell death in plant immunity. *Nature* **478**, 264-8.
Zemojtel T, Frohlich A, Palmieri MC*, et al.*, 2006. Plant nitric oxide synthase: a never-ending story? *Trends Plant Sci* **11**, 524-5; author reply 6-8.
Zhang J, Zhao X, Sun P, Ma Z, 2014. PSNO: predicting cysteine S-nitrosylation sites by incorporating various sequence-derived features into the general form of Chou's PseAAC. *Int J Mol Sci* **15**, 11204-19.
Zhang X, Henriques R, Lin SS, Niu QW, Chua NH, 2006. Agrobacterium-mediated transformation of Arabidopsis thaliana using the floral dip method. *Nat Protoc* **1**, 641-6.
Zhao Y, Lin YH, 2010. Whole-cell protein identification using the concept of unique peptides. *Genomics Proteomics Bioinformatics* **8**, 33-41.
Zheng L, Baumann U, Reymond JL, 2004. An efficient one-step site-directed and site-saturation mutagenesis protocol. *Nucleic Acids Res* **32**, e115.

Supplements

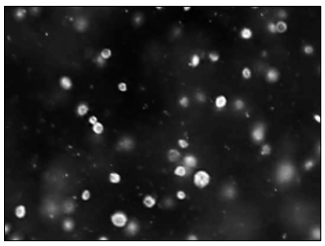

Fig. S1. Isolated nuclei of *Arabidopsis* cell cultures visualized with DAPI.

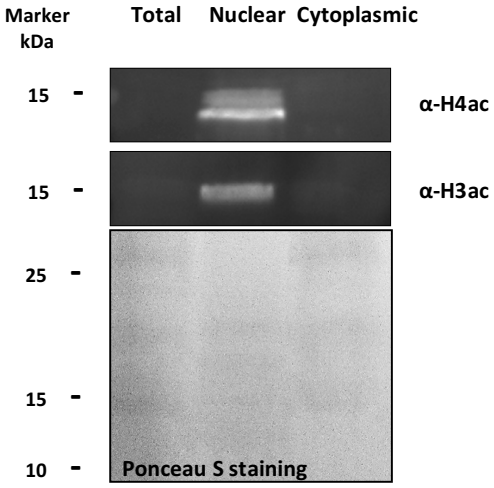

Fig. S2. Immunoblot analysis of nuclear extracts. 15 µg of total cell culture, nuclear and cytoplasmic extract were separated by SDS-PAGE and immunoblotted with anti-H3acantibodies. Anti-rabbit-IgG-Horseradish Peroxidase was used as secondary antibody. The relative masses of protein standards are shown on the left. (The SDS-PAGE and immuonoblat analysis of nuclear extracts was performed by Alexandra Ageeva and Alexander Mengel).

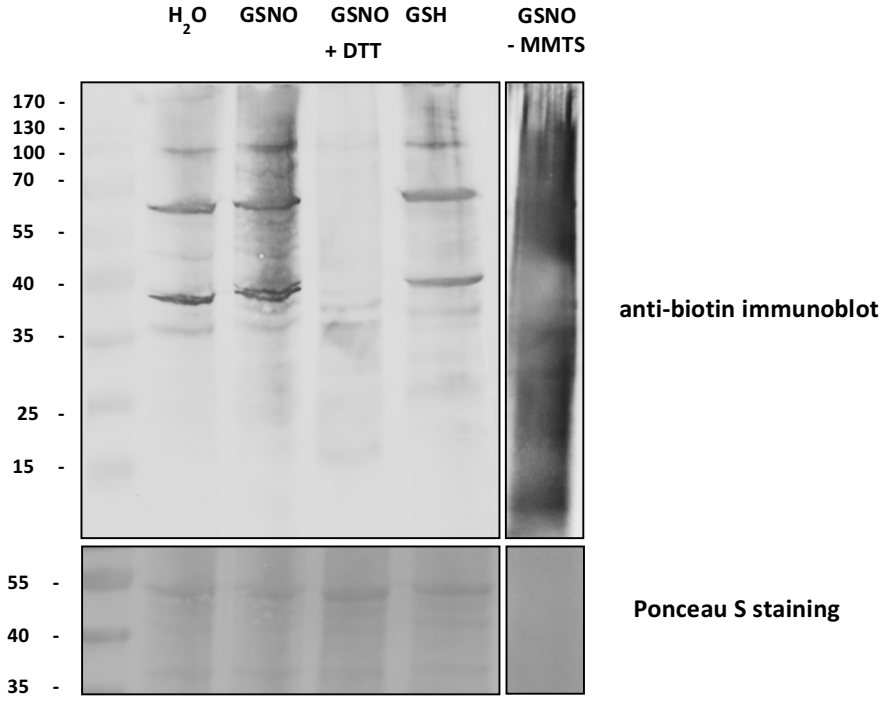

Fig. S3. Control treatments demonstrating the specificity of the biotin switch assay. The nuclear protein samples were treated as indicated and subjected to the biotin switch assay. The protein sample was separated by SDS-PAGE and immunoblotted by monoclonal antibiotin antibody. The relative masses of protein standards are shown on the left. (Left) In the water-treated sample a distinct protein pattern could be detected, which was more intensive after GSNO-treatment. After treatment with 100 mM DTT only two weak protein bands could be detected, which might represent *in-vivo* biotinylated proteins or indicate cross reaction of the anti-biotin antibody. After treatment with 250 µM GSH the protein pattern was very similar to the pattern of the water-treatment, demonstrating the applied GSH concentration cannot reduce the *in-vivo* S-nitrosylated proteins. (Right) Without a blocking step a strong biotinylation signal could be detected. Taken together, these results demonstrate that *in-vivo* S-nitrosylated proteins were detected in the water treated sample. The left gel was produced by Elke Mattes.

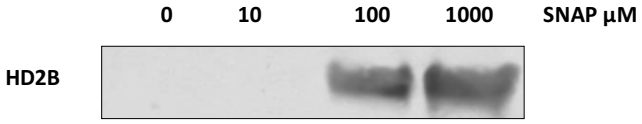

Fig. S4. Immunoblot analysis of S-nitrosylation of recombinant protein of HD2B treated with SNAP *in-vitro*. 5 µg of recombinant HD2B was treated with different concentrations of SNAP and subjected to the biotin switch assay. Biotinylated proteins were visualized by immunoblotting using anti-biotin monoclonal antibody.

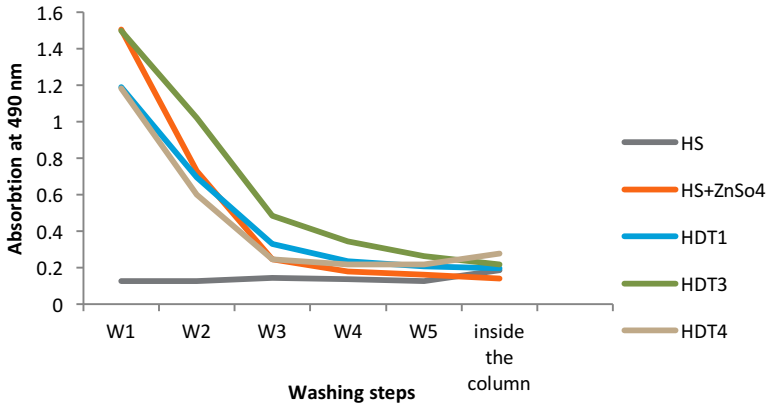

Fig. S5. Washing steps of removing extra zinc ion from recombinant proteins. 0.1 mM $ZnSO_4$ was loaded on recombinant protein samples for 1h at RT, and then protein samples were washed 5-7 times using 10kd spin columns until the follow trough of all protein samples had an absorption similar to HS buffer. The absorption was measured by adding PAR at 490 nm after each washing step using Tecan reader.

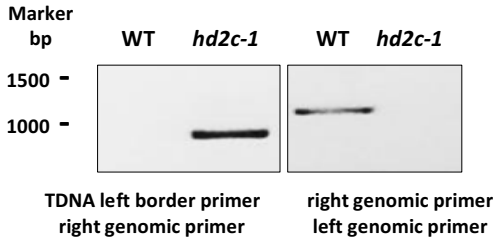

Fig. S6. Genotyping *hd2c-1* T-DNA insertion line (Salk_129799.19.60). To verify the homozygous mutants, a PCR-based genotyping was performed using specific primers (LBa1 of pBIN-pROK2 for SALK lines (T-DNA left border primer), *HD2C*-LP (left border primer) and *HD2C*-RP (right border primer)) from the website of SIGnal Salk Institute Genomic Analysis Laboratory (http://signal.salk.edu/cgi-bin/tdnaexpress) and Extract-N-AmpTM plant PCR kit (sigma, Germany) following the manufacturer's instructions. The DNA fragments were separated by agarose gel electrophoresis.

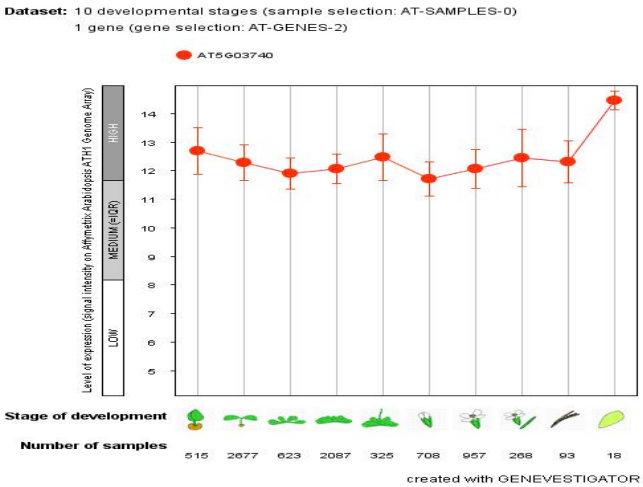

Fig S7. Expression level of *HD2C* in developmental stages of *Arabidopsis* using GENEVESTIGATOR Data-based protein expression tool was used to estimation of expression level of HD2C in developmental stages of *Arabidopsis* (https://genevestigator.com/gv/user/userProfile.jsp).

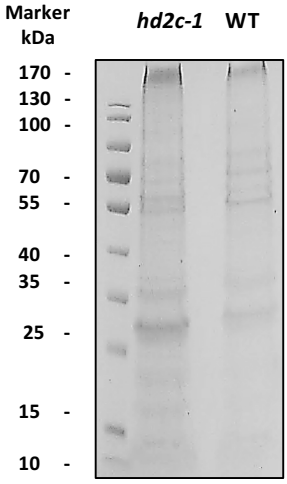

Fig S8. Quality control of nuclear enriched protein extraction from *Arabidopsis* WT and *hd2c-1* line for Co-IP experiment. The nuclear enriched protein fractions obtained from 0.5 gram of plant starting material and whole the sample were loaded on the gel. The proteins were separated by SDS-PAGE and the gel was stained by coomassie blue staining solution. The relative masses of protein standards are shown on the left.

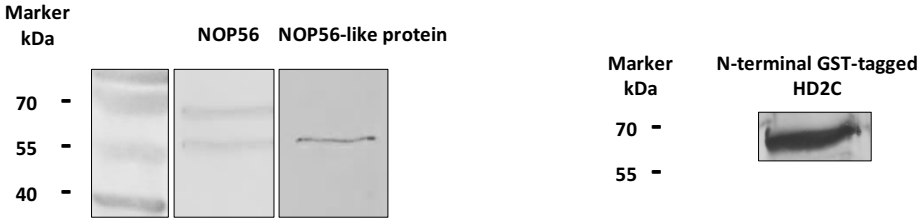

Fig. S9. Immunoblot analysis of purified recombinant proteins. 5 µg recombinant proteins of C-terminal-6X histidine tagged NOP56 (AT3G05060) and N-terminal-6X histidine tagged NOP56-like protein (AT1g56110) and N-terminal-GST tagged HD2C were loaded in the SDS-PAGE and detected via western blot using primery monoclonal anti-histidine antibody and monoclonal anti-GST primery antibody and anti-mouse IgG–alkaline phosphatase secondary antibody. The relative masses of protein standards are shown on the left.

Table. S1. Identified S-nitrosylation nuclear candidate proteins from *Arabidopsis* cell cultures. *Arabidopsis* cell cultures were treated with avirulent and virulent *Pst* DC3000 for 2 h and 13 h and only 13 h, respectively. Control samples were treated with $MgCl_2$. Nuclear enriched fractions were treated with either ddH_2O or 250 µM GSNO and subjected to the biotin switch assay. Biotinylated proteins were visualized by immunoblotting and purified by neutravidin agarose. The biotinylated proteins were identified by LC-MS/MS analysis in which the scaffold settings were used 2 unique peptides. Peptide identifications were accepted if they could be established at greater than 95.0% probability as specified by the Peptide Prophet algorithm. Protein identifications were accepted if they could be established at greater than 99.0% probability and contained at least two identified peptides. MW: Molecular weight, N: Nucleus, N^N: Nucleolus, C: Cytosol, Cy: cytoskeleton, ER: Endoplasmic reticulum, E: Extracellular, G: Golgi, PM: Plasma membrane, P: Plastid, Pe: peroxisome, V: Vacuole and M: Mitochondrion. Bold letters shows the highest localization of protein in the corresponding organelle (eFP browser). The black and blue colored proteins correlate with the right and left gels of Fig 5b, respectively.* indicates the proteins with no cysteine residue.

	AGI code	Description	MW kDa	Localization eFP browser	Peptide number									
					2h						13h			
					$MgCl_2$		*Pst* avr		$MgCl_2$		*Pst* avr		*Pst* vir	
					H_2O	GSNO	H_2O	GSNO	H_2O	GSNO	H_2O	GSNO	H_2O	GSNO
1	AT1G03860.1*	ATPHB2, PROHIBITIN 2	32	C, ER, E, G, PM, P, V								2		
2	AT1G06220.1	MEE5, Ribosomal protein S5/Elongation factor G/III/V	110	***N***, C, PM, M				2						
3	AT1G07660.1*	Histone H4	11	***N***, C, PM, P, V, M			2							
	AT1G07660.1	Histone H4	11	***N***, C, PM, P, V, M							3			2
4	AT1G07670.1	ATECA4, Endomembrane-type CA-ATPase 4	116	N, C, ***ER***, ***PM***, M				3						
5	AT1G07920.1	GTP binding Elongation factor Tu family protein	50	N^N, ***C***, PM, P, V, M	2	5	3	4			5	3		
	AT1G07920.1	GTP binding Elongation factor Tu family protein	50	N^N, ***C***, PM, P, V, M					2			4		2
6	AT1G08880.1 *	HTA5, DNA binding	15	***N***, C, PM, P, M										3
7	AT1G09100.1	RPT5B, 26S proteasome AAA-ATPase subunit	47	***N***, ***C***, PM, M				2						
8	AT1G09640.1	Translation elongation factor EF1B, gamma chain	47	N, ***C***, ER, E, G, ***PM***, V, M				3						
9	AT1G12270.1	Hop1, Stress-inducible protein, putative	65	***N***, ***C***, M		2		3						
10	AT1G15690.1*	AVP1, Inorganic H pyrophosphatase family protein	81	C, ER, E, G, ***PM***, P, ***V***, M		2	2	3						
11	AT1G15930.1	Ribosomal protein L7Ae/L30e/S12e/Gadd45	15	N, ***C***, PM, M				2						
12	AT1G17745.1	PGDH, D-3-phosphoglycerate dehydrogenase	66	N, C, PM, Pe, ***P***, M		2		3						
13	AT1G20960.1	Emb1507, U5 small nuclear ribonucleoprotein helicase	247	***N***^{N}, C, PM, P, M				2						
14	AT1G22780.1	PFL, Ribosomal protein S13/S18 family	18	N, ***C***, ER, E, G, PM, P, V, M		2								

Table. S1. Continued.

	AGI code	Description	MW kDa	Localization eFP browser	Peptide number									
					2h						13h			
					$MgCl_2$		*Pst* avr		$MgCl_2$		*Pst* avr		*Pst* vir	
					H_2O	GSNO	H_2O	GSNO	H_2O	GSNO	H_2O	GSNO	H_2O	GSNO
15	AT1G24360.1	NAD(P)-binding Rossmann-fold superfamily protein	34	***N***, ***P***, ***M***	2			2						
16	AT1G27400.1	Ribosomal protein L22p/L17e family protein	20	N, ***C***, ***PM***, ***P***, V, M		2								
17	AT1G43170.1	ARP1, emb2207, Ribosomal protein 1	45	***N***^{N}, ***C***, PM, P, V, M				2						
18	AT1G44835.1	YbaK/aminoacyl-tRNA synthetase-associated domain	34	N, ***C***, P, M								2		
19	AT1G48920.1	ATNUC-L1, Nucleolin like 1	59	***N***^{N}, C, PM, P, M				2			4			
	AT1G48920.1	ATNUC-L1, Nucleolin like 1	59	***N***^{N}, C, PM, P, M					2					
20	AT1G50570.1	Calcium-dependent lipid-binding family protein	42	***N***, ***C***, ER, E, G, P, M				4						
21	AT1G52360.1	Coatomer protein complex, subunit beta 2, putative	104	N, ***C***, ER, E, G, PM, M					2					
22	AT1G54220.1	Dihydrolipoamide acetyltransferase protein	58	N, C, P, V, ***M***				2			2			
23	AT1G54270.1	EIF4A-2, ATP-dependent helicase/ translation initiation	47	N, ***C***, G, PM, P, V, M		2	2	4			2	2		
	AT1G54270.1	EIF4A-2, ATP-dependent helicase/ translation initiation	47	N, ***C***, G, PM, P, V, M								3		
24	AT1G55490.1	CPN60B, Chaperonin 60 beta	64	N, PM, ***P***, M								2		
25	AT1G56070.1	LOS, Ribosomal protein S5/Elongation factor G/III/V	94	N^{N}, ***C***, E, G, PM, P, V, M	3	6		3		3	2	5		
26	AT1G56110.1	NOP56, Homolog of nucleolar protein NOP56	59	***N***^{N}, C, PM, P			4	5			2			
	AT1G56110.1	NOP56, Homolog of nucleolar protein NOP56	59	***N***^{N}, C, PM, P								3		3
27	AT1G57720.1	Translation elongation factor EF1B, gamma chain	46	N, ***C***, ER, E, G, ***PM***, V, M				5			2	3		
28	AT1G62740.1	Hop2, Stress-inducible protein, putative	65	***N***, ***C***, ***PM***, P, M				4				2		
29	AT1G67230.1	LINC1, Little nuclei1	129	***N***, C, Cy, PM, P, M				2			2	2		
30	AT1G71380.1	ATGH9B3, Cellulase 3	53	N, ER, ***E***, G, PM, P, V, M				3						
31	AT1G72370.1	P40, 40s ribosomal protein SA	32	***N***, ***C***, ER, E, G, PM, ***P***, M	2	3	3	5			2	4		
32	AT1G78850.1	D-mannose binding lectin protein with Apple-like carbohydrate-binding domain	49	N, C, ER, ***E***, G, ***PM***, V							2			
33	AT1G78900.1	VHA-A, Vacuolar ATP synthase subunit A	69	N, C, ER, E, G, PM, P, ***V***, M	5	3		4			3	2		

Table. S1. Continued.

	AGI code	Description	MW kDa	Localization eFP browser	Peptide number									
					2h				13h					
					$MgCl_2$		*Pst* avr		$MgCl_2$		*Pst* avr		*Pst* vir	
					H_2O	GSNO	H_2O	GSNO	H_2O	GSNO	H_2O	GSNO	H_2O	GSNO
34	AT2G02160.1	CCCH-type zinc finger family protein	76	***N***, C, M				3						
35	AT2G06850.1*	Xyloglucan endotransglucosylase hydrolase 4	34	C, ER, ***E***, G, PM, ***P***, V			2	3			3			
36	AT2G17360.1	Ribosomal protein S4 (RPS4A) family protein	30	N, ***C***, ***PM***, ***P***, V, M		2		3		2		2		
37	AT2G19480.1	NFA02, Nucleosome assembly protein 1;2	44	***N***, C, ER, PM , M				2						
38	AT2G21390.1	Coatomer, alpha subunit	136	***N***, ***C***, ***ER***, E, G, PM, P, M				3						
39	AT2G30490.1*	ATC4H, Cinnamate-4-hydroxylase	58	C, ***ER***, E, G, PM, P, V, M				2						
40	AT2G31610.1	40S ribosomal protein S3 (RPS3A)	28	N, ***C***, ***PM***, ***P***, V, M	2			2				3		
	AT2G31610.1	40S ribosomal protein S3 (RPS3A)	28	N, ***C***, ***PM***, ***P***, V, M								2		
41	AT2G33150.1	PKT3, Peroxisomal 3-ketoacyl-CoA thiolase 3	49	N, C, ***Pe***, PM, P, V, ***M***				3				2		
42	AT2G33340.1	MOS4-associated complex 3B	57	***N***, C, ***P***, M				2						
43	AT2G34680.1	AIR, Outer arm dynein light chain 1 protein	187	N, C, ***PM***, P, M				3						
44	AT2G37190.1	Ribosomal protein L11 family protein	18	***N***^{N}, ***C***, ER, E, G, PM, ***P***, V, M			2	2		2	2	2		
45	AT2G37270.1	ATRPS5B, Ribosomal protein 5B	23	N, ***C***, Cy, PM, P, V, M	2	3								
	AT2G37270.1	ATRPS5B, Ribosomal protein 5B	23	N, ***C***, Cy, PM, P, V, M										2
46	AT2G37470.1*	Histone H2B, putative	15	***N***, C, PM, P, V, M										2
47	AT2G39990.1	EIF2, Eukaryotic translation initiation factor 2	32	***N***, ***C***, ER, E, G, P				2						
48	AT2G40290.1	Eukaryotic translation initiation factor 2 subunit 1	39	***N***, ***C***, PM, P, M				2						
49	AT2G40660.1	Nucleic acid-binding, OB-fold-like protein	42	***N***, ***C***, E, PM, P, M				2						
50	AT2G41840.1	Ribosomal protein S5 family protein	31	***N***^{N}, ***C***, PM, M	2	5								
51	AT2G42740.1	RPL16A, Ribosomal protein large subunit 16A	21	N^{N}, ***C***, ER, E, G, PM, P, V, M		2		2						
	AT2G42740.1	RPL16A, Ribosomal protein large subunit 16A	21	N^{N}, ***C***, ER, E, G, PM, P, V, M					2		2			2
52	AT2G44530.1	Phosphoribosyltransferase family protein	43	N, C, ***P***, M				2						
53	AT2G47000.1	MDR4, ATP binding cassette subfamily B4	139	N, C, G, Pe, ***PM***, M				3						
54	AT2G47110.1	UBQ6, Ubiquitin 6	18	N, ***C***, G, PM, M	2									

Table. S1. Continued.

	AGI code	Description	MW kDa	Localization eFP browser	Peptide number									
					2h						13h			
					$MgCl_2$		*Pst* avr		$MgCl_2$		*Pst* avr		*Pst* vir	
					H_2O	GSNO	H_2O	GSNO	H_2O	GSNO	H_2O	GSNO	H_2O	GSNO
55	AT2G47470.1 *	ATPDIL2-1, Thioredoxin family protein	39	C, ***ER***, E, G, PM, V				2				3		
56	AT3G01280.1	VDAC1, Voltage dependent anion channel 1	29	N, C, ER, E, G, PM, P, V, ***M***				2						
57	AT3G01290.1	SPFH, PHB domain-containing membrane-associated	31	N, C, ER, E, G, ***PM***,V, ***M***	2	2						2		
58	AT3G01800.1	Ribosome recycling factor	29	***N***, ***P***, ***M***				3						
59	AT3G02080.1	Ribosomal protein S19e family protein	16	N, ***C***, Cy, PM, P, M		2								
60	AT3G02880.1	Leucine-rich repeat protein kinase family protein	68	C, ER, E, G, ***PM***, P, V, M			2	2		2				
61	AT3G03960.1	TCP-1, cpn60 chaperonin family protein	59	N, ***C***, PM, P	2			4			3			
62	AT3G05060.1	NOP56-like pre RNA processing ribonucleoprotein	59	***N***^{N}, C, ER, E, G, PM			3	2						
	AT3G05060.1	NOP56-like pre RNA processing ribonucleoprotein	59	***N***^{N}, C, ER, E, G, PM								3		2
63	AT3G08580.1	AAC1, ADP/ATP carrier 1	41	***N***^{N}, ***PM***, ***P***, ***V***, ***M***	4	3	3	8		3	2	6		
	AT3G08580.1	AAC1, ADP/ATP carrier 1	41	***N***^{N}, ***PM***, ***P***, ***V***, ***M***					4	2		4		4
64	AT3G09440.1	Heat shock protein 70 (Hsp 70) family protein	71	N, ***C***, ER, E, G, ***PM***, ***P***, V, M				2			2			
65	AT3G11130.1	Clathrin, heavy chain	193	N, C, ER, E, G, ***PM***, P, ***V***, M	5	3	2	4				2		
66	AT3G11400.1	EIF3G1, Eukaryotic translation initiation factor 3G1	33	N, ***C***, ***PM***, P, M		2		2						
67	AT3G13290.1	VCR, Varicose-related	146	***N***, C, PM, P, M	2									
68	AT3G13930.1	Dihydrolipoamide acetyltransferase protein	58	N, PM, P, ***M***	2			3						
69	AT3G17390.1	MTO3, Methionine adenosyltransferase	43	***N***^{N}, C, Cy, ER, E, G, ***PM***,P,M					3			3		3
70	AT3G23990.1	HSP60, Heat shock protein 60	61	N, C, PM, P, V, ***M***						2	2			
71	AT3G25520.1	ATL5, Ribosomal protein L5	34	***N***, ***C***, PM, P, V, ***M***		2		2						
72	AT3G26618.1	ERF1-3, Eukaryotic release factor 1-3	49	N, ***C***, P, M				2						
73	AT3G53990.1	Adenine nucleotide alpha hydrolases-like	18	N, ***C***, ER, E, G, ***PM***, M				2						
74	AT3G54110.1	ATPUMP1, Plant uncoupling mitochondrial protein 1	33	C, ER, E, G, Pe, PM, P, V, ***M***				2						
75	AT3G55410.1	2-oxoglutarate dehydrogenase, E1 component	115	N, C, PM, P, ***M***				5						

Table. S1. Continued.

	AGI code	Description	MW kDa	Localization eFP browser	Peptide number									
					2h						13h			
					$MgCl_2$		*Pst* avr		$MgCl_2$		*Pst* avr		*Pst* vir	
					H_2O	GSNO	H_2O	GSNO	H_2O	GSNO	H_2O	GSNO	H_2O	GSNO
76	AT3G56190.1	Alpha-soluble NSF attachment protein 2	33	N, C, ER, G, ***PM***, V, M				4		3	2	2		
77	AT3G57330.1*	ACA11, Autoinhibited Ca2+-ATPase 11	112	C, ER, G, Pe, ***PM***, P, V, M		2								
78	AT3G58510.1	DEA(D/H)-box RNA helicase family protein	66	***N***^{N}, C, E, ***Pe***, ***PM***, P, M				3						
79	AT3G60240.2	EIF4G,Eukaryotic translation initiation factor 4G	188	***N***, C, PM, P, ***M***		2		6			2			
80	AT4G11010.1	NDPK3 | nucleoside diphosphate kinase 3	26	N, C, PM, ***P***, ***M***						2				
81	AT4G14960.1	TUA6, Structural constituent of cytoskeleton	47	***N***, C, Cy, ***PM***, P, V	2	3	2	3		3	2	4		
	AT4G14960.1	TUA6, Structural constituent of cytoskeleton	47	***N***, C, Cy, ***PM***, P, V, M						2		2		2
82	AT4G16143.1	IMPA-2, Importin alpha isoform 2	59	***N***^{N}, ***C***, PM, M				4						
83	AT4G18100.1	Ribosomal protein L32e	16	N^{N}, ***C***, PM, P, M		2								
84	AT4G20890.1	TUB9, Tubulin beta-9 chain	50	***N***, ***C***, Cy, G, ***PM***, P, V, M		2		3			3			
85	AT4G21150.1	HAP6, Ribophorin II (RPN2) family protein	75	N, ***ER***, E, G, PM, V, M	2									
86	AT4G24190.1	SHD, Chaperone protein htpG family protein	94	N, C, ***ER***, E, G, PM, P, V, M							2			
87	AT4G25210.1	DNA-binding storekeeper transcriptional regulator	40	***N***^{N},C, P, M			3							
88	AT4G27500.1	PPI1, Proton pump interactor 1	69	N, C, ***ER***, ***PM***, P, M								3		
89	AT4G30190.1	AHA2, H(+)-ATPase 2	104	N, C, ER, E, G, ***PM***, P, V, M			3	3				2		
90	AT4G31480.1	Coatomer, beta subunit	106	N, ***C***, ER, G, PM, M				2						
91	AT4G31880.1	Unknown protein	94	***N***, C, ***P***, M				2						
92	AT4G34200.1*	EDA9, D-3-phosphoglycerate dehydrogenase	63	C, PM, ***P***, ***M***	4	8	4	7	2	2	3	5		
93	AT4G34450.1	Coatomer gamma-2 subunit, putative	98	N, ***C***, ER,G, PM, P, M	2			2						
	AT4G34450.1	Coatomer gamma-2 subunit, putative	98	N, ***C***, ER,G, PM, P, M										2
94	AT4G35000.1	APX3, Ascorbate peroxidase 3	32	N, C, ***Pe***, PM, P, V, M						2				
95	AT4G36020.1	CSDP1, Cold shock domain protein 1	30	***N***, C, E, G, P, M				4		3				
96	AT4G37910.1*	MtHsc70-1, Mitochondrial heat shock protein 70-1	73	PM, P, V, ***M***				4						
97	AT4G39680.1	SAP domain-containing protein	69	N, ***C***, ***P***, M				6						

Table. S1. Continued.

	AGI code	Description	MW kDa	Localization eFP browser	Peptide number									
					2h						13h			
					$MgCl_2$		*Pst* avr		$MgCl_2$		*Pst* avr		*Pst* vir	
					H_2O	GSNO	H_2O	GSNO	H_2O	GSNO	H_2O	GSNO	H_2O	GSNO
98	AT4G39980.1*	3-deoxy-D-arabino-heptulosonate 7-phosphate synthase	58	PM, ***P***, M				2						
99	AT5G02490.1	Heat shock cognate 70 kDa protein 2 (HSC70-2)	71	N, ***C***, G, PM, P, M				3						
	AT5G02490.1	Heat shock cognate 70 kDa protein 2 (HSC70-2)	71	N, ***C***, G, PM, P, M					3					6
100	AT5G02500.1	HSC70-1, Heat shock cognate protein 70-1	71	N^N, ***C***, ER, G, Pe, PM,P,V, M	6	4	7	7	4	5	6	7		
101	AT5G03740.1	HD2C, HDT3, Histone deacetylase 2C	32	***N***^{N}, C, ER, E, G, M										4
102	AT5G08670.1	ATP synthase alpha/beta family protein	60	N, ***C***, Pe, PM, P, V, ***M***		2	2	3				4		
103	AT5G09590.1	MTHSC70-2, Mitochondrial HSO70 2	73	N, PM, P, V, ***M***							2			
104	AT5G09810.1	ACT7, Actin 7	42	N, ***C***, Cy, PM, P, ***M***		3		3				3		
	AT5G09810.1	ACT7, Actin 7	42	N, ***C***, Cy, PM, P, ***M***					2					
105	AT5G10010.1	Unknown protein	51	***N***^{N}, C, ER, E, G, PM, P, M				3			2			
106	AT5G10840.1 *	Endomembrane protein 70 protein family	74	***ER***, E, G, ***PM***, P, V, M				2						
107	AT5G11900.1	Translation initiation factor SUI1 family protein	22	N, ***C***, ER, E, G, Pe, M				2						
108	AT5G14040.1	PHT3;1, Phosphate transporter 3;1	40	N, E, Pe, PM, ***P***, V, ***M***				2						
	AT5G14040.1	PHT3;1, Phosphate transporter 3;1	40	N, E, Pe, PM, ***P***, V, ***M***								3		4
109	AT5G15090.1 *	VDAC3, Voltage dependent anion channel 3	29	***N***, ER, E, G, PM, ***P***, V, ***M***	2					2		2		
110	AT5G19510.1	Translation elongation factor EF1B/ribosomal protein S6	24	N, ***C***, E, ***PM***, V, M						2	2			
111	AT5G19760.1	Mitochondrial substrate carrier family protein	32	N, C, ER, E, Pe, ***PM***, ***P***, V, ***M***				2						
	AT5G19760.1	Mitochondrial substrate carrier family protein	32	N, C, ER, E, Pe, ***PM***, ***P***, V, ***M***								2		
112	AT5G19770.1	TUA3, Tubulin alpha-3	50	N, ***C***, Cy, ER, E, G, PM, V, M				2						
113	AT5G20290.1	Ribosomal protein S8e family protein	25	***N***^{N}, C, PM, P, M				2						
114	AT5G22060.1	ATJ2, DNAJ homologue 2	46	N, C, Pe, ***PM***, M				2						
115	AT5G22650.1	HD2B, HDT2, Histone deacetylase 2B	32	***N***^{N}, C, ER, E, G, PM, V, M				2				2		
116	AT5G23740.1	RPS11-BETA, Ribosomal protein S11-beta	18	N, ***C***,PM, P, M				2						

Table. S1. Continued.

	AGI code	Description	MW kDa	Localization eFP browser	Peptide number									
					2h						13h			
					$MgCl_2$		*Pst* avr		$MgCl_2$		*Pst* avr		*Pst* vir	
					H_2O	GSNO	H_2O	GSNO	H_2O	GSNO	H_2O	GSNO	H_2O	GSNO
117	AT5G23890.1	Unknown protein	104	N, PM, ***P***, M								2		
118	AT5G26710.1	Glutamyl/glutaminyl-tRNA synthetase, class Ic	81	N, ***C***, ER, E, G, PM, P										2
119	AT5G27640.1	TIF3B1, Translation initiation factor 3B1	82	***N***, ***C***, PM, M				2			2			
120	AT5G28540.1	BIP1, ATP binding	74	N, C, ***ER***, E, G, PM, P, V										2
121	AT5G40770.1*	ATPHB3, PROHIBITIN 3	30	N, C, ER, E, G, PM, P, V								3		
122	AT5G40870.1	Uridine kinase/uracil phosphoribosyltransferase 1	54	N, C, ***P***, M				2						
123	AT5G42020.1	BIP, Heat shock protein 70 (Hsp 70) family protein	74	N^N, C, ***ER***, E, G, PM, V	6	5	5	10	2	6	6	8		
124	AT5G46070.1	Guanylate-binding family protein	123	***N***^{N}, C, ***P***, M				2						
125	AT5G47210.1*	Hyaluronan, mRNA binding family	38	N, C, ER, E, G, Pe, ***PM***, M		2					3			
126	AT5G48650.1	Nuclear transport factor 2 (NTF2) family protein	50	***N***, ***C***, ER, E, G, P, M				2						
127	AT5G50920.1*	CLPC, CLPC homologue 1	103	PM, ***P***, M				2						
128	AT5G52470.1	FIB1, FIBRILLARIN 1, snoRNA binding	33	***N***^{N}, C, PM, P, M								4		2
129	AT5G52840.1*	NADH-ubiquinone oxidoreductase-related	19	C, PM, P, ***M***						2	2			
130	AT5G55070.1	Dihydrolipoamide succinyltransferase	50	N, C, PM, P, ***M***	2		3	3			2	2		
131	AT5G56000.1	Heat shock protein 81-4 (HSP81-4)	80	***N***, ***C***, ER, E, G, PM, P, V, M										2
	AT5G56000.1	Heat shock protein 81-4 (HSP81-4)	80	***N***, ***C***, ER, E, G, PM, P, V, M		2	2	5			3	2		
132	AT5G56630.1	PFK7, phosphofructokinase 7	53	N, ***C***, ER, E, G, M				2						
133	AT5G57120.1	Unknown protein	38	***N***^{N}, C, M				2						
134	AT5G57870.1	eIFiso4G1, MIF4G domain-containing protein	86	***N***, C, PM, P, M				2						
135	AT5G61780.1	Tudor2, TUDOR-SN protein 2	108	N, C, PM, P, M								2		
136	AT5G62690.1	TUB2, Tubulin beta chain 2	51	***N***, C, Cy, ER, E, G, PM, M	5	7	7	9	2	2	4	3		
	AT5G62690.1	TUB2, Tubulin beta chain 2	51	***N***, C, Cy, ER, E, G, PM, M					3			3		4
137	AT5G67630.1	P-loop containing nucleoside triphosphate hydrolases	52	***N***^{N}, C, Cy, ***P***, M				2						

Table. S2. *Arabidopsis* S-nitrosylation nuclear candidate proteins analyzed by GPS-SNO 1.0 software. *Arabidopsis* S-nitrosylated nuclear candidate proteins were analyzed by GPS-SNO 1.0 software using the high threshold condition.

	AGI code	Cys position	NO sensitive-peptide sequence	Score	Cutoff	Cluster
1	AT1G06220.1	677	ADPVVSFCETVVESS	1,738	1,484	Cluster A
2	AT1G07670.1	8	MGKGGEDCGNKQTNS	2,213	1,484	Cluster A
		376	PSVETLGCTTVICSD	3,25	2,443	Cluster B
		381	LGCTTVICSDKTGTL	3,745	2,443	Cluster B
3	AT1G12270.1	297	EMGKYNECIEDCNKA	2,918	2,443	Cluster B
		494	LLDGVKRCVQQINKA	4,098	2,443	Cluster B
4	AT1G15930.1	51	VVRGLHECAKLIEKR	2,837	2,443	Cluster B
5	AT1G17745.1	7	*MAFSSSCSSVKAVN	8,443	1,484	Cluster A
6	AT1G20960.1	526	KAENILLCAPTGAGK	2,647	2,443	Cluster B
		1382	TGSGKTICAEFAILR	2,663	2,443	Cluster B
7	AT1G24360.1	192	NLTGVFLCTQAAVKI	3,065	2,443	Cluster B
		255	NINVNVVCPGFIASD	2,63	2,443	Cluster B
8	AT1G27400.1	15	PDNITKSCKARGADL	3,71	1,484	Cluster A
9	AT1G44835.1	265	SEVAKGECVEALAET	4.049	2.443	Cluster B
10	AT1G52360.1	221	WDYQTKSCVQTLEGH	2,826	2,443	Cluster B
		690	KLQMAEECMKYAMDL	3,859	2,443	Cluster B
11	AT1G54220.1	342	YYLTVDTCVDKLMAL	3,103	2,443	Cluster B
		510	YMPVTLSCDHRVVDG	2,69	2,443	Cluster B
12	AT1G56070.1	131	GALVVVDCIEGVCVQ	2,652	2,443	Cluster B
		448	ETVEDVPCGNTVAMV	2,505	2,443	Cluster B
13	AT1G56110.1	324	SLTNLAKCPSSTLQI	4,38	2,443	Cluster B
		387	SIASRIDCFADGATT	2,641	2,443	Cluster B
14	AT1G62740.1	296	EMGKYDECIKDCDKA	2,647	2,443	Cluster B
		425	AYSNRAACYTKLGAM	3,261	2,443	Cluster B
		493	LLDGVKRCVQQINKA	3,478	2,443	Cluster B
15	AT1G67230.1	795	KVSWFRKCTSKMLKL	3,435	2,443	Cluster B
		1044	QQEEGIHCTQATATA	2,56	2,443	Cluster B
16	AT1G71380.1	358	ATKHTFNCGSSVIVP	3,386	2,443	Cluster B
17	AT1G72370.1	23	EADVRMMCAAEVHLG	1,732	1,484	Cluster A
18	AT1G78850.1	10	FSITLALCFTLSIFL	2,552	1,484	Cluster A
		348	LLGWDETCKSPSLAS	2,995	2,443	Cluster B
19	AT1G78900.1	256	AIPGAFGCGKTVISQ	3,332	2,443	Cluster B
20	AT2G19480.1	376	AGERPPECKQQ****	3,429	2,443	Cluster B
21	AT2G21390.1	623	MIKNSQLCGQAMIAY	3,022	2,443	Cluster B

Table. S2. Continued.

	AGI code	Cys position	NO sensitive-peptide sequence	Score	Cutoff	Cluster
22	AT2G33150.1	371	FASQFVYCRNKLGLD	2,723	2,443	Cluster B
		402	LGATGARCVATLLHE	2,88	2,443	Cluster B
23	AT2G33340.1	3	*****MNCAISGEVP	27,854	26,728	Cluster C
24	AT2G34680.1	627	CGGTPGKCITSWLRR	2.451	2.443	Cluster B
		1440	ALSSEISCSYKVRFE	2,772	2,443	Cluster B
25	AT2G40290.1	274	LNKAIAACTETIETH	3,071	2,443	Cluster B
26	AT2G40660.1	14	QMILSALCKHFSLDP	3,432	1,484	Cluster A
27	AT2G41840.1	137	HVGLGVKCSKEVATA	3,326	2,443	Cluster B
28	AT3G05060.1	81	RKFLKANCQGETLAV	1,863	1,484	Cluster A
29	AT3G08580.1	130	PYKGIGDCFGRTIKD	2,739	2,443	Cluster B
30	AT3G09440.1	319	NIDLFRKCMEPVEKC	3,353	2,443	Cluster B
		326	CMEPVEKCLRDAKMD	2,603	2,443	Cluster B
		609	MKELESICNPIIAKM	2,033	1,484	Cluster A
31	AT3G11130.1	472	LAEDKLECSEELGDL	5,37	2,443	Cluster B
		680	SSEWAMECMKDLLLV	2,777	2,443	Cluster B
		940	VAYRRGQCDEELINV	4,245	2,443	Cluster B
		1309	EYYQNRGCFNELISL	3,027	2,443	Cluster B
32	AT3G13930.1	510	YMSVTLSCDHRVIDG	2,75	2,443	Cluster B
33	AT3G23990.1	121	VAGDGTTCATVLTRA	2,728	2,443	Cluster B
34	AT3G53990.1	83	GVKTDIACLDMLDTG	2,81	2,443	Cluster B
35	AT3G55410.1	948	PNAEIVWCQEEAMNM	3,897	2,443	Cluster B
36	AT3G56190.1	82	AYAEAAKCYKKVDTN	3,533	2,443	Cluster B
		94	DTNEAASCLERAVNI	4,81	2,443	Cluster B
		205	TAGMCHLCKADVVSI	2,5	2,443	Cluster B
37	AT3G60240.1	716	PQEKDLKCDNRTASD	3,152	2,443	Cluster B
		1242	TEKIMHACIQKLLGY	2,886	2,443	Cluster B
		1293	EKMKMLSCKQELSSR	2,87	2,443	Cluster B
		1559	DENEIGMCMKDMNSP	2,788	2,443	Cluster B
38	AT4G11010.1	6	**MSSQICRSASKAA	5,825	1,484	Cluster A
39	AT4G14960.1	20	GIQVGNACWELYCLE	1,858	1,484	Cluster A
		347	TIQFVDWCPTGFKCG	1,82	1,484	Cluster A
40	AT4G20890.1	12	LHIQGGQCGNQIGAK	4,598	2,443	Cluster B
41	AT4G30190.1	327	MAGMDVLCSDKTGTL	3,663	2,443	Cluster B
42	AT4G31480.1	262	SSAVIYECAGTLVSL	3,266	2,443	Cluster B
		477	GISTITQCLGELPFY	2,484	2,443	Cluster B

Table. S2. Continued.

	AGI code	Cys position	NO sensitive-peptide sequence	Score	Cutoff	Cluster
43	AT4G31880.1	82	VKVAVAACISEITRI	2,946	2,443	Cluster B
		251	SNIVASICEGTFSAL	1.497	1.484	Cluster A
		147	VVMLDLECDALLIEM	3,136	2,443	Cluster B
44	AT4G34450.1	46	PQVDPRRCSQVITKL	2,973	2,443	Cluster B
45	AT4G36020.1	213	VGHFARDCTQKVAAG	2,777	2,443	Cluster B
46	AT5G02490.1	319	NMDLFRKCMEPVEKC	3,321	2,443	Cluster B
		326	CMEPVEKCLRDAKMD	2,674	2,443	Cluster B
		609	MKELESVCNPIIAKM	2,328	1,484	Cluster A
47	AT5G02500.1	319	NMDLFRKCMEPVEKC	3,527	2,443	Cluster B
		326	CMEPVEKCLRDAKMD	2,603	2,443	Cluster B
		609	MKELESICNPIIAKM	2,481	1,484	Cluster A
48	AT5G09590.1	25	SPFSAYRCLSSSGKA	2,538	2,443	Cluster B
49	AT5G09810.1	12	EDIQPLVCDNGTGMV	3,152	2,443	Cluster B
		287	TYNSIMKCDVDIRKD	2,973	2,443	Cluster B
50	AT5G14040.1	194	IIADIALCPFEAVKV	3,158	2,443	Cluster B
51	AT5G19760.1	170	VLALWKGCGPTVVRA	2,902	2,443	Cluster B
52	AT5G19770.1	20	GIQVGNSCWELYCLE	1,858	1,484	Cluster A
		347	TVQFVDWCPTGFKCG	1,82	1,484	Cluster A
53	AT5G22060.1	416	GGAQRVQCAQQ****	3	2,443	Cluster B
54	AT5G26710.1	682	SNMRNLKCGDVIQLE	2,658	2,443	Cluster B
55	AT5G28540.1	298	LGKLRRECERAKRAL	1,689	1,484	Cluster A
		635	LKEVEAVCNPIITAV	2,53	1,484	Cluster A
56	AT5G40870.1	460	VTSEIDQCLNQEFRV	2,587	2,443	Cluster B
57	AT5G42020.1	298	LGKLRRECERAKRAL	1.65	1.484	Cluster A
		635	LKEVEAVCNPIITAV	2,53	1,67	Cluster A
58	AT5G46070.1	436	FMEADLRCTSTIQRM	2,625	2,443	Cluster B
		451	EKQLRAACHASNANM	1.557	1.484	Cluster A
59	AT5G52470.1	252	VISIKANCIDSTVAA	3,201	2,443	Cluster B
60	AT5G57120.1	34	ERCGFSKCFKKLLSE	3,935	2,443	Cluster B
61	AT5G57870.1	640	LLGEALQCVEELGLP	3,424	2,443	Cluster B
		777	QAADIEACRNL****	1.519	1.484	Cluster A
62	AT5G61780.1	358	LKATELQCKKNRVKM	2,902	2,443	Cluster B
63	AT5G62690.1	12	LHIQGGQCGNQIGAK	4,598	2,443	Cluster B
64	AT5G67630.1	224	AQTKFVQCPEGELQK	2,625	2,443	Cluster B

Table. S3. Analysis of 54 putative partner proteins of HD2C identified by Co-IP. Nuclear protein fractions from WT and *hd2c-1* line were incubated with the Dynabeads wh have already been bound to the antibody to HD2C. The eluted samples were analyzed by mass spectrometry. 324 of identified proteins demonstrated the thresh confidence score of 30. 90 of proteins were identified with higher abundance in WT in compare with *hd2c-1* in 3 replicates. The proteins which showed any spectral coun *hd2c-1* were eliminated. A variation analysis among replicates of WT *and hd2c-1* samples besides a t-test was performed. The proteins were arranged by variation in samples from smallest to largest. The proteins with p-value bigger than 0.05 were marked by red (lowest fidelity), this way the proteins with WT variations more than 0.4 w marked red automatically. Then the proteins with *hd2c-1* variation more than 1 and/or with identified unique peptides less than 2 in any replicate were marked ora (medium fidelity). The 7 uncolored remained proteins are the partner candidates of HD2C with highest fidelity (Table. 4). Gene regulation is the maximum fold change of g up- or down-regulation by ABA and glucose according to GENEVESTIGATOR using p-value ≤ 0.05 and fold changes ≥ 2.

	AGI code	Description	Unique peptides		Normalized abundance								t-t
					hd2c-1				WT				
			Exp1	Exp2/3	Exp1	Exp2	Exp3	Variation	Exp1	Exp2	Exp3	Variation	
1	AT4G21150.1	HAP6, ribophorin II (RPN2) family protein	2	3	0	436.1	3969.6	1.48232	11576.2	10349.5	10240.5	0.06917	0.0
2	AT5G47690.1	Binding	1	3	0	2770.1	2690.1	0.86630	9170.4	9526.4	7840.0	0.10049	0.0
3	AT4G02840.1	Small nuclear ribonucleoprotein family	2	3	4083.2	11281.1	42496.8	1.05873	36679.5	43004.9	46324.7	0.11665	0.1
4	AT5G03740.1	HD2C, histone deacetylase 2C	11	15	59357.3	171576.1	366684.7	0.78067	5791779	5291988	4093217	0.17254	0.0
5	AT4G22010.1	sks4, SKU5 similar 4	8	12	89340.5	85093.6	434734.1	0.98815	991204.5	667471.4	940973.8	0.20105	0.0
6	AT3G15190.1	Chloroplast 30S ribosomal protein S20	2	2	1338.2	1450.4	16652.8	1.35941	22074.4	14652.7	18577.6	0.20140	0.1
7	AT4G31480.1	Coatomer, beta subunit	1	2	571.9	10498.9	1639.6	1.28618	13649	11464.1	8679.7	0.22110	0.1
8	AT1G33120.1	Ribosomal protein L6 family	2	3	11610.0	23275.0	4088.5	0.74415	38466.4	25362.8	27511.8	0.23081	0.0
9	AT3G49720.1	Unknown protein	1	2	518.2	1380.9	5869.6	1.10948	18861.7	13159.0	21308.5	0.23524	0.0
10	AT4G02520.1	GSTF2, glutathione S-transferase PHI 2	1	2	4205.5	12308.8	1902.8	0.89032	23817.2	16313.6	27878.1	0.25880	0.0
11	AT4G25630.1	FIB2, fibrillarin 2	2	5	8133.1	29623.7	20191.0	0.55767	258900.9	182884	157508.9	0.26411	0.0
12	AT1G16720.1	HCF173, high chlorophyll fluorescence	3	6	4015.7	5713.7	27066.2	1.04736	82518.0	60478.8	45505.2	0.29631	0.0
13	AT3G05060.1	NOP56-like pre RNA processing	4	7	3609.6	5149.7	4220.7	0.17923	142949.3	131635.2	77482.3	0.29816	0.0
14	AT1G56110.1	NOP56, homolog of nucleolar NOP56	6	8	3290.1	26533.7	33442.4	0.74904	195428.7	108996	126287.9	0.31855	0.0
15	AT3G23820.1	GAE6, UDP-D-glucuronate 4-epimerase 6	1	3	0	1405.9	1264.9	0.86963	25845.7	49555.0	48878.8	0.32582	0.0
16	AT5G63420.1	RNA-metabolising metallo- lactamase	4	3	5420.6	26885.2	25625.1	0.62377	89393.2	66046.5	45475.9	0.32809	0.0
17	AT5G26742.1	emb1138, DEAD box RNA helicase (RH3)	8	11	11937.2	83909.7	99274.6	0.71687	579245.7	345641.7	325605.5	0.33829	0.0
18	AT5G28740.1	Tetratricopeptide repeat (TPR)-like	4	4	8789.7	13784.5	3200.3	0.61628	80852.1	81591.8	39526.0	0.35761	0.0
19	AT3G06810.1	IBR3, acyl-CoA dehydrogenase-related	3	2	871.5	4171.5	349.2	1.15306	37800.3	26561.8	17934.8	0.36312	0.0
20	AT5G22650.1	HD2B, histone deacetylase 2B	6	8	3620.1	72724.6	205171.3	1.09145	964004.1	580538.1	493096	0.36878	0.0
21	AT3G57150.1	NAP57, homologue of NAP57	7	10	33153.5	19546.1	79813.2	0.71558	324222.5	605306.2	300213.6	0.41384	0.0
22	AT5G20290.1	Ribosomal protein S8e family	2	6	995.9	27161.8	13666.0	0.93858	45301.4	82689.6	111080.4	0.414	0.0
23	AT5G26000.1	TGG1, thioglucoside glucohydrolase 1	6	7	11281.8	68601.7	381016.1	1.29525	393102.6	923927.5	585948.9	0.42359	0.0
24	AT1G68830.1	STN7, STT7 homolog STN7	1	4	744.2	25188.8	13900.8	0.92138	16986.6	43023.1	30498.2	0.43160	0.1

Table. S3. Continued.

	AGI code	MW[kDa]	Spectral count						Confidence score		Max fold change (WT: *hd2c-1*)			Expression value eFB browser	Hints to S-nitrosylation	Gene regulatio by	
			hd2c-1			WT											
			Exp1	Exp2	Exp3	Exp1	Exp2	Exp3	Exp1	Exp2/3	Exp1	Exp2	Exp3			ABA	Glucos
1	AT4G21150.1	74.66	0	0	0	2	3	2	71.7	92.4	infinity	23.7	2.5	433.5	This work (Table. S1)	-2.24	2.30
2	AT5G47690.1	181.45	0	0	0	2	2	2	47.8	61.8	infinity	3.4	2.9	-	(Hu et al., 2015)	No probe	
3	AT4G02840.1	141.08	0	0	0	2	1	3	50.8	71.2	8.9	3.8	1.0	291.4	-	-2.41	-
4	AT5G03740.1	31.83	0	0	0	24	49	49	475.7	769.5	97.5	30.8	11.1	255.0	This work (Table. S1)	-2.41	2.68
5	AT4G22010.1	60.45	0	0	0	10	20	32	191.1	499.7	11.0	7.8	2.1	441	-	-10.19	2.57
6	AT3G15190.1	21.82	0	0	0	2	1	2	56.9	87.5	16.4	10.1	1.1	2144.1	-	-2.32	-
7	AT4G31480.1	106.14	0	0	0	1	1	3	33.2	51.2	23.2	1.0	5.2	378.4	This work (Table. S1)	-3.28	-
8	AT1G33120.1	22.01	0	0	0	3	1	2	71.1	93.9	3.3	1.0	6.7	1484.4	-	-2.02	-
9	AT3G49720.1	28.53	0	0	0	2	0	2	37.3	82.6	36.3	9.5	3.6	386.0	-	-	2.46
10	AT4G02520.1	24.12	0	0	0	1	0	3	44.7	68.8	5.6	1.3	14.6	207.5	(Hu et al., 2015)	-4.35	-
11	AT4G25630.1	33.65	0	0	0	2	5	4	44.9	126.5	31.8	6.1	7.8	443.6	-	-9.50	7.0
12	AT1G16720.1	65.70	0	0	0	3	3	7	102.1	150.8	20.5	10.5	1.6	25.0	-	-2.55	-4.80
13	AT3G05060.1	59.00	0	0	0	5	9	4	269.8	342.2	39.6	25.5	18.3	210.6	This work (Table. S1)	-4.72	3.52
14	AT1G56110.1	58.67	0	0	0	7	10	10	138	269.0	59.3	4.1	3.7	480.4	This work (Table. S1)	-5.54	5.31
15	AT3G23820.1	50.56	0	0	0	2	4	4	62.0	143.1	infinity	35.2	38.6	968.7	-	-5.62	4.60
16	AT5G63420.1	100.55	0	0	0	4	2	3	98.3	68.5	16.4	2.4	1.7	111.6	-	-3.76	-
17	AT5G26742.1	81.15	0	0	0	10	8	16	250.1	389.5	48.5	4.1	3.2	-	-	No probe	
18	AT5G28740.1	107.05	0	0	0	4	4	4	94.2	96.0	9.1	5.9	12.3	137.6	-	-3.09	-
19	AT3G06810.1	91.71	0	0	0	3	1	2	66.6	42.2	43.3	6.3	51.3	125.5	-	4.09	-
20	AT5G22650.1	32.34	0	0	0	7	12	10	161.2	258.9	266.2	7.9	2.4	564.2	This work (Table. S1)	-3.07	3.84
21	AT3G57150.1	63.02	0	0	0	10	13	14	247.8	371.6	9.7	30.9	3.7	531.2	-	-4.80	3.96
22	AT5G20290.1	24.99	0	0	0	2	2	10	60.0	191.7	45.4	3.0	8.1	3484.5	This work (Table. S1)	-	-
23	AT5G26000.1	61.13	0	0	0	8	23	23	227.8	455.8	34.8	13.4	1.5	2137.4	(Hu et al., 2015)	-2.58	-
24	AT1G68830.1	63.25	0	0	0	1	3	5	32.1	80.8	22.8	1.7	2.1	7.9	-	-4.17	-2.17

Table. S3.Continued.

	AGI code	Description	Unique peptides		Normalized abundance								t-t
					hd2c-1				WT				
			Exp1	Exp2/3	Exp1	Exp2	Exp3	Variation	Exp1	Exp2	Exp3	Variation	
25	AT4G39960.1	Molecular chaperone Hsp40/DnaJ family	1	2	107.8	1432.4	608.5	0.93378	11179.4	5060.7	5829.4	0.45305	0.0
26	AT4G34980.1	SLP2, subtilisin-like serine protease 2	5	10	3697.0	46710.4	156462.7	1.14238	79426.2	197821.6	236960.7	0.47853	0.1
27	AT3G55200.1	Cleavage and polyadenylation factor A	2	2	1736.6	2919.9	5331.8	0.55031	21506.2	31785.1	10802.9	0.49108	0.0
28	AT3G63490.1	Ribosomal protein L1p/L10e family	2	3	609.1	3372.0	3918.6	0.67373	16880.5	21990.4	42362.2	0.49786	0.0
29	AT1G43170.1	ARP1, ribosomal protein 1	2	8	528.4	42919.2	16239.7	1.07714	29168.1	94266.8	92519.7	0.51525	0.1
30	AT5G09440.1	EXL4, EXORDIUM like 4	1	1	157.2	737.1	405.5	0.67146	11173.6	9343.7	23351.4	0.52071	0.0
31	AT5G51750.1	SBT1.3, subtilase 1.3	3	3	4545.7	1342.9	557.3	0.98328	68464.5	35008.5	24441.9	0.53899	0.0
32	AT5G35530.1	Ribosomal protein S3 family protein	1	1	4307.2	831.0	3354.2	0.63451	14935.2	4631.4	6775.1	0.61918	0.1
33	AT3G07010.1	Pectin lyase-like superfamily protein	2	3	2.2	14888.8	4614.9	1.17203	46496.2	210383.5	139084.3	0.62258	0.1
34	AT4G22890.1	PGR5-LIKE A	2	1	276.9	1317.5	4.0	1.30092	9923.0	4447.7	3051.4	0.62540	0.1
35	AT3G27830.1	RPL12-A, ribosomal protein L12-A	2	1	6073.8	299.7	1531.2	1.24878	55527.2	7090.0	7780.3	0.63689	0.1
36	AT3G06530.1	ARM repeat superfamily protein	4	5	431.7	1753.7	8517.0	1.21572	59078.5	23813.2	14593	0.72254	0.1
37	AT1G10580.1	Transducin/WD40 repeat-like	2	2	5166.0	8696.0	6901.1	0.25503	123631.4	60710.5	22291.4	0.74278	0.1
38	AT1G02840.1	SR34, RNA-binding (RRM/RBD/RNP)	1	5	436.4	11020.4	25869.6	1.02683	3975.6	25123.9	37365.2	0.76243	0.4
39	ATCG00170.1	RPOC2, DNA-directed RNA polymerase	2	2	4400.3	175.5	34460.2	1.06981	7698.7	9536.2	17231.7	0.8675	0.2
40	AT3G21540.1	Transducin family protein/WD-40 repeat	4	5	2426.4	1712.6	441.3	0.65857	98064.9	29661.9	14480.4	0.93933	0.2
41	AT3G18035.1	Winged-helix DNA-binding TF	1	2	0	3128.2	554.0	1.35998	4721.3	20798.7	56380.3	0.96834	0.2
42	AT4G21660.1	Proline-rich spliceosome-associated	2	1	114.8	292.0	0	1.08477	27215.3	9369.6	2618.1	0.97252	0.2
43	AT5G16750.1	Transducin family protein/WD-40 repeat	3	2	2789.4	99.5	1913.9	0.85696	46064.7	13219.8	5496.2	0.99759	0.2
44	AT4G04940.1	Transducin family protein/WD-40 repeat	3	2	998.7	4299.8	599.9	1.03285	57222.9	9689.7	12382.4	1.01014	0.2
45	AT5G62390.1	BAG7, BCL-2-associated athanogene 7	4	4	2977.0	4130.5	30465.1	1.24142	253080.8	46842.2	44666.7	1.04215	0.2
46	AT3G11964.1	RNA binding	4	2	4514.1	1009.9	419.4	1.11723	61184.9	12335.4	7182.1	1.10786	0.2
47	AT5G46580.1	Pentatricopeptide (PPR) repeat	2	1	237.7	0	2222.0	1.48801	19109.6	1865.9	4020.6	1.12764	0.2
48	AT3G18600.1	P-loop containing nucleoside	2	2	37.9	102.4	973.5	1.40727	28221.1	3255.3	4496.6	1.17331	0.2
49	AT2G36620.1	RPL24A, ribosomal protein L24	1	1	1561.6	2164.8	16273.2	1.15417	38702.6	9999.6	19949.6	1.18333	0.3
50	AT4G30440.1	GAE1, UDP-D-glucuronate 4-epimerase 1	2	1	6145.1	261.9	434.5	1.46803	57268.6	5416.7	4995.9	1.33237	0.3
51	AT5G17920.1	Cobalamin-independent synthase	2	1	5523.8	266.5	0	1.61392	42353.3	2302.7	4827.7	1.35982	0.3
52	AT3G04260.1	PTAC3, plastid transcriptionally active 3	3	2	1793.4	1148.7	3865.2	0.62549	109884.9	12584.2	5578.2	1.36600	0.3
53	AT4G07410.1	Transducin family protein/WD-40 repeat	4	2	371.8	0	279.4	0.89176	39761.7	1139.6	4449.0	1.41611	0.3
54	AT5G09810.1	ACT7, actin 7	2	1	4240.0	0	0	1.73205	31748.1	216.0	2061.0	1.56029	0.4
55	AT1G59610.1	ADL3, dynamin-like 3	5	1	2966.8	304.6	0	1.49663	81705.9	397.1	3214.2	1.62283	0.4

Table. S3. Continued.

	AGI code	MW[kDa]	Spectral count						Confidence score		Max fold change (WT: *hd2c-1*)			Expression value eFB browser	Hints to S-nitrosylation	Gene regulation k	
			hd2c-1			WT											
			Exp1	Exp2	Exp3	Exp1	Exp2	Exp3	Exp1	Exp2/3	Exp1	Exp2	Exp3			ABA	Gluc
25	AT4G39960.1	48.03	0	0	0	1	0	3	49.9	48.6	103.6	3.5	9.5	220.9	-	-	2.17
26	AT4G34980.1	81.04	0	0	0	6	7	13	104.4	278.6	21.4	4.2	1.5	316.8	-	-2.96	2.44
27	AT3G55200.1	134.96	0	0	0	3	3	1	56.8	65.7	12.3	10.8	2.0	245.2	-	-3.13	-
28	AT3G63490.1	37.63	0	0	0	3	0	3	49.1	86.8	27.7	6.5	10.8	1517.1	(Hu et al., 2015)	-2.28	-
29	AT1G43170.1	44.55	0	0	0	3	1	8	56.6	198.3	55.1	2.1	5.6	3055.3	This work (Table. S1)	-3.38	-
30	AT5G09440.1	29.47	0	0	0	1	0	5	34.2	39.0	71.0	12.6	57.5	77.7	-	47.79	-2.24
31	AT5G51750.1	84.94	0	0	0	4	1	2	71.3	74.9	15.0	26.0	43.8	594.3	-	-	2.85
32	AT5G35530.1	27.45	0	0	0	1	0	1	46.6	117.0	3.4	5.5	2.0	1890.5	-	-2.19	-
33	AT3G07010.1	46.17	0	0	0	3	6	5	62.1	165.9	20319.3	14.1	30.1	80.5	-	-2.78	-
34	AT4G22890.1	35.72	0	0	0	2	1	1	51.7	52.0	35.8	3.3	761.2	1691.4	-	-4.28	-
35	AT3G27830.1	200.74	0	0	0	2	0	1	58.2	33.6	9.1	23.6	5.0	2819.3	-	-2.43	-
36	AT3G06530.1	24.63	0	0	0	5	3	6	111.0	122.9	136.8	13.5	1.7	107.8	-	-5.66	4.59
37	AT1G10580.1	65.12	0	0	0	5	2	2	84.8	98.1	23.9	6.9	3.2	-	-	No probe	
38	AT1G02840.1	33.72	0	0	0	1	2	4	63.2	176.8	9.1	2.2	1.4	366.2	-	-	-
39	ATCG00170.1	156.36	0	0	0	2	2	3	50.8	60.9	23.1	1.7	54.3	-	-	-2.56	-
40	AT3G21540.1	106.06	0	0	0	5	3	4	126.1	134.1	40.4	17.3	32.8	40	-	-3.89	3.81
41	AT3G18035.1	51.32	0	0	0	1	5	2	32.9	116.3	infinity	6.6	101.7	350.3	-	-2.41	-4.34
42	AT4G21660.1	68.51	0	0	0	2	1	1	46.8	72.6	236.9	32.0	infinity	103.1	-	-4.40	-
43	AT5G16750.1	96.69	0	0	0	3	2	2	75.0	38.8	16.5	132.7	2.8	91.1	-	-3.79	2.96
44	AT4G04940.1	102.21	0	0	0	4	0	3	139.9	52.9	57.2	2.2	20.6	59.1	-	-5.69	7.47
45	AT5G62390.1	51.56	0	0	0	4	3	4	102.9	129.9	85.0	11.3	1.4	803.2	-	-3.63	-
46	AT3G11964.1	211.60	0	0	0	4	2	2	83.8	47.0	13.5	12.2	17.1	125.8	-	-4.91	3.33
47	AT5G46580.1	80.87	0	0	0	2	0	1	37.7	38.2	80.3	infinity	1.8	407.4	-	-3.23	2.08
48	AT3G18600.1	63.81	0	0	0	2	1	2	68.6	66.2	743.9	31.7	4.6	282.9	-	-7.14	5.89
49	AT2G36620.1	18.85	0	0	0	1	0	3	34.9	43.2	24.7	4.6	1.2	1474.9	-	2.88	3.00
50	AT4G30440.1	47.45	0	0	0	2	0	1	59.2	65.5	9.3	20.6	11.4	374.4	-	2.03	-
51	AT5G17920.1	84.35	0	0	0	2	0	3	132.8	127.8	7.6	8.6	infinity	1773.9	(Hu et al., 2015)	-2.13	2.64
52	AT3G04260.1	102.91	0	0	0	4	2	1	99.8	75.5	61.2	10.9	1.4	449.2	-	-3.28	-
53	AT4G07410.1	90.26	0	0	0	5	0	2	70.8	42.5	106.9	infinity	15.9	124.6	-	-2.23	-
54	AT5G09810.1	41.73	0	0	0	2	0	1	222.6	202.5	7.4	Infinity	Infinity	1616.0	This work (Table. S1)	-	2.21
55	AT1G59610.1	100.22	0	0	0	5	0	1	162.9	156.4	27.5	1.3	infinity	184.8	-	-2.29	-

ACKNOWLEDGMENT

I would like to warmly thank my PhD supervisors Prof. Dr. Jörg Durner and Dr. Christian Lindermayr for providing the opportunity of doing my PhD work in their laboratory and their supporting even in non-scientific difficult times of my study.

Prof. Dr. Jörg Durner's enthusiasm and encouragement made my entire Ph.D study an enjoyable journey. He offered me key ideas and criticisms during institute seminars and three thesis committee meetings which I deeply appreciate. I am highly thankful to him also for reading and correction of my dissertation.

I specially thank Dr. Christian Lindermayr for awarding me an interesting thesis topic, his professional supervision during whole my PhD study and careful review of my dissertation. His excellent guidance and willing to discussion, besides his patience to provide me freedom and confidence of developing my own ideas have strongly contributed to the success of this work.

I am highly grateful to Prof. Dr. Erich Glawischnig for appearing as the second examiner and Prof. Dr. Siegfried Scherer for accepting the chairmanship of my final examination.

I would like to especially acknowledge Dr. Harald Schempp for appearing as my thesis committee member and his kind encouragement and constructive criticisms during three thesis committee meetings.

I am thankful to Dr. Dieter Ernst for forwarding my first application to Prof. Dr. Jörg Durner and Dr. Christian Lindermayr and kindly introducing me to them.

I would also like to express my gratitude to 'protein core facility' in Helmholtz Zentrum München especially Dr. Christine von Törne for performing nano LC-MS/MS analyses of this work and preliminary quantification analysis of Co-IP data.

My special thanks go to 'staff' of 'BIOP' especially Dr. Anton Schäffner and Dr. Corina Vlot-Schuster for their encouragement and valuable advices during my institute seminars.

I am very grateful to Dr. Areli Herrera Diaz, Dr. Sanjukta Dey and Alexander Mengel for their kindness, encouragement and very motivated scientific open discussions. I thank Dr. Areli Herrera Diaz for her nice advices about cloning. I thank Alexander Mengel for kindly performing HDAC activity for HD2C recombinant protein and his interesting suggestions regarding biochemical aspects in some of my experiments.

Thanks very much to Dr. Izabella Kovacs, Dr. Frank Gaupels and Dr. Jeremy Astier for their interesting and critical advices during lab meetings.

I would like to appreciate cooperation of Dr. Mounira Chaki in identification of nuclear targets of S-nitrosylation.

I would like to thank very warm and friendly advices and cooperation of Dr. Francesca Verillo in first month of my work in BIOP.

My warm thanks go also to other group members specially Dr. Antonie Bernhard, Dr. Christian Holzmeister and Dr. Gitto Kuruthukulangarakoola.

I sincerely thank my colleagues Elke Mattes, Rosina Ludwig, Birgit Geist, Lucia Gößl, Marion Wenig and Evi Bieber for their friendly technical assistance and collaboration. I thank Karoline Stoll for her kind helps for doing official works.

My deep thanks go to Dr. Chen Liu, Dr. Wei Zhang, Rafał Maksym, Alexandra ageeva, Dr. Jin Zhao, Dr. Ming Jin, Dr. Feng Zhao, Jiangli Zhang and Birgit Lange for enjoying lunch times together in a friendly atmosphere and their kind supports during hard times of study and in writing time. I thank Dr. Chen Liu for her nice advices for generation of transgenic lines and very tasty Chinese snacks. I thank Rafał Maksym for his funny jokes during lunch times and for his friendly ‘ciao’s every evening. I thank Alexandra Ageeva for her nice cooperation and her kindly smiles and nice chocolates.

I express my gratitude to all my formal teachers, supervisors and colleagues and also my nice Iranian friends.

I heartily appreciate kind support of people - without naming anyone - who made it possible that I can leave my country again and complete this study.

Finally, I would like to say ‘Thank you’ to my parents for their endless love and supports during my studies and difficult times of my life. And, I heartily thank my lovely sisters and brother for their kindness and always open hugs.